An Economic Analysis of Injecting Energy Storage into Power Systems Containing Renewables

By

Kelsey Bekr McGlashan

A Thesis submitted to the Faculty of the

Worcester Polytechnic Institute
In partial fulfillment of the requirements for the
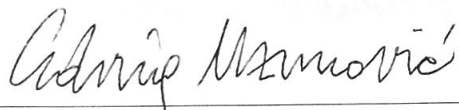Degree of Master of Science
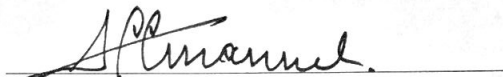In
Electrical and Computer Engineering
by

June 2017

Approved:

_____
Professor Edvina Uzunovic, Major Advisor

_____
Professor Alexander Emanuel, Advisor

_____
Professor Yousef Mahmoud, Advisor

Abstract

Large amounts of renewable energy generation are being introduced into modern power systems to decrease the environmental impact of power generation. Despite benefits, increased renewable energy penetration will likely create additional system instability and unpredictability. Increasing line capacity via redundancy of transmission networks and utilizing energy storage are two methods that can be used to increase transmission power system stability. This study investigates the economic effects of energy storage and line capacity in isolated test systems. Utilizing Powerworld Simulator test systems based off two common industry test bed standards (WECC 9-bus, IEEE 14-bus) were built using scaled real-world generation and load data. Multiple Optimal Power Flow studies performed on the test systems with and without the addition of an energy storage model revealed the incremental change in overall system cost of adding energy storage and highlighted the impact energy storage has on isolated systems with renewable energy.

Acknowledgments

I would like to thank my thesis advisor Professor Edvina Uzunovic of the Electrical and Computer Engineering/Power Systems Engineering Department at Worcester Polytechnic Institute for supporting me throughout the entire process of planning, developing, creating and writing my Master's Thesis. Despite corresponding almost exclusively via email and phone, you provided your support through every step of the way, and helped me continuously achieve my goals and meet my deadlines, without the need for meetings on campus. I really would not have been able to complete this project without you, and for that I am truly appreciative to have had the privilege of your counsel.

I would also like to thank my thesis committee, Professor Alexander Emanuel and Professor Yousef Mahmoud, for being willing and able to support the completion of my thesis, albeit at a relatively short notice towards the end of the process. You both were readily available despite scheduling and communication errors, and have been fairly flexible in order to support me, and for that I am grateful.

Finally, I would like to thank Mike Ahern and Stephanie Papia for helping support me through this process in less obvious ways. You both have helped me through the formalities, procedures and paperwork necessary to complete my thesis (and for that matter, my degree), and for that I cannot thank either of you enough.

Table of Contents

List of Figures

List of Tables

List of Terms

AA-CAES:	Advanced Adiabatic Compressed Air Energy Storage
BES:	Battery Energy Storage
CAES:	Compressed Air Energy Storage
EES:	Electrical Energy Storage
FCDV:	Fixed Cost Dependent Value
FCIV:	Fixed Cost Independent Value
FBES:	Flow Battery Energy Storage
FES:	Flywheel Energy Storage
HES:	Hydrogen Energy Storage
HTS:	High Temperature Superconducting Coils
IEEE:	Institute of Electrical and Electronics Engineers
ISO:	Independent System Operator
ISONE:	Independent System Operator of New England
LAES:	Liquid Air Energy Storage
LTS:	Low Temperature Superconducting Coils
NERC:	North American Electric Reliability Corporation
OPF:	Optimal Power Flow
PHS:	Pumped Hydro Storage
PNNL:	Pacific Northwest National Laboratory
PSB:	Polysulfide Bromine Flow Battery
RE:	Renewable Energy
REG:	Renewable Energy Generation
SMES:	Superconducting Magnetic Energy Storage
TSS:	Time Step Solution
TES:	Thermal Energy Storage
UFC:	Unit Fuel Cost
VOM:	Variable Operation and Maintenance Cost

VBR:	Vanadium Redox Flow Battery
WECC:	Western Electricity Coordinating Council
WSCC:	Western System Coordinating Council (dissolved. See: WECC)
ZnBr:	Zinc Bromide Flow Battery

1. Introduction

Power system design theory has changed dramatically over the past three decades. Not long ago, power system design consisted of utilizing power generation around a very simple and familiar load demand curve [1]. With some variance, this 24-hour load demand curve was easily represented by a curve similar to that of a sine wave; peak load demand would occur around midday, and lowest demand would occur very late in the evening. To cater to the relatively stable and relatively predictable load, electric utilities generated power using large-scale prime mover generation plants that were optimized for predictable dispatch with little down-time. Typically, large-scale coal, oil or nuclear power plants were utilized to supply the network's base load, while large natural gas plants supplied any load that exceeded the base load (such as peak load) [2, 3, 4, 5, 6]. For a long time, power networks remained relatively stable as the predictable load could be matched by the easy-to-control power generation.

However, modern power system design now includes a growing effort to produce more sustainable power with fewer emissions to combat climate change [1, 7]. This has dramatically increased the amount of renewable generation installed in power networks [8, 9, 10, 6], challenging the traditional roles of coal, oil and natural gas power plants. One unanticipated result of increased renewable penetration is a more dynamic load demand curve such that now at the very least two models are needed to represent it. The traditional curve is still applicable during the summer season, but during the fall, winter and spring seasons a new model is needed to represent the load pattern. This new 24-hour model coined as the "duck curve" has two peaks and a local minimum; one peak in the morning just after sunrise, one peak in the evening just after sunset and a new minimum during midday (in between the two peaks) [11, 12]. The harshness of the duck curve is only projected to increase as the amount of renewable energy installed increases.
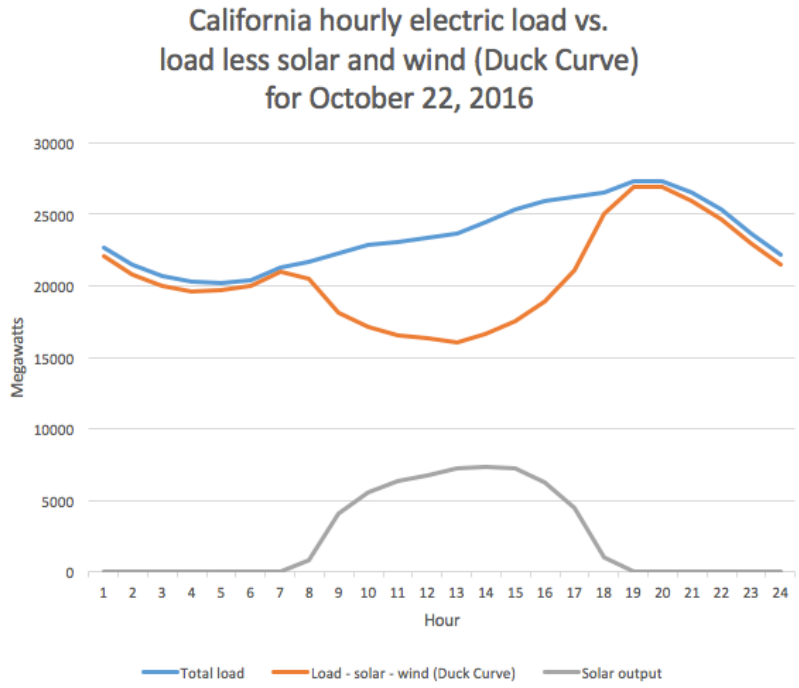
Figure 1-1: Example of Duck Curve **[12]**

A greater defined duck curve indicates larger variance in the load demand profile, only making it harder for power utilities to balance supply with demand. Thus, there is a need to address the decreased stability and reliability of the modern power system design due to the increase of renewable energy penetration.

Introducing line redundancy to a power transmission network is one popular method that is frequently used to increase power system stability [9, 13]. The addition of transmission line connectivity and capacity not only allows for more power transfer within a network and thus less congestion, but also decreases the power losses due to transmission. Another method gaining momentum in the modern utility industry is the addition of bulk energy storage (ES) into a transmission network [10, 14, 15]. Bulk ES allows for easy power dispatch and could absorb excess power during low demand, high supply and discharge power into the network during high demand and low supply, thus balancing supply and load without the need for installing additional transmission lines [5, 10, 16]. The concept of bulk ES is becoming increasingly popular as it may serve as a cost effective alternative solution, fixing many of the problems facing the modern power grid [17].

Regardless, there are still many challenges that many utilities face when attempting to install and apply ES to an electrical network. While storage isn't a new concept, the industry is still developing and there are few resources detailing common storage heuristics. Since most electrical networks are very complex it can often be difficult to determine properties such as the storage size, storage location, and the actual storage technique itself that would be best suited for certain applications [5]. In addition, it is hard to quantify the actual technical or economic value of installing storage into a network [18]. Typically, the actual economic value of storage depends heavily on the properties of the network in which it is installed. Thus, while the direct costs can be calculated easily, quantifying the overall economic impact of storage is much more complicated.

1.1   Scope

The purpose of this thesis was to determine the economic effects of introducing energy storage into an isolated power network that utilizes conventional and renewable generation sources. Utilizing PowerWorld Simulator, two test systems based off two common industry test bed standards (the WECC 9 bus, IEEE 14 bus) were built using scaled real-world generation and load data from one typical day in the summer, and one typical day in the fall. Then a generator in each model was replaced with a renewable generator, either a wind or solar plant of the same size. Weather data was recorded for the two days chosen such that estimates of the hourly power generation for either wind or solar energy could be constrained within the model. Multiple Optimal Power Flow (OPF) studies were performed on the model test systems with and without the addition of an energy storage module. The size of the module, as well as the placement of the module in the test systems were varied to determine the economic effects of location and sizing of energy storage in an isolated system. Next, original test models were altered to allow for additional line capacity by creating redundant lines across the network. The same original tests were performed to see the economic effects of additional line capacity. Finally, the overall daily cost results

from the OPF tests were compared to determine the optimum location and sizing of energy storage in each system, as well as highlight any additional economic trends that were present.

1.2   Literature Review

There are multiple resources [19, 20, 21] available that have studied the economics of applying ES in distribution networks [22]. One such resource [19] is quite simply a comprehensive assessment on numerous additional studies regarding the economics of energy storage for distribution purposes. However, as [22] suggests, methods used for determining the optimum sizing and placement of ES into distribution networks should not be directly applicable to the utilization of bulk ES within transmission networks. Transmission networks have various properties that differ from distribution networks. The power flows across transmission lines fluctuate much more over time with larger magnitudes than those of distribution lines, depending on the status of connected electric generation sources such as renewables or ramp-up power plants. Thus, it is much harder to determine the best methods for ES transmission integration, let alone determining the economics of such projects.

Two reports [23, 24] each presented methods for determining the maximum ES requirement or potential within networks of many variable generation sources such as wind energy. However, neither considered the costs of installing storage into the networks in question. Both found a large potential for storage integration, but without considering the costs or economic benefits, it would be unwise to move forward with installing storage based on the results of these studies alone.

Additionally, [25] proposed scheduling and operating a wind power plant with ES to optimize the cost benefits within the electric market. By simulation of a simple 2-bus network, it was determined that a wind power plant operator could utilize storage to take advantage of the spot price of electricity, increasing the value of wind power plants in electric markets. But the actual costs of storage installation and integration were not considered in the analysis.

A complex, three-stage algorithm is utilized in [26] to determine the best locations and parameters of distributed storage units in the IEEE RTS-96, a large transmission network test system. Various scenarios were tested considering not only the technical properties of the system, but the actual costs and economics of storage as well. However, this report did not consider the installation of bulk ES at a single location within the network.

The costs of installing various storage technologies in two transmission-constrained networks were studied in [27] using a DC OPF framework. Both networks were modified from the IEEE 14-bus network to include wind generation. The first network was used to determine the economical location and operation of various storage technologies installed independently, while the second network was used to determine economical operation of a mix of storage technologies. In a similar fashion, [28] focused on determining the optimum location of ES in a network with high wind generation penetration while minimizing system costs. This paper utilized the Probabilistic OPF method on the IEEE 24-bus network, and considered scenarios in which the system was constrained to limited power flows, maximizing the wind power utilization while minimizing the hourly system cost. Yet a third report [17], proposed utilizing the Dynamic OPF method on an IEEE 30-bus network with large amounts of wind generation to test the economics and impact of integrating ES. This report also focused on improving network operation by utilizing the four hour-ahead and 24 hour-ahead wind generation forecasts to mitigate prediction errors to better optimize the economic dispatch of power reserves or other conventional power plants. However, this report did not look at determining the optimum location or size of storage in the network.

Finally, [22] outlined a Mixed-Integer Linear Programming method to reduce the operating and investment costs of installing storage in a network by looking at the optimum placement and sizing of storage. The proposed methodology utilized a realistic 240-bus 448-line model from the WECC interconnection but it was suggested that the optimization strategy could apply to other networks of various sizes and properties with various amounts of renewable energy as well.

2. Background

To maintain a stable power transmission network there needs to be an instantaneous balance between generated electric power and stochastic demand [7]. The modern electric grid does not contain enough substantial energy storage capacity and the demand is supplied directly from power generation plants [1, 7]. Maintaining the balance of supply and demand in this way is difficult due to the complexity of electricity networks; thousands of power plants need to produce enough energy in real-time to supply millions of consumers. In 2012, global electric generation reached approximately 22,000 TWh, 70 percent of which was generated using fossil fuels like coal, natural gas or oil [5]. Up until a couple of decades ago, power system stability was maintained almost exclusively through the use of either fossil fuel or nuclear generation units matching the load demand balance, with operators making minor adjustments to rebalance the supply as necessary.

Over the last few years alone there have been many technical, economic, regulatory and social factors that have changed not only the electric grid, but also the way load management is viewed. One major change in particular is the wide scale installation of renewable energy (RE) sources in order to reduce fossil fuel pollution and emissions [1, 8, 10, 7]. While the majority of generation capacity is still conventional large prime movers, the amount of RE is only expected to increase, as renewable generation holds many benefits over conventional plants [16]. After considering the fixed capital investment and maintenance costs associated with renewables, there are no variable costs needed to maintain or produce additional power. In addition, for every unit of power produced there are no polluting emissions as there is no physical fossil fuel to be burned or consumed. The "fuels" of RE are mainly wind density or solar irradiance, which are largely considered to be virtually unlimited sources.

Despite all the benefits of RE, there are still uncertainties and issues that it brings to the electric network. The most common sources of RE are intermittent in nature; their output cannot be controlled or easily

predicted without added investment and infrastructure [7]. This makes the tasks of load demand management and maintaining network stability even more challenging. The combination of massive deployment of unpredictable renewable sources along with rising power demands from consumers in more liberalized trade markets is creating new opportunities for load management technology.

Electrical Energy Storage (EES) is one promising approach to the load management problem that is becoming increasingly relevant in industry [16, 10]. Unlike demand control or additional transmission interconnectivity, EES is extremely controllable and easily customizable. In addition to improving the system reliability, there are numerous benefits to utilizing EES [7, 10]. By providing time varying energy management (energy that is easy to dispatch), EES has the capability to: help meet peak electric load demands instantly, alleviate the intermittence of REG, meet remote and future electric vehicle load requirements, support the realization and integration of smart grids, help manage distributed or standby power generation and reduce the electrical energy imported during a peak demand period [1, 5, 7]. In other words, EES could relieve the stringent load balancing requirement altogether, creating a more flexible electrical network for various future or present applications.

2.1   Types of Electrical Energy Storage

There are many types of EES each with different storage mechanisms, operating procedures and functional properties. Grouping EES based on the type of energy stored in the system is currently the most widely used method of EES classification. There are currently five main groups of EES that will be discussed further: Mechanical, Electrochemical, Electrical, Thermochemical and Chemical, and Thermal Energy Storage. One publication [1] analyzed each type of Energy Storage in what is referred to as a SWOT analysis, in which the Strengths, Weaknesses, Opportunities and Threats of each type are discussed and compared. A similar method will be used here to better highlight the differences of each type of storage.

2.1.1   Mechanical Energy Storage

Mechanical Energy Storage methods utilize mechanical energy conversion to store energy. When charging, these units consume electrical energy to convert it to and store it as mechanical energy, and the opposite is true when discharging. There are three main techniques of mechanical energy storage that will be discussed further in detail: Pumped Hydro Storage, Compressed Air Energy Storage, and Flywheel Energy Storage.

2.1.1.1   Pumped Hydro Storage

Pumped Hydro Storage (PHS) accounts for approximately 99 % of the worldwide bulk energy storage capacity which equates to about 3 % of worldwide electric generation [5]. The properties of PHS make it an ideal technology for time shifting load demand, controlling system frequency and non-spinning generation supply reserve.

In Pumped Hydro units, pumps consume electricity to force water from a reservoir of low elevation to a reservoir of higher elevation [1, 5, 10]. To generate electricity, water from the high reservoir is then allowed to flow through a turbine generator towards the lower reservoir. The potential energy stored depends on the difference in elevation between the higher and lower reservoirs as well as the total volume of water available. Conventional operating procedure comprises of pumping water into the higher reservoir during off-peak demand hours (i.e. when electricity demand is low) as the cost of consuming electricity is typically cheaper. Water is allowed to power the turbines driving the generators during peak demand hours (when electricity demand is at its highest), as the electricity sell price is typically higher.

The rated power of PHS depends entirely on the design water pressure and flow rate allowable through the pump and/or turbine generator shafts as well as the rated power of the pump/turbine and generator/motor units.

Strengths

PHS has the highest technical maturity of any EES method due to the simple design based on systems that have been around for decades [1, 15]. Hydroelectric generation and pump technology are both very mature and well-established industries that are in use across the world. The operation costs are very low and the technology is very reliable with a long lifetime of typically well over 40 years and a cycle efficiency of 70-85%. PHS has the capability of being able to store large amounts of energy, with capacities typically ranging from 1 MW to well over 3000 MW. Despite such large power ratings, PHS typically has relatively fast response times usually taking only minutes to ramp up to full load pumping or discharging.

Weaknesses

PHS design depends heavily on geological location: either multiple existing reservoirs of varying heights are required or locations in which to create reservoirs are required. Regardless of whether the reservoirs are man-made or natural, PHS is disruptive to local ecosystems. Taking up so much land and water resources can negatively affect water quality and watershed flows which can threaten local species. In addition, PHS development often requires high fixed capital investment costs to support such a large system infrastructure [1, 5, 15].

Opportunities

The negative environmental impacts of PHS can still be limited by smart design [5]. The larger the difference in elevation between the two reservoirs, the smaller land size needed to generate the same amount of electricity [1, 10]. Variable speed drives could be utilized to enhance efficiency and dynamic behavior alongside intelligent control systems. Development is trending towards higher speed units with larger capacity, as there are few physical limitations. In addition, modern technology now allows for the utilization of PHS in abandoned flooded mine shafts, underground caves and even within ocean caverns.

Threats

The only major threats to PHS are the large geological constraints limiting construction, high initial fixed investment and capital costs, and the local public opposition of PHS due to the environmental costs associated with it [1].

2.1.1.2 Compressed Air Energy Storage

Compressed Air Energy Storage (CAES) is a newer method of energy storage that is quickly becoming more popular in the power industry. Currently it is being used for time shifting load demand, peak load shaving, controlling system frequency and voltage [5].

In Compressed Air units, air is forced into underground caverns or above ground tanks via a compressor train. The potential energy is stored as high-pressure air. To generate electricity, the compressed air runs through an expander train that drives a generator [10]. Conventional operating procedure has been to utilize electricity during off-peak demand hours to drive a reversible motor/generator unit that in turn runs a chain of compressors for injecting air into the storage vessels. During peak demand hours, released compressed air is heated by a heat source and then used to drive turbine generators [1, 5, 10].

Conventional CAES facilities consumed fossil fuels as the primary heat sources before expansion. Newer technology utilizes recuperators to capture and reuse the waste heat from the exhaust, reducing fuel consumption by 22-25 % and thus improving cycle efficiency from approximately 42 % without recuperators to 54 % with the technology [1].

The rated power of CAES depends entirely on the design air pressure and decompress-able flow rate allowable, as well as the rated power of the compressor/turbine and generator/motor units.

Strengths

CAES plants can be very large with very little storing losses. The size of a CAES plant currently ranges from around 100 MW to well over 2700 MW. The energy from the compressed air can be stored for more

than 1 year if necessary. CAES units have relatively fast response times usually taking about 12 minutes to ramp up to full load charging or discharging. This is much faster than conventional generation plants, and extremely reliable with 91.2-99.5 % starting/running reliabilities [1].

Weaknesses

Conventional CAES design depends heavily on geological location: either multiple salt or rock caverns are needed or locations in which to create such caverns or install tanks are required. While CAES has less geographical restrictions than PHS, the high capital investment costs vary depending on location, and are very high for the construction of artificial caverns [1]. In addition, while reliability is extremely high, most CAES plants have lower round trip efficiency compared to PHS or other storage technology available.

Opportunities

Newer technologies have improved the efficiency of CAES significantly as well as reduced or eliminated the use of fossil fuels altogether. Advanced Adiabatic CAES has a higher efficiency than conventional CAES as it utilizes thermal energy storage during the air expansion phase, thus using significantly less energy to heat the air before expansion [1]. More research is being done on using geological structures (such as abandoned mine shafts) other than salt caverns either underground or otherwise to store compressed air. Above-ground small-scale CAES has increased in popularity and development to be used as alternatives to battery packs for Uninterruptible Power Supplies or back-up power systems. Other technological developments include Liquid Air Energy Storage methods which operate in a similar fashion but are considered to be thermal energy storage since the heat energy stored is utilized for charging and discharging and not the potential energy of the stored air.

Threats

The only major threats to CAES are the costs associated with it. The fixed capital costs can be high, and the operating costs are heavily dependent on the fuel used for the heat source. As fossil fuels prices continue to rise as projected, the operating costs will also increase. While CAES does not disrupt as large

of an ecological area such as PHS, there are still some environmental costs due to the burning of fossil fuels [1].

2.1.1.3 Flywheel Energy Storage

Flywheel Energy Storage (FES) can be classified into two groups: Low speed and High-speed FES. Low speed FES is used for short-term and medium/high power applications, while high speed FES was originally used for high power quality and ride-through power applications in the aerospace industry, but is now being considered for more general applications as well [1], [5].

Flywheel units utilize the concept of stored mechanical energy in a spinning mass around an axis. A modern flywheel system is composed of 5 parts: the flywheel, a group of bearings, a reversible electric motor/generator, a power electronic unit and a vacuum chamber in which it operates [1]. Electricity is consumed to accelerate or decelerate the Flywheel in an FES. Ideally the flywheel is constantly spinning such that any time the flywheel velocity is increased or decreased, stored energy is transferred to or from the flywheel via the integrated motor/generator.

The amount of energy stored is dependent on the rotating speed of the flywheel and its inertia. Since Kinetic Energy increases proportional to mass and quadratic to velocity, low density and high tensile strength materials are used for high velocity spinning [1]. Low speed FES typically utilizes rotating steel as the flywheel material at a speed below 6,000 rpm. Accordingly, low speed FES has a specific energy of about 5 Watt-hours per kilogram (Wh/kg) of mass in motion. High speed FES typically uses advanced composite materials such as carbon fiber rotating at speeds up to 100,000 rpm. High speed FES has a specific energy of about 100 Wh/kg and utilizes magnetic bearings to improve efficiency by alleviating bearing wear. High speed FES is typically more expensive than low speed FES due to the higher quality materials used for the parts.

Strengths

Flywheel systems are extremely efficient with cycle efficiency approaching 95 %. Any maintenance that is required is fairly easy as FES has a very simple design. Friction can continue to be reduced using magnetic suspension and the use of well-sealed vacuum chambers. Better sealed chambers also reduce wind shear and thus energy loss from less air resistance [1].

Flywheel systems have long lifetimes and high energy densities and have very little environmental impact. Since the charging or discharging rate is limited solely by the motor/generator, energy can be transferred extremely quickly with several charge/discharge cycles able to occur within a few minutes.

Weaknesses

While relatively easy and straightforward, the maintenance requirements are typically very high for FES. Both low and high-speed FES still have fairly low specific energy compared to other storage systems. The costs associated with FES are high compared with batteries utilized for any application longer than 10 minutes. In addition, Flywheel devices can have high self-discharge up to roughly 20 % of stored capacity per hour during standby or when idling [1]. Thus, while the cycle efficiency is high, overall efficiency can be quite low if FES is in standby for any large amount of time.

Opportunities

Better and more advanced materials have lowered production costs significantly and will likely continue to lower the costs associated with building and maintaining flywheels. Research has focused heavily on usage of different materials allowing for increased rotational speeds and power densities, high bearing carrying capacity, flywheel array technology as well as high speed electrical machines in general. One promising area of study in particular is in the utilization of high temperature superconductor bearings that has increased overall bearing performance [1].

Threats

The threats associated with FES technology are mainly regarding the safety and cost of the technology [1]. Increasing the size of flywheels is associated with a decrease in operational safety. Thus, safety concerns are limiting the overall size of FES systems. Vacuum containment vessels are needed for efficient flywheel operation, but these vessels are costly and negatively affect the weight and size of installation.

2.1.2   Electrochemical Energy Storage

Electrochemical Energy Storage methods apply chemical energy conversion methods to store energy. These units utilize chemical reactions to move electrons when discharging. To charge, the chemical reactions are simply reversed. There are two main methods of electrochemical energy storage that will be discussed further in detail: Battery Energy Storage and Flow Batteries.

2.1.2.1 Battery Energy Storage

Battery Energy Storage (BES) technology is one of the most widely used and most diverse technology in the industry. BES stores energy via electrochemical reactions, with a BES unit comprising of electrochemical cells coupled together in either series or parallel to produce a current and desired voltage. While the structure of BES remains the same, there are many different reactions that can be applied to store energy. Currently batteries are used in many different applications including power quality, energy management, ride-through power and in the transportation sector [1, 5].

Types of BES

Table 2-1 details some qualities of six common types of batteries used for BES. Ideal battery candidates have high energy density and specific energy, low self-discharge rates, high cycle efficiency and low cycle response time. As can be observed in Table 2-1, most batteries share many common qualities but all

come with very high capital costs. Lead-Acid batteries are currently the most widely used in industry for BES [1, 5, 10]. The lithium-ion industry has experienced significant growth recently, gaining popularity due to its ideal properties for size sensitive limitations [1]. Li-ion BES has the largest energy density of any other battery type, allowing for extremely portable electronic devices. Sodium-sulfur batteries use inexpensive and non-toxic materials, making them useful for environmental considerations.

Table 2-1: Battery Technology Comparison

Type	Energy Density (Wh/L)	Specific Energy (Wh/kg)	Self-Discharge Rate	Cycle Efficiency	Cycle Response Time	Capital Costs ($/kWh)
Lead-Acid [5, 10]	50-90	25-50	Low	64-90 %	~2,000 sec	50-600
Lithium-Ion [29]	1,500-10,000	75-200	Low	97 %	Few ms	350-700
Sodium-Sulfur [30] [31]	150-300	150-760	Negligible	72-90 %	Few sec	300-500
Nickel-Cadmium [15] [31] [32]	50-150	50-75	Low	70-90 %	Few sec	1,000
Nickel-metal Hydride [32] [33] [34]	170-420	70-100	High (5-20 % per 24 hr)	66-92 %	Few sec	800-1,500
Nickel Chloride [35]	150	94-120	Low	~99 %	Few sec	109-240

Strengths

There is a wide variety of batteries available with varying characteristics that can satisfy most energy storage applications. Batteries have very fast response times (ranging from milliseconds to seconds) and fairly low standby losses with high energy densities and high cycle efficiencies [1]. Despite such a diversity in the technology the construction of BES systems typically doesn't take that long compared to other storage systems, with a newly built BES unit ready to be online in roughly 12 months [5]. Battery installations don't rely on geographical location and can be installed anywhere that is convenient. BES

systems can be used for multiple purposes at once and are easily scalable since they are made up of multiple battery units tied together. In other words, BES systems are very flexible.

Weaknesses

While there are many benefits to battery technology, currently, most battery cells have limited lifetimes, expiring in a relatively small number overall charge/discharge cycles or in a few years [1, 5]. In an effort to improve service life, certain types of batteries are not completely discharged meaning that for some BES units more capacity is required than the design capacity to yield the expected or desired output. Batteries have high maintenance requirements and thus high maintenance costs. While other energy storage systems can be scaled up to large sizes easily, large BES units are not economically nor chemically feasible since they are built off of many individual cells. Most types of BES are very heat sensitive with reduced service lifetimes if the operating temperatures are not close to the design operating temperature. Thus, costly climate control systems are often required.

Opportunities

While most battery technology isn't new to the industry, there has been a large push to improve existing technology such that there will likely be more competition and higher quality batteries in the near future with fewer associated costs [1].

Threats

Most of the battery types used for BES are hard to dispose of or recycle at the end of their service life due to the fact that they contain toxic chemicals [1]. This also means that there could be possible negative ecological effects of using BES. Currently most types of BES are very costly, with large initial investment capital costs, although battery technology has been developing rapidly so the prices will likely drop in the near future.

2.1.2.2 Flow Battery Energy Storage

Flow Battery Energy Storage (FBES) is a relatively new technology that involves an electrochemical reaction between two salt solutions. FBES systems with dissolved electroactive components in the electrolyte are called redox flow battery systems while those that lack these dissolved components in the electrolyte are called hybrid flow battery systems. Similar to BES units, there are a wide variety of salt solutions that can be used, each with varying properties [1], [5]. Despite their differences the power of a FBES system can be determined by the size of the electrodes and the number of cells. Storage capacity is determined by the concentration and the amount of electrolyte present.

Types of FBES

There are currently three main types of flow batteries that are being considered for FBES systems: Vanadium Redox Flow Batteries, Zinc Bromide Flow Battery and Polysulfide Bromine Flow Battery [5]. VBR is currently the most mature FBES available with extremely quick response times of less than 0.1 ms and has a long service life, lasting well over 15,000 cycles. VBR also has high efficiencies, up to 85 % and can be designed to provide constant, continuous power. VBR could be used for enhancing power quality, improving load leveling and power security. The major downsides to VBR include the fact that VBR has low electrolyte stability and solubility which equates to low energy density for the high operating costs.

The Zinc Bromide unit is a hybrid FBES and has relatively high energy density of 30-65 Wh/L [5]. ZnBr units can utilize their full capacity (deep discharging) while still easily able to reverse the process for recharging. These units also have long service lives between 10-20 years. Downsides to ZnBr units include relatively low cycle efficiencies of 65-75 %, material corrosion and dendrite formation. ZnBr units can only operate within a certain temperature range, which is a major drawback for many applications.

The Polysulfide Bromine unit is a redox FBES in which the two electrolyte materials are highly soluble in the aqueous electrolytes [5]. PSB units are typically fairly cost effective with fast response time of around

20 ms. While PSB-FBES systems are undeveloped and require additional research and testing before implementation, they have the potential to be suitable for frequency and voltage control applications. Currently the only major drawback to PSB implementation is the fact that they utilize potentially hazardous materials, with potentially hazardous byproducts.

Strengths

Overall, FBES systems are useful due to their overall high discharge depths, very small self-discharge, high service life, high capacities, and reduced maintenance requirements [5] [1]. One major advantage over most other types of storage is the fact that FBES systems have the capability of decoupling power from its storage capacity. In other words, the storage capacity does not determine the power rating of the system.

Weaknesses

Weaknesses of FBES systems include low efficiencies and energy densities, performance limitations due to physical properties of the reactions, relatively high manufacturing costs and complicated system requirements [1] [5].

Opportunities

FBES systems are still a relatively new technology in industry. More research is being done on improving cost, efficiency, reliability and the power and energy management of large-scale systems [5].

Threats

The main threat for certain types of FBES is the fact that some units utilize hazardous materials, with potentially hazardous byproducts [5].

2.1.3 Electrical Energy Storage

Electrical Energy Storage methods utilize physical properties of classical electrical components to store energy. These units absorb electrical energy directly without the need for energy conversion during

charging or discharging. There are three main methods of electrical energy storage that will be discussed further in detail: Capacitors, Supercapacitors and Superconducting Magnetic Energy Storage Devices.

2.1.3.1 Capacitors and Supercapacitors

Capacitors are widely used in not just the utility industry, but the electric industry in general as they have many applications and can be easily scaled either by combining smaller units in series or parallel or by building larger units. [1] Capacitors are built using two metal foil conductors separated by a thin insulator made up of usually ceramic, glass or plastic. Supercapacitors apply the same theory of two conductor electrodes, but an electrolyte is used with a porous membrane separator instead of a thin insulator. With an applied DC voltage, electrical energy is stored between the two electrodes as an electrical field.

The maximum operating voltage of a capacitor is heavily dependent on the materials used. The majority of capacitors are idea for small energy storage but modern technology with better materials is allowing for the use of supercapacitors with higher power and higher energy storage capacity [1], [5]. Today, capacitors are used for high voltage power correction, smoothing output of power supplies, bridging and energy recovery in mass transit systems, while supercapacitors are used for pulse power, hold-up/bridging power to equipment, solenoid and valve actuation in factories as well as uninterruptable power supply devices.

Strengths

The physical properties of capacitors allow for extremely fast charging and discharging rate (much faster than conventional batteries) with a virtually unlimited life cycle and no required maintenance since there are no moving parts [1]. Capacitors and Supercapacitors have high energy densities and high-power densities. They are safe to use and environmentally friendly.

Weaknesses

While most of the physical properties of capacitors make them ideal for energy storage, there are still properties of capacitors that limit their usage. For instance, in order to use capacitors in most electrical networks, a DC converter is required to apply the DC voltage necessary for energy storage [5]. This not only increases the associated costs, but also lowers the overall efficiency of a supercapacitor unit. Capacitors have high energy dissipation and thus high self-discharge losses, reducing the overall efficiency if they are not being used frequently [1]. Compared to conventional batteries capacitors in general still have lower energy density and limited capacity, although as stated previously newer technology is constantly improving the current physical limitations.

Opportunities

Large-scale capacitors and supercapacitors have the benefit of being very low-weight with very long lifetimes, making them ideal for low-weight applications such as the transportation industry [5] [1]. Capacitors could be combined with applications involving batteries to reduce the cycling-duty on the batteries that have a limited cycling lifetime. Along with improving materials and capacity, research has also focused heavily on utilizing chemical capacitive energy storage which combines both the physical and chemical properties of materials to store energy.

Threats

The main threats associated with utilizing capacitors as energy storage devices are simply the cost: other technologies are more mature and more cost-effective for storing bulk amounts of energy [1]. While research for supercapacitors is promising, they are not yet ready for implementation or mass production.

2.1.3.2 Superconducting Magnetic Energy Storage

Superconducting Magnetic Energy Storage (SMES) utilizes current flowing through a coil to store energy via a magnetic field [1], [5]. SMES systems are composed of a superconducting coil unit, a power supply

unit, a refrigeration unit and a vacuum system. The superconducting coil is cryogenically cooled below its superconducting critical temperature to store energy with very little losses. Since a portion of current passing through a coil is dissipated as heat energy due to the resistance in the wire, SMES systems can be optimized for zero-resistance coils (and thus lossless energy storage) by cooling and physical properties of the material used. SMES systems discharge by means of sending current through an AC power converter. The size of the SMES unit depends on the self-inductance of the coil as well as the amount of current flowing through it.

Superconducting Magnetic Storage can be classified into two groups: Low Temperature Superconducting Coils (LTS) and High Temperature Superconducting Coils (HTS). LTS devices operate at around 5 Kelvin and are more mature than HTS technology with relatively small sized units available for industry applications [1] [5]. HTS devices in theory would be able to operate around 70 Kelvin, but they are not yet ready for mass production or implementation.

Strengths

As with Capacitors, Superconducting Magnets have extremely high efficiency and exceptional dynamic performance since they can store electrical energy directly and are capable of full deep discharge cycles with hardly any degradation [1] [5]. Combined with little maintenance required, most SMES systems can have a lifetime of well over 30 years. SMES systems can have high power densities and are environmentally friendly with no toxic chemicals or byproducts.

Weaknesses

The cooling systems for LTS-SMES systems are very expensive, bringing the already high initial capital investment costs to upwards of $10,000 per kWh with high variable operation costs [5] [1]. SMES systems have high self-discharge rates of 10-15 % over a period of 24 hours, lowering the overall efficiency if they are not in constant use. While there are no toxic chemicals involved in SMES, there is still a large negative immediate environmental impact from the strong magnetic fields involved.

Opportunities

As mentioned above, utilizing HTS-SMES could reduce the overall costs as the need for expensive cooling would be reduced [5] [1]. Additional research is focused on reducing overall costs, creating larger units, developing coil materials that are less sensitive to temperature variations.

Threats

The main threats associated with utilizing SMES devices are the costs and health effects of the surrounding electromagnetic fields [1]. While there is research being done to reduce both either via shielding or higher cryogenic temperatures, these properties will still severely limit SMES from being used expansively in industry.

2.1.4   Thermochemical and Chemical Energy Storage

Thermochemical Energy Storage methods utilize a combination of chemical and thermal properties to store energy. These units harvest energy from a combination of naturally occurring thermodynamic processes with similar artificial processes or reactions taking advantage of thermodynamic principles. There are two main methods of thermochemical energy storage that will be discussed further in detail: Solar Fuels and Solar Hydrogen/Fuel Cells.

2.1.4.1 Solar Fuels

Solar fuels are a relatively new concept growing in popularity in which hydrogen or carbon-based fuels are produced and then harvested for their energy [5]. Solar fuels are created by naturally occurring photosynthesis, artificial photosynthesis or a fusion based variant. In natural or artificial photosynthesis processes, solar energy is absorbed and stored within the chemical bonds of the materials used (usually water and/or carbon dioxide). While natural processes can rely on plant matter to absorb the solar energy, artificial processes must rely on catalysts that are typically hard to find due to limited supply. In a third

approach, thermal processes are used to separate water into its components using high temperatures in a closed environment. Once produced, these fuels can be stored in tanks to eventually be used as fuels for electric generation. Solar Fuels differ from Biomass Power Plants as the fuels used are created or produced specifically for the purpose of energy generation.

Strengths

Solar fuel technology is still in development but is promising since the storage duration of fuels is much longer than that of any other type of energy storage. Solar fuel could be stored for hours to several months at a time before being used with virtually no "self-discharge" (since fuels do not easily dissipate out of storage tanks) [5]. Due to the chemical properties of combustible fuels, the power rating of solar fuels could exceed 20 MW, with high specific energy densities ranging from 800 to 100,000 Wh/kg, much higher than most other types of energy storage currently available.

Weaknesses

Solar fuel technology is heavily dependent on large amounts of sunlight, so large areas would be required to concentrate solar energy [5]. As mentioned earlier, water-splitting catalysts used in artificial photosynthesis processes are very scarce elements, making them very expensive.

Opportunities

Research is focused heavily on increasing the photosynthesis efficiency and creating solar collectors, as well as utilizing cheaper more available catalysts to drive the costs for solar fuels down [5].

2.1.4.2 Hydrogen Energy Storage and Fuel Cells

Hydrogen Energy Storage (HES) differs from the previously mentioned storage devices in that it is the only major storage type that is not considered a renewable source of energy [1], [5]. HES is less of a storage system and more of two processes combined to yield similar effects of storage. In HES systems, a source of energy is developed by utilizing previously stored energy from other methods. In other words,

hydrogen is produced and placed into storage containers for later consumption to generate electricity. A common hydrogen production method is utilizing water electrolysis units.

Currently fuel cell technology is the most popular method of harvesting power from stored hydrogen [5] [1]. Fuel cells work by converting the energy stored in the chemical bonds of hydrogen and oxygen into water and power, with the output power being used to drive a generator shaft, creating electricity. Fuel cells are characterized depending on the fuel and electrolyte used.

Strengths

Fuel cells generate electricity much quieter and more efficiently than conventional methods like fossil fuel combustion [1] [5]. The only emission of fuel cells is water which is non-polluting and not harmful to the environment. Hydrogen is an idea fuel source as it is the most abundant element in the universe and has high mass energy density. As long as hydrogen can be created easily and cheaply, fuel cells can continuously generate electricity as needed. Fuel cells are also very easy to scale in size and could range from a few kWs to a few hundred MWs.

Weaknesses

While fuel cells are cheaper and more efficient than combustion, they are still less efficient than other energy storage methods and have a comparably high energy consumption with relatively low volumetric energy density [5] [1]. The volumetric energy density can be improved, but the additional storage techniques are energy intensive. Most of the electrode or catalysis metals used are toxic, reducing the ability for recycling old fuel cells. Additionally, while it may be easy to convert the hydrogen into energy, it is much more difficult to reverse the process; converting energy back to hydrogen to complete the cyclic process is expensive.

Opportunities

The combination of fuel cells with the production and storage of hydrogen could offer stationary, distributed or even transportation power [5] [1]. HES alongside fuel cells create a very flexible storage method since the capacity is independent of energy production, storage and consumption.

Threats

The main threats to the combination of utilizing hydrogen and fuel cells as an energy storage technique is simply the high costs low efficiency of the technology, and safety concerns [1]. There has been little push for additional research into further development since other more effective technologies are more readily available. It would be much easier to utilize renewable energy generation and other storage methods than to harvest hydrogen as an energy source.

2.1.5   Thermal Energy Storage

Thermal Energy Storage (TES) methods encompass many different technologies that utilize direct thermodynamic properties to store heat energy [5], [15]. Most thermal storage methods consist of a storage medium in a tank or reservoir, a packaged chiller or refrigeration system, pumps and controls, and insulated piping to transfer the medium throughout the system. TES system operators maintain the temperature of the thermal tank above or below that of ambient temperature.

Thermal storage methods are fundamentally different than previously mentioned energy storage methods since they do not convert or store electric energy but only utilize thermal energy [5]. This allows them to be flexible in nature such that they could be developed for Heating, Ventilation and Air Conditioning (HVAC) purposes as well [15]. TES units can act as heat pumps, transferring thermal energy from one location to another. For instance, during low cooling demand the unit could be removing heat and chilling the storage medium. During periods of high cooling demand, the unit would work in reverse and release

the stored cooling medium to absorb heat, meeting air-conditioning loads. Other applications include load shifting and electric generation for heat engine cycles.

The benefits of TES include being able to store large amounts of energy with very few safety hazards or concerns, small self-discharge (less than 1 % per 24 hours) due to the adiabatic properties of the system, decent energy density and specific energy (80-500 Wh/L and 80-250 Wh/kg respectively) and all while having very low capital investment costs (between $3-60/kWh) [15] [5]. Regardless, TES has low cycle efficiency (between 30-60 %), making it currently not ideal for supporting the electric system. Research is being done to focus on optimizing TES systems for peak load reduction and load shifting, but those applications are still limited. There are two groups of Thermal Storage that will be discussed further: Low-Temperature TES and High-Temperature TES.

2.1.5.1 Low-Temperature Thermal Energy Storage

There are two Low-Temperature TES methods currently in development: aquiferous and cryogenic energy storage. Aquiferous Low-Temp TES utilizes water as a thermal storage medium. Water is already abundantly used as a heat energy storage medium in many industries due to its favorable thermal properties, making aquiferous systems the most promising for peak load shaving as well as industrial cooling. Cryogenic Low-Temp TES utilizes nitrogen or air in liquid cryogen form to transfer heat in a similar fashion [5]. Liquid Air Energy Storage, a form of cryogenic thermal storage is becoming more popular since liquid air has a high expansion ratio from the liquid state to the gaseous state, as well as having a higher power density than gaseous air. Cryogenic thermal storage is expected to be used for future power management as LAES and other types could operate similar to CAES systems [15].

2.1.5.2 High-Temperature Thermal Energy Storage

There are three High-Temperature TES methods currently in development: latent fusion heat, sensible heat and concrete thermal storage. Latent fusion heat storage involves using Phase Change Materials (PCMs) as the thermal storage media, holding them at a constant temperature for PCMs to absorb energy as they change from liquid to solid phases [15] [5]. The properties of latent heat storage allow for high storage density will a small reservoir. Thus, latent heat storage is ideal for managing heating and cooling loads for large buildings. Sensible heat storage works in a similar fashion to latent fusion with the exception that heat energy is transferred to a storage medium holding that medium in a single phase. Concrete thermal storage uses synthetic oil to transfer heat energy to concrete or ceramics.

2.1.6 Hybrid Electrical Energy Storage

Another method of energy storage that should be considered is the concept of Hybrid Electrical Energy Storage, or integrating at least two of the technologies as described above into a single system or application [5]. This concept could prove to be useful since there are both advantages and disadvantages to each method. Placing two methods together could optimize overall system performance by providing less drawbacks or compromises. For example, combining supercapacitor techniques with batteries could create a system with improved storage capacity, fast charging and discharging rates and long service life due to the split cycle usage of each technology. Another example could be the combination of a liquid hydrogen refrigeration-based SMES system within a fuel cell system that could be used for back-up power generation for renewable generation applications. Regardless of the type of energy storage, there are many method combinations that could work for many different applications. Certain storage methods should not be ruled out for a particular combination simply due to their individual drawbacks, when utilizing an additional method could compensate for the original method's drawbacks.

2.2 Electrical Energy Storage Applications

There are many scenarios within an electrical network in which utilizing EES could be beneficial. In fact, some types of EES are already commonly in use in industry. Other types of EES have potential to be used for various applications with specific requirements. With each type of EES having differed operational properties with various strengths and weaknesses, it might be difficult to decide which storage method best meets the necessary criteria for operation. In some cases, a combination of technologies might work best while in other applications, a single method might suffice. Regardless, the majority of EES applications focus on improving efficiency of networks on the transmission and distribution level and improving the output of variable renewable energy generation, with a few growing applications in the transportation and smart grid sectors [18].

2.2.1 Transmission and Distribution Applications

An ideal electrical network is constantly running at steady state with smooth transitions from one state to the next as loads fluctuate. Of course, an ideal network is not feasible, and there will always be disturbances that affect the operation and efficiency of an electrical transfer network. For instance, the voltage of a heavily loaded line will sag below its optimum voltage requiring additional stabilization devices or techniques to rebalance the line voltage. During high voltage switching or a thunderstorm power surges could negatively affect the network as well with the potential to damage other network components if protection devices do not respond properly. Alternatively, a network might be loaded normally with balanced lines yet due to the nature of complex networks there might simply be small disturbances or flickers that escalate to create additional problems. While there are many solutions already in use in electrical transmission and distribution networks to combat these non-ideal situations, EES could be used as additional support devices, aiding in the stability of an unbalanced network [1].

37

One major area of application in which storage could be useful (and already is useful in many networks [15]) is in the stabilization of both electrical transmission and distribution. With so many synchronous components and variables in constant flux, ESS methods could be implemented to help smooth out any changes in the power network. Storage could help maintain power quality, reduce line congestion under heavy loads or simply smooth out small disturbances to ensure that the network is operating under normal conditions [5]. For these applications near instant response time and relatively large power capabilities would be required. FES and PHS are good examples of storage methods already in place for these issues. While FES has small power capacities, it does have near instant response times, making it ideal for correcting small disturbances or maintaining good power quality. On the other hand, PHS has much slower response times (although still faster than conventional generators), but can have large power capacities, making it ideal for smoothing out loads and reducing line congestions over a longer period.

Another major area of application is the necessity for voltage regulation and control [36]. Constant load and generation changes yields changes in active and reactive power loads, influencing the voltage magnitude and angle profiles in networks. Some amount of variation is expected, and most operation parameters allow for small changes in voltage. However, controlling of dynamic voltage performance could be improved with EES utilization.

One method of implementation which is typically mentioned less often is the potential for Black-Start Capability [1], [5]. Most large-scale generators are not able to come online when starting from a total network black-out. Usually smaller black-start engines distributed near or at critical power plant sites are utilized to bring plants back to full capacity during a black-out, starting the process of bringing the larger network out of black-out status. EES with relatively large power capabilities could be extremely useful for black-start applications as they would already have energy stored ready to be used either to bring plants back online or simply provide power to critical load centers.

2.2.2   Renewable Energy Applications

Despite the many benefits renewable generation has over conventional generation plants there are still problems that they bring to electric networks. The power outputs of solar and wind plants, the two most common REG methods are hard to control regardless of the expertise and planning executed by operational engineers. Wind Turbines rely on wind volume which can be intermittent based on weather patterns [18], and solar panels rely on solar irradiance, thus only generating power proportional to the amount of sunlight available. The output of both methods depends heavily on location, surrounding area and seasonal weather patterns. Often wind and solar farms are placed in locations with optimum weather and/or solar conditions for maximum utilization. While this increases the overall actual power output, these locations tend to be more remote and farther from actual load centers such as cities and towns. Thus, the likelihood of congestion on transmission lines connecting generation farms to the rest of the network is greatly increased and a common occurrence, adding to overall network instability.

Many of these problems however could be solved with the integration of EES. As mentioned previously, EES systems already have excellent properties that allow for good voltage, power and congestion correction leading to better system stability. Most types of EES could aid in the reduction of congestion of transmission lines with REG. EES could be used to smooth out the output of REG farms, allowing for better control and management of the generation output.

The value of EES will increase greatly as the amount of REG installed on electric networks increase [37]. More installation of REG will likely create larger generation variance profiles that will need to be smoothed out in order to maintain the balance of load demand and supply and thus, maintain network stability. Most storage types have the unique property of fast-response, scheduled charging and discharging, allowing for quick absorption of supply during times of high REG output and/or low load, as well as quick generation dispatch during times of low REG output and/or high demand. Additionally, almost all the storage types have response times in minutes or less, making them very flexible for large variations in REG output typically occurring within a scale of minutes to hours.

39

On the other hand, improving weather forecasting accuracy, better generation scheduling and improving line connectivity and capacity may reduce the value and usefulness of EES for REG applications. Better weather forecasting would mean that engineers could better predict the amount of REG output and thus rescheduled conventional generation to fill gaps created by the REG output expected [38]. Improving line connectivity would allow better overall power flow, meaning that ideally any abnormal generation conditions from REG output could be absorbed by or compensated for somewhere else on the surrounding networks, even if not in the original network. Adding line capacity would help with any congestion issues, especially during high REG outputs. Despite these factors, EES will likely still play a key role in future power networks with REG as there is still a large potential for EES to reduce overall costs by improving overall network efficiency [5] [39].

2.2.3 Transportation and Smart Grid Applications

In many ways, the transportation and smart grid sectors are already utilizing certain types of EES, and their utilization is only expected to increase in the future [40]. Batteries and BES are becoming more prevalent in mass transit and personal transit as hybrid and electric vehicles grow in popularity [36]. Due to lightweight, small dimension, high energy density and fast response properties [5], lithium-ion BES units are being adopted for use in electric or hybrid electric vehicles to replace the need for utilizing gasoline as a transportation fuel source [15]. On mass transit systems, BES units are being utilized for electric light-rail train systems, storing any recovered energy from braking to be used for reacceleration after stopping at a station [41].

In the smart grid sector BES units are being developed as small distributed units among residential or commercial customers to be used for individual load-levelling [36], [37]. Smart BES units can be controlled by the local utility or via automatic software to optimize the load profile within a community. The smart units could be used to discharge energy during high or peak demand periods, benefitting both the customer and local utility by reducing the overall electric load during peak demand, and recharge during low demand periods. In addition, industrial and commercial customers typically require high

reliability and availability of electric supply [15]. Thus, BES units would provide additional power security for these customers, discharging energy during power outages. Overall the smart grid realization is still far from complete, but some utilities are beginning to deploy smart grid technology (including EES), creating a far more flexible and interactive electric network while improving both stability and reliability [39].

2.3   *Challenges of Electrical Energy Storage Implementation*

There are many benefits to the application and realization of EES, but the technology is still not perfect, and there are still various challenges associated with EES deployment and installation. Electrical networks are so complex that even with plenty of research and industry knowledge on storage systems it is still challenging to determine which methods of EES should be applied for which scenarios. Many storage methods still have relatively high costs associated with them, making largescale deployment uneconomical. Additionally, while direct costs of EES methods can be determined, there is little resources regarding how to quantify the actual technical or economic value that deployed EES units would provide. There are still many scenarios in which utilizing other technologies would be more beneficial, reducing the usefulness of storage [5] [18].

For example, [18] looked at varying the levels of generation flexibility, interconnection and demand flexibility to determine which technologies in the electric industry compete with storage, and which would be complementary. In general, any competing options that exist in the industry would reduce market share of storage and reduce the operation cost savings of utilizing storage, as other alternatives could be utilized instead. In many scenarios, the application of controlling demand directly via smart grid implementation, known as flexible demand side response was the most direct alternative to storage, with the potential to reduce the market size for storage in 2030 by more than 50 %. In cases with high

41

interconnection, reduced operation cost savings of storage were observed, but those savings were partly compensated as storage might be less expensive than adding interconnectivity to a network.

In addition, [18] found that due to typical network demand profiles, any storage with capacity in excess of six hours yielded little additional value, but fast response storage options also have a limited market value. The substantial cost savings of storage come from the options that both replace or reduce the need for conventional generation, and allow the system to absorb additional renewable generation. Thus, flexible generation with fast frequency regulations services could also compete with the storage market.

In [6], utilizing storage without renewables negatively affected the value of storage. Storage operation would still be controlled based on the prices of electricity by charging when demand is low and discharging when demand is high, but the energy being absorbed would be coming from non-renewable sources, thus increasing the CO_2 emissions released into the environment, not reducing them. Many regions still utilize conventional coal or oil plants for base load (instead of nuclear) with natural gas plants used during peak demand. Because of this, the value of storage may be heavily dependent on the location of storage placement. In other words, placing storage close to renewable generation may greatly increase the overall value of its usage as there will be increased renewable power utilization, and decreased emissions, while the opposite would be true for placing storage closer to conventional fossil fuel plants.

2.4   Case Studies

Many network utilities and operators in the United States and around the world are starting to take advantage of bulk EES technologies. Methods such as PHS or CAES are being built and installed for a broad range of grid applications. On the other hand, some utilities have already benefited from the operation of bulk storage, having previously invested in such projects.

According to [14], there are numerous storage projects in the US alone, many of which that have been in operation for years. The Bath County Pumped Storage Station in Bath County Virginia is one operation

that has been in use since 1985. As of 2013 it was still the largest pumped hydro project in the world, with a capacity of 3,003 MW and cycle efficiency of 78 %. Another large, utility-scale project already in operation is the McIntosh CAES Facility located in the small town of McIntosh Alabama. It was installed in 1991 and was the first CAES unit of its kind in the United States. Similarly, the Golden Valley Electric Association in Fairbanks Alaska installed a 27 MW BES system in 2003 utilizing NiCd batteries, the only project to do so in the US. These projects and others like them support their surrounding electric system in many ways, providing many benefits with few drawbacks, but most of the older projects were installed independent of any existing REG.

Only within the past decade or so have utilities begun to pair existing or new REG with EES units. The EESI report listed three projects that were installed with the purpose of aiding in the operation of REG, and all three were installed after 2010. Looking at the United States Department of Energy Global Energy Storage Database [42], there are over 711 ESS planned or installed projects in the US as of April of 2017. Of those, only a single project relating to REG applications was commissioned before 2009 out of the nearly 233 planned or installed EES-REG projects in the US.

One interesting large-scale development installed after 2009 is the Notres Battery Storage facility in Ector County Texas [42]. Commissioned in 2012, it is currently the world's largest BES system specifically used for wind energy. The 36 MW lead-acid BES supports a large 153 MW wind farm and can provide power for up to 40 minutes during periods of low or non-existent wind. However, the Winkler project was not cheap, costing roughly $44 million to build the BES system alone (or roughly $1.2 million per MW of built storage capacity).

Another similar project is the AES Laurel Mountain Wind Farm in Laurel Mountain, West Virginia [43]. The project consisted of building a 98 MW wind farm with a 32 MW Li-Ion BES unit. The facility was completed in late 2011 and has been in operation ever since. The project can provide its rated power for 15 hours and dispatches energy to the transmission network on demand. As with the project in Texas, the

Laurel facility was expensive, with a capital cost of $29 million to build the BES (roughly $900,000 per MW of built storage capacity).

In addition to the above two cases there are only three other similarly sized, operational projects in the US that paired ESS with wind energy, but many more planned for commissioning and construction [42]. When looking at projects that involved solar (specifically photovoltaic) energy, only one large-scale operational project appeared in the US database. Known as the Imperial Irrigation District BESS in El Centro, California, the ESS unit provides 30 MW of li-ion storage capacity in conjunction with about 50 MW of solar generation. The BESS unit became operational in October of 2016 and can provide rated power for about 40 minutes. The project costs totaled $68 million ($2.1 million per MW). As with the ESS wind energy projects, many more ESS solar energy projects are planned or commissioned for construction, and more are expected as the technology develops.

Overall, while there appears to be many storage projects in the US, most of them are quite small and provide only small contributions to the surrounding transmission or distribution networks. The majority of any large-scale projects already existing are not heavily involved with aiding in the penetration of renewable energy. Almost every project that does involve REG applications was installed within the last ten years, and a large portion of the planned or commissioned ESS projects will likely involve REG as well. Regardless, ESS is not cheap, and large capital investments are required for construction, especially for BESS. Thus, it would be difficult to see the economic effects of BESS paired with REG on a small timeframe since the capital costs are so high. Other bulk EES technologies are certainly a bit cheaper than BESS, but it is hard to evaluate the overall value of ESS by just comparison or observation alone.

3. Methodology

This thesis aimed to determine the value ESS adds to an electrical network with renewable energy by observing how storage affects the economics of an isolated network. Specifically, the focus was to determine the economic importance of size of injected storage as well as the injection location within the system. In order to do this, it was first necessary to determine a simulation software that could be used to build and test economics of a network as well as determine a software power flow testing technique in which to use that would best simulate the dispatch of generation in a typical real-world power network.

3.1   Determination of Software for Optimal Power Flow Studies

There are many programs available that can be used to simulate an electric transmission or distribution network, but most are extremely expensive and require the purchase of software licenses in bulk. For instance, two popular programs that were considered were PSSE and Powerworld Simulator. Initially the full versions of either were unavailable due to the associated costs, but both programs had demo options that allowed full functionality for a limited network with a limited number of busses. PSSE allowed full functionality for any sized network up to 30 busses, and Powerworld allowed most functionality for any network up to 13 buses. Despite the smaller network limit Powerworld Simulator was chosen over PSSE as it had more options for economic optimization within power flow studies.

Today the majority of grid operators utilize some form of economic dispatch to determine how much power will be produced from which generators at what time of the day. The Optimal Power Flow approach is one method that is widely used to determine the economic dispatch in a network subject to any power flow constraints or operational limits. With the OPF method, everything from generator minimum and maximum power output limits to transformer or transmission line power capacity limits to capacitor or reactor bank limits can be modeled as constraints on the system. OPF programs use the

constraints along with generator cost models to calculate the optimal settings of various system parameters to create the most economical scenario. This type of programming has become extremely useful in the modern operation and planning of power systems as the OPF method is very flexible, able to solve a large number of complex network power flow problems with reasonable computing power and accuracy.

An OPF optimization study is initially defined by minimizing an objective function **f(x, u)**, subject to equality constraints, **g**, and system constraints, **h**, where **u** is a vector of independent variables and **x** is a vector of dependent variables. As mentioned previously, almost any system constraints can be defined and ordered in this way, allowing for flexible problem solving. Once all system constraints are defined, the algorithm can minimize the objective function determining the best settings for each variable given all constraints.

For all purposes of this project the OPF program method was utilized in Powerworld Simulator to solve for the generation dispatch in each network model built. The Powerworld OPF allowed for determination of the economic dispatch within a system, as well as the recording of overall system cost. This would allow for a cost comparison between various scenarios involving the addition of EES to a given constrained system.

3.2   *Building a Test Bed (WSCC 9-bus Network)*

After choosing the simulation and power flow software, the next step was to determine a base test bed system that could be modified to include REG. While a test system could have been created from nothing, there are many resources available from national organizations that already contained frameworks for strong test systems. Within the North American Electric Reliability Corporation [44] there are eight regional entities that aim to improve the reliability of the respective eight regional systems as well as the reliability of the North American system as a whole. NERC and each regional entity have extensive

databases consisting of operational guidelines, procedures, and regulations. The Institute of Electrical and Electronics Engineers has an additional vast array of information including reports and academic studies on power system operation, theory as well as test systems. In order to pick a strong model, ideal test bed system properties needed to be defined.,

A good base model for analyzing the economics of adding storage to a system should have properties that allow it to be easily manipulated. This would make it fairly easy to determine the trends regarding power flows and the variables affecting system cost. One regulating entity under NERC [45], the Western Electric Coordinating Council (formally known as Western System Coordinating Council) endorsed a flexible 9-bus test system for considering system reliability at a smaller scale [46], [47]. IEEE also had a 9-bus test system that was almost identical with a few modifications [48]. The 9-bus model was considered to be a good candidate with a fairly balanced system consisting of three generators and three loads, each connected with the same number of lines in a ring-like network. In addition, since the system was under 13 buses, it could be created in Powerworld Simulator without the need for simplification or bus reduction. With strong specifications, the WECC 9-bus test system was chosen as the bed model. Additional specifications of the WECC 9-bus model can be found in Appendix A.
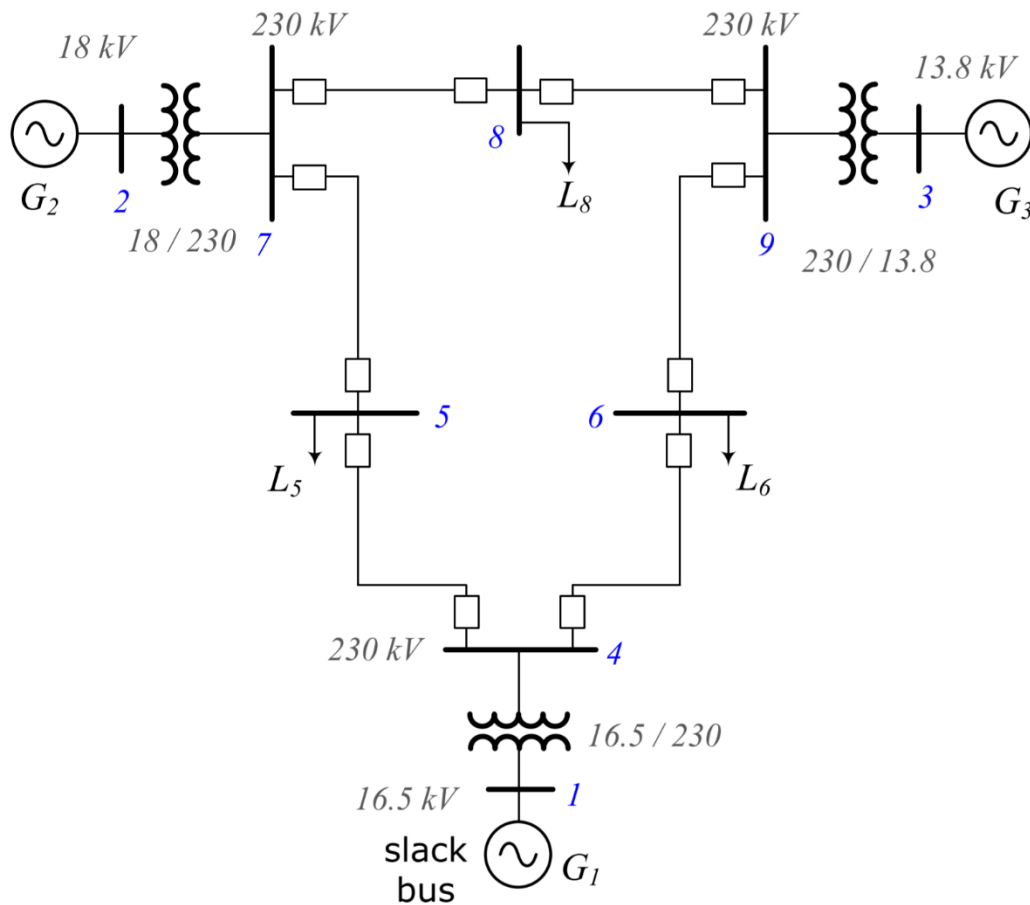
Figure 3-1: WSCC 9-bus Test System

After determination of the test bed, the next step was to build it into Powerworld and modify it such that it could contain REG. Using the Powerworld One-line builder, the original generator and load specifications were inputted and embedded into the provided buses. Transmission lines with the provided parameters were inputted and connected to the necessary buses as defined in the base model.

3.2.1 Load Modelling

A typical day in the fall with a well-defined duck curve and atypical day in the summer with a well-defined traditional sine wave curve were chosen to observe the effects different load profiles have on the network, providing more realistic load and REG modelling. In order to successfully simulate the two

separate days, it was necessary to create two separate models, each with almost identical properties, apart from the load profiles. For all purposes of this study October 15, 2016 was chosen as the fall day and July 15, 2016 was chosen as the summer day.

Actual hourly load data for both days was gathered from [49]. The 24 model load profiles were created using the following scaling calculation:

$$S(t) = \frac{L_M}{L_{A,Max}} L_A(t) \tag{3-1}$$

Where S is the scaled load for t hour of the day, L_M is the given load from the model, $L_{A,\,Max}$ is the maximum load from the ISONE data [49] over the 24-hour period, and L_A is the actual occurring load for t hour of the day from the ISONE data. Thus, the scaling factor for any given hourly load was the load of the model divided by the maximum occurring load from the ISONE data. Each hour of load from ISONE was scaled down in this way to maintain accurate proportions of the loads in the model. The scaled load calculation data can be found in Appendix B.

The scaled loads were then entered into the Time Step Simulation program within Powerworld. The TSS program in Powerworld is a powerful tool that can be used to complete power flow studies with the ability to manually control certain variables across units of time. The TSS program completes power flow studies and records data for each time unit determined. For all purposes, the TSS program was utilized to create and control 24 hours of data for each test system. The TSS provided for independent control over each hour, creating separate OPF solutions for each hour simulated.

3.2.2   Generator Cost Models

In addition to determining accurate load models, it was necessary to determine the generator cost models. Since the majority of electric generation capacity in New England is power by natural gas [50], it was assumed that the two larger generators in the 9-bus model would be powered by Natural Gas, leaving the

49

third, smaller generator for the REG. Generator cost data was retrieved from [51]. The report summarized various cost variables associated with installing or operating a variety of different electric generators, including various natural gas plants. To simplify cost calculations and representation it was assumed that any of the cost data collected from the EIA report [51] was proportional to the total size of the generator. For the purposes of this study it was assumed that both gas turbines in the model would be Conventional Combined Cycle Turbines.

There are seven total parameters that control the Powerworld cubic cost model for each generator: The Unit Fuel Cost, Variable Operation and Maintenance Cost, Fuel Cost Independent Value, Fuel Cost Dependent Value, and Cubic Cost Values B, C, and D parameters. The UFC, VOM, FCIV and Cubic Cost Value B needed to be derived as they would be utilized in the cost model. The FCDV and the Cubic Cost Values C and D however would not be used in the model and thus could be set to zero. The UFC was derived by taking the wholesale price of natural gas on the respective fall and summer days [52]. The wholesale price of bulk natural gas was approximately 2.756 $/MMBTU and 3.285 $/MMBTU for July 15, 2016 and October 15, 2016 respectively. Since there was no fuel for REG, the UFC cost was 0.000 $/MMBTU. The VOM was taken from the [51] as the Variable O&M cost in $/MWh. The Cubic Cost Value B was taken as the Heat Rate in BTU/kWh from the [51]. The FCIV was derived using the following equation:

$$FCIV = \frac{XY}{Z} \tag{3-2}$$

Where X was taken as the total generator size in MW, Y was the Overnight Fixed Cost Value in $/kW from [51] converted to $/MW, and Z was the plant capacity factor in hrs/yr. Since the price data from [51] was in 2013 dollars, the values provided in Powerworld were adjusted to 2016 dollars given a cumulative 3.6 % inflation rate from 2013 to 2016 [53].

The Overnight Fixed Cost from [51] represented the total amount per kW that would've been spent on the plant if it were built in one night. To better represent how fixed capital costs are considered when building

a power plant, it was assumed that any fixed capital costs were spread over the course of 6.25 years, equal to a 16 % annualized adjustment. Because of this, Y was altered before being included in the FCIV calculation to take into account the annualized adjustment.

However, since the models were to be run over the course of a single day and not an entire year, the FCIV needed to be adjusted further such that the cost model only considered the fixed capital costs of a single day out of the 6.25 years. Thus, Y was further adjusted to equal approximately 0.044 % of the total overnight fixed capital cost value from [51].

The plant capacity factor represents the total hours in a year of which that the generator is running. In all cases, it was assumed that the capacity factors would always be equivalent to 8760 hr/yr (or a capacity ratio of 1). This was assumed for two reasons: first, the simulations were only across a 24-hour period so it would make sense that the generators in the model were running constantly throughout that period. Second the TSS OPF program automatically controls the generator dispatch such that there is no need to assume that the generator isn't running for the entire duration of the 24-hour period as the program would determine that if it deemed it uneconomical for any reason.

Thus, with all variables accounted for, a summary of the cost models for each generator can be observed in Appendix C.

3.2.3 Renewable Generation Modelling

The final step to completing the test network was to create and build the renewable generation into the models. As mentioned previously, the two larger generators of the two base systems (fall and summer) were already assumed to be natural gas generators, leaving the third, smaller generator of each to be replaced by REG. To evaluate the performance of the two most common forms of REG, two additional models were developed for each day, one model containing solar generation, and one model containing wind generation. Thus, there were four total base models for the 9-bus test system, characterized by load

51

profile and type of REG: a fall load profile with solar generation, a fall load profile with wind generation, a summer load profile with solar generation and a summer load profile with wind generation.

In order to create the solar generators, it was first necessary to gather locational solar irradiance data for the fall and summer days to create 24-hour solar generation profiles. It was assumed that that the solar generation farm would be located at the site of the Worcester Regional Airport in Worcester, MA. While occupied by an airport, this area is extremely flat with high elevation within the city of Worcester, meaning no tall objects or hills nearby casting any major shadows. Under normal circumstances this would be an ideal location for a solar farm in Worcester.

In addition, it was assumed that the only variables affecting the solar irradiance at the determined location were the seasonal angles of the sun. In other words, it was assumed that there would be no major cloud cover or weather events other than sunshine affecting the region during the two days. This was considered while picking the days, and further verified by observing the historical weather data. The solar farm was assumed to be all fixed axis panels, facing due south to maximize sun exposure. All panels were assumed to be fixed at a tilt angle equal to that of the Latitude of Worcester (42.26 degrees) to maximize yearly sun exposure. It was also necessary to assume that any solar insolation hitting the panels was proportional to the total energy produced by the panels. The actual relationship may differ depending on the type of panels used, material, manufacturer, placement etc.

With these assumptions, 24-hour solar generation profiles could be created given historical solar data for the two days chosen [54]. There are many calculations and angle data required to estimate the hourly solar insolation at the location chosen. The process was taken from [55], and it can be found along with calculations, equations and resulting angle data in Appendix D. Utilizing the calculated solar insolation data, the solar generation profiles were derived using the following equation:

$$\textbf{\textit{Scaled Energy Produced}} \ [\textbf{\textit{MW}}] = \textbf{\textit{IC}}(\textbf{\textit{t}}) \frac{S_G}{IC_{MAX}} \tag{3-3}$$

Where IC was the total solar insolation at hour t, S_G was the total size of the renewable generator in the model and IC_{max} was the maximum total solar insolation out of the 24-hour period. Thus, the generation was scaled such that the maximum generation (and thus the total size of the generator) occurred at the time of maximum solar insolation, with the remaining hours of generation scaled proportionally. The resulting solar generation profiles created can be observed below in Figures 3-2 and 3-3. The solar generators were then built into the Powerworld one-line, the cost models created and inputted as defined previously, and the generation profiles defined in the TSS specifications such that the generation was fixed and not controllable by the OPF.
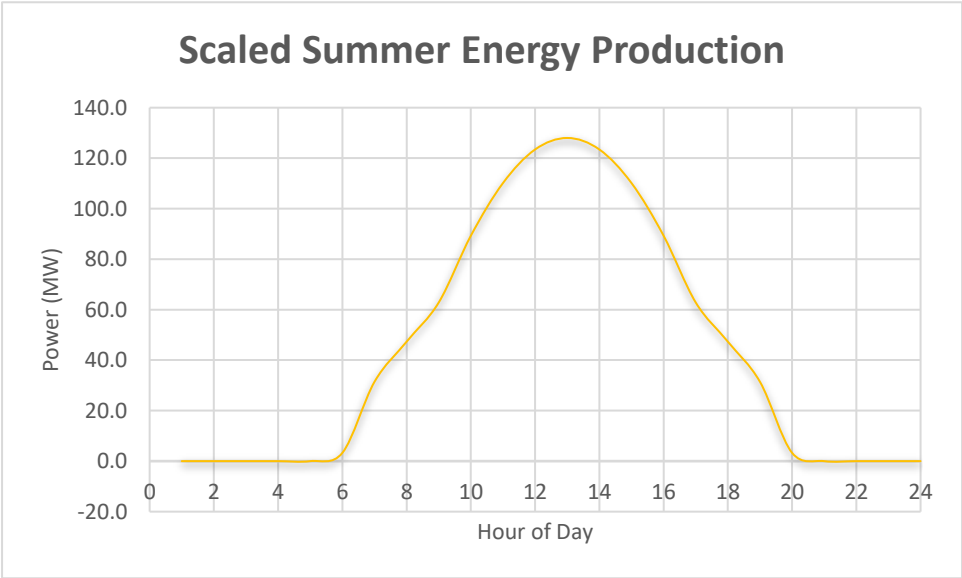
Figure 3-2: 9-bus Solar Generation Profile: Summer
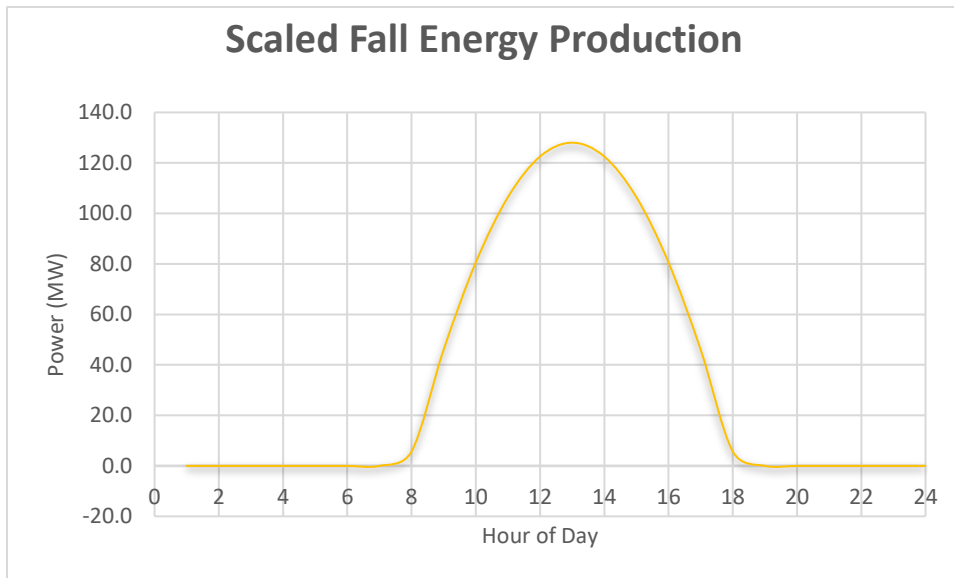
Figure 3-3: 9-bus Solar Generation Profile: Fall

The creation of the wind generators was like that of the solar generators, with a few key differences in creating the generation profiles. To create the wind generators, it was first necessary to gather locational wind volume data for the fall and summer days [54]. Again, it was assumed that that the wind generation farm would be located at the site of the Worcester Regional Airport in Worcester, MA. While occupied by an airport, this area is extremely flat with high elevation within the city of Worcester, meaning no tall objects or hills nearby, allowing for consistent, unobstructed wind patterns. Under normal circumstances this would also be an ideal location for a wind farm in Worcester.

Again, it was also assumed that there would be no major weather events such that only average wind velocities were present during the two days. The wind turbines were assumed to be able to rotate freely such that the wind direction would not influence the power generated. It was also necessary to assume that the wind velocity spinning the turbines was proportional to the total energy produced. The actual relationship may differ depending on the type of turbines installed, material, manufacturer, placement etc. However, this made calculations much more straightforward since historical wind velocity data is already available.

With these assumptions, 24-hour wind generation profiles could be created given historical weather data for the two days chosen [54]. Utilizing the historical wind velocity data, the wind generation profiles were derived using the following equation:

$$\textit{Scaled Energy Produced } [MW] = V(t)\frac{S_G}{V_{MAX}} \qquad\qquad (3\text{-}4)$$

Where V was the wind velocity at hour t, S_G was the total size of the renewable generator in the model and V_{max} was the maximum velocity out of the 24-hour period. Thus, the generation was scaled such that the maximum generation (and thus the total size of the generator) occurred at the time of maximum wind velocity, with the remaining hours of generation scaled proportionally. The resulting wind generation profiles created can be observed below in Figures 3-4 and 3-5. The wind generators were then built into the Powerworld one-line, the cost models created and inputted as defined previously, and the generation profiles defined in the TSS specifications such that the generation was fixed and not controllable by the OPF.
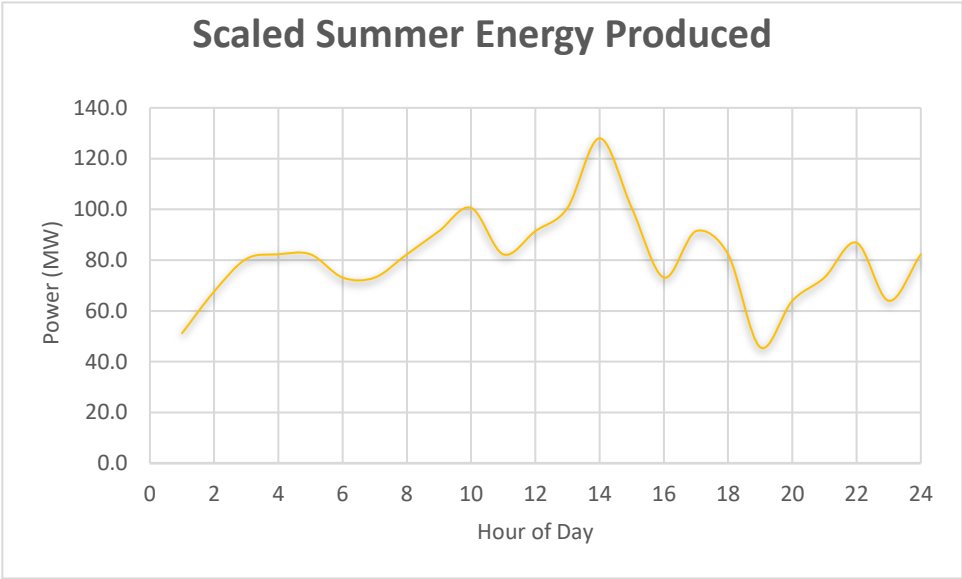
Figure 3-4: 9-bus Wind Generation Profile: Summer
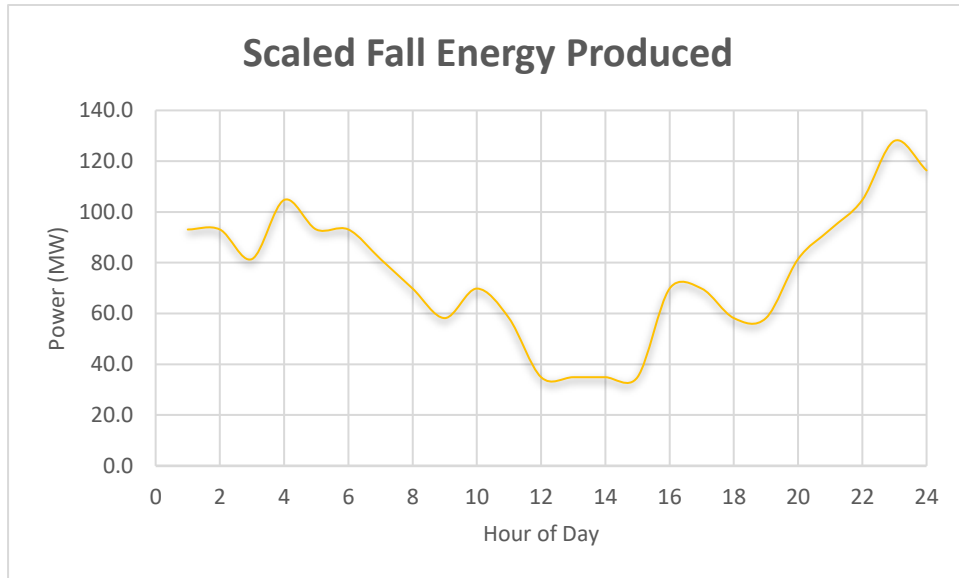
Figure 3-5: 9-bus Wind Generation Profile: Fall

3.3   Building Energy Storage into the 9-bus Models

With all four 9-bus base models completed, the next phase of the project involved building the energy storage into the models such that the overall system economics could be observed. Building the energy storage required picking an actual energy storage method, determining a cost model, and determining a state of charge for each hour of operation.

As discussed in section 2.1, there are many types of energy storage, but many are still relatively expensive and not very mature in the electric power industry. While there are many stages to technological development, the properties of under-developed technology are often just uneconomical and impractical for daily operation. Thus, a good storage technology for testing would be one that is already heavily developed and utilized in the electric industry. This leaves Pumped Hydro Storage as a very clear choice; PHS is by far the most developed and most common storage type in industry to date, even when considering the new or planned installments.

Many of the newer case studies regarding REG applications involved Battery Energy Storage (mainly li-ion or lead-acid). While BES costs are expected to decrease significantly within the next decade or so, batteries are still for the most part much more expensive per MW of capacity than PHS [1], [5], [15], [29], [42]. Because of this, BES was not included in the scope of this study.

The next step in building energy storage into the 9-bus model for testing was to determine the fixed and variable costs to input into the Powerworld cost model. In 2013, the Pacific Northwest National Laboratory published [56] that heavily assessed the energy storage industry. The associated costs of PHS were taken from the second volume of [56]. Since the cost data retrieved was in 2011 dollars, it was adjusted to 2016 dollars given a cumulative 7.5 % rate of inflation from 2011 to 2016 [53].

As with the previous generator cost models in Powerworld, The Unit Fuel Cost, Variable Operation and Maintenance Cost, Fuel Cost Independent Value, and Cubic Cost Value B parameters were derived, while the Fuel Cost Dependent Value and the Cubic Cost Values C and D were not used and thus set to zero. Since there was no fuel for PHS, the UFC cost was assumed to be 0.000 $/MMBTU. For all purposes of this study, the round-trip energy conversion losses of PHS were not considered, as it would be somewhat difficult to estimate the cost of such losses. Had they been considered; the UFC cost would not have been negligible. The VOM was taken from [56] as the Variable O&M cost in $/MWh. The Cubic Cost Value B was taken as the Heat Rate for renewables in BTU/kWh from [51]. The FCIV was derived using Equation 2.

The System Fixed Cost from [56]represented the total amount per kW that would've been spent on the plant if it were built in one night. As with the generators, to better represent how fixed capital costs are considered when building a storage facility, it was assumed that any fixed capital costs were spread over the course of 6.25 years, equal to a 16 % annualized adjustment on the Y variable of the FCIV. Since the models were to be run over the course of a single day and not an entire year, the FCIV Y value was adjusted further to equal approximately 0.044 % of the total overnight fixed capital cost value from [51].

The plant capacity factor represented the total hours in a year of which the storage facility would be running. In all cases, it was assumed in a similar fashion to the generators that the capacity factors would always be equivalent to 8760 hr/yr (or a capacity ratio of 1).

It was further assumed that the data from [56] was proportional to the total size of the storage. In reality, this may not necessarily be the case due to many various factors, but this was assumed in order to remain consistent with the previous assumptions regarding the generator cost models. Thus, with all variables accounted for, a summary of the cost models for the energy storage can be observed in the cost tables in Appendix C.

Determining a state of charge for each hour of operation required analysis on the prepared base models. For all purposes of this study it was assumed that the storage would only be allowed to charge or discharge at a single static rate. Some EES units may be more flexible to allow for variable rates of charging or discharging, however this was assumed to simplify the TSS control and maintain a focused scope. It was further assumed that the storage cycle would cover 12 hours. In this way, the charge and discharge states would be determined based on the 12 cheapest and 12 most expensive hours of the base model without storage. The charging or discharging hours did not have to be consecutive.

Taking these assumptions into account, it was necessary to run TSS OPF studies on each of the four base models to determine the base costs of each system. Once the TSS OPFs determined overall system cost per hour, the hours could be compared and used for assigning the storage states of charge. With charging and discharging states assumed for each EES unit in each of the four models, the 9-bus systems were ready for further economic analysis and testing.

3.4   Testing PHS in the 9-bus System

At this point in the process, a simple iterative step-by-step procedure was needed to utilize the Powerworld TSS-OPF program to observe the system costs of the four built 9-bus test models with the insertion of the PHS models. The following procedure was used to test many various cases of injected PHS in the isolated 9-bus test systems, while altering both the size and location of the injected storage.

1. Place PHS model into 9-bus network
   a. Connect PHS model to REG bus
   b. Set storage size to 10 MW, adjust cost model
2. Run TSS OPF to calculate cost per hour of network
3. Record results into Excel spreadsheet
4. Increase storage size by 10 MW, adjust cost model
5. Repeat steps 2-4 until size of storage reaches total size of REG
6. Move PHS model to a different bus in the 9-bus network
7. Repeat steps 1b-6, stop when all buses except for the slack bus have been tested.

This process was utilized until all four cases had been tested with all possible combinations. Thus, a total of 416 cases of the 9-bus test model were tested (13 storage sizes, 8 bus placements within 4 base models) and hourly results were recorded for later comparison and analysis.

The results were compiled by taking the hourly cost data for each test from the Powerworld TSS OPF results and summing them to get the overall cost per day per test. This allowed for easier comparison between the overall daily costs of the base cases and the overall daily costs of the cases with injected storage. The results can be found in Appendix E.

3.5   *Introducing Line Redundancy to the 9-bus System*

Once the testing of the original base models was complete, the focus shifted towards looking at systems with more line capacity. Utilizing the original base models, four new test beds were created by introducing line redundancy into the networks. Every transmission line between each bus in the network now had two total lines with equivalent properties, effectively doubling the available power flow capacity between each bus while reducing line resistance by half. By creating systems with more line capacity, the goal was to test the networks in a similar fashion as before, varying the properties of injected energy storage such that comparisons could be made between the economics of the original models without redundancy and the new models with line redundancy.

With new models, new states of charge for each hour of operation needed to be configured. TSS OPF studies were completed on each of the four line-redundant base models to determine the base costs of each system. The charging states were assigned to the 12 cheapest hours, and the discharging states assigned to the 12 most expensive hours of the base systems.

A similar procedure was used to test the line-redundant base models.

1. Place PHS model into modified 9-bus network

   a.   Connect PHS model to REG bus

   b.   Set storage size to 10 MW, adjust cost model

2. Run TSS OPF to calculate cost per hour of network

3. Record results into Excel spreadsheet

4. Increase storage size by 20 MW, adjust cost model

5. Repeat steps 2-4 until size of storage reaches total size of REG

6. Move PHS model to a different bus in the 9-bus network

7. Repeat steps 1b-6, stop when all buses except for the slack bus have been tested.

This process was utilized until all four cases had been tested with all possible combinations. Thus, a total of 224 cases of the modified 9-bus test model were tested (7 storage sizes, 8 bus placements within 4 base models) and hourly results were recorded for later comparison and analysis. As with the original 9-bus cases, results were compiled by taking the hourly cost data for each test from the Powerworld TSS OPF results and summing them to get the overall cost per day per test. The results can be found in Appendix E.

3.6 Building a Larger Test Bed (Modified IEEE 14-Bus Network)

After completing extensive testing on the 9-bus bed set, many trends became apparent. To compare and verify the trends realized with the 9-bus tests, a new set of test beds were required. As with the creation of the 9-bus test bed many national resources and databases were considered for finding a good base model. The IEEE 14-bus test system [57], [58], [59] was chosen as a good candidate for the new test set. Containing five generators and eleven loads in multiple ring loops it would likely perform differently than the 9-bus sets, while remaining easy to manipulate and control with only 14 buses. In addition, since the Powerworld version used contained a 13-bus limit, the 14-bus test bed would need to be modified only by a single bus to reduce the system to 13 buses. Additional specifications of the original model chosen, as well as the modified model specifications can be found in Appendix F.
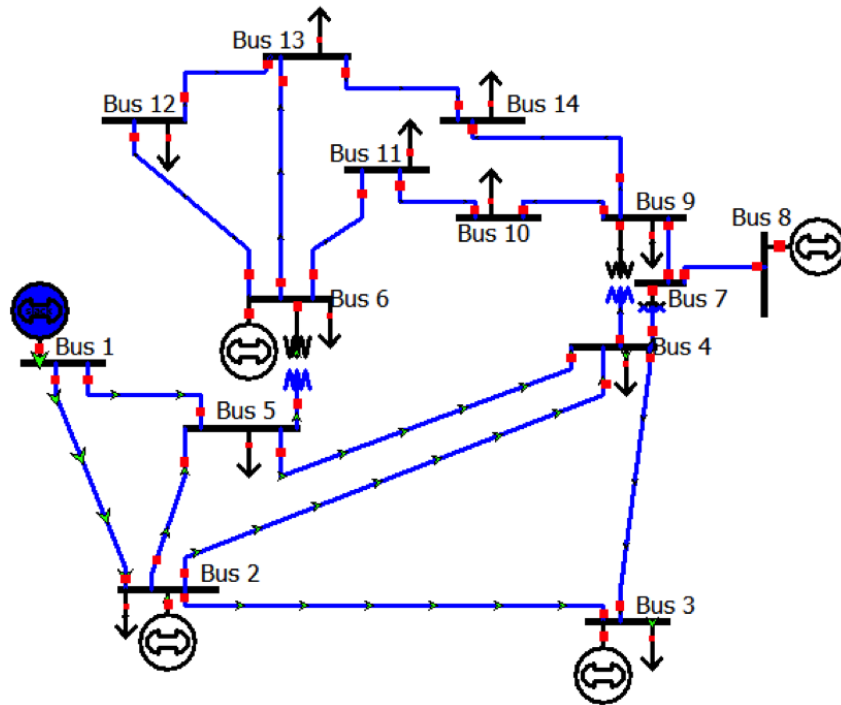
Figure 3-6: IEEE 14-Bus Network

With the modified IEEE 13-bus network, the process to build it into Powerworld was almost identical to that detailed in Section 3.2 with few key changes. The same load data gathered for the fall and summer days were used to create accurate 24-hour load profiles in the TSS program. The loads were scaled using Equation 1 as before, with the exception that the loads data in question was coming from the 13-bus model. The scaled load calculation data can be found in Appendix G.

The same methods were used as before to develop the generator cost models. Since there were five generators in the 13-bus network with various sizes, it was assumed that the most isolated generator in the network would be reserved for the REG, as often that is the case with REG in modern networks. The remainder of the generators were assumed to be conventional combined cycle natural gas turbines. Having reserved the single generator for renewables, building the REG into the models was also completed as previously described for the 9-bus network, determining the generation profiles and scaling

them using Equation 3 and 4 to be able to input them into the TSS program. The energy storage models were built into the four 13-bus test models as previously described in section 3.3.

3.7   Testing PHS in the 14-Bus System

With a completed 13-bus test bed set, a similar simple iterative step-by-step procedure was needed as before to utilize the Powerworld TSS-OPF program to observe the system costs of inserting PHS models. The following procedure was used to test many various cases of injected PHS in the isolated 13-bus test systems, while altering both the size and location of the injected storage.

1. Place PHS model into 13-bus network
   a. Connect PHS model to REG bus
   b. Set storage size to 10 MW, adjust cost model
2. Run TSS OPF to calculate cost per hour of network
3. Record results into Excel spreadsheet
4. Increase storage size by 20 MW, adjust cost model
5. Repeat steps 2-4 until size of storage reaches total size of REG
6. Move PHS model to a different bus in the 13-bus network
7. Repeat steps 1b-6, stop when all buses except for the slack bus have been tested.

This process was utilized until all four cases had been tested with all possible combinations. Thus, a total of 336 cases of the 13-bus test model were tested (7 storage sizes, 12 bus placements within 4 base models) and hourly results were recorded for later comparison and analysis. As with the previous 9-bus cases, results were compiled by taking the hourly cost data for each test from the Powerworld TSS OPF results and summing them to get the overall cost per day per test. The results can be found in Appendix J.

4. Results and Discussion

The goal of this thesis was to observe the economic effects of injecting various sizes of storage in various locations within isolated power networks containing conventional and renewable generation sources. By developing multiple hypothetical test beds and recording the overall system costs with and without the introduction of storage models, data could be obtained and organized to determine what, if any economic trends existed. To better highlight the results the overall daily cost data was normalized by taking the percent cost difference between the costs of the test case in question and the base case. The data was further organized into grids with size of storage on one axis and distance (in buses) from REG on the other. Taking it one step further, the relationships in the grid could be plotted in various forms to better observe trends. The following results are grouped by the base test bed utilized, to illustrate the differences between each base case.

4.1   9-bus Single-Line Cases

The first data set to be discussed are the 9-bus single-line cases. This set consisted of all the cases that utilized the modified 9-bus test bed with only single transmission lines connecting each bus as described in Section 3.2. There were four test beds in this set: two beds with solar REG and two beds with wind REG each on a fall and summer day respectively.

For each case set, percentage cost difference grids were created to observe the initial trends. The values within the grids were color-coded to better highlight the changes in cost at each bus. Grid values in green represented cases in which it was more economical to inject storage. Grid values in blue represented cases in which it was more expensive to inject storage, but cost difference was very little. Grid values in shades of orange represented cases in which it was significantly more expensive to inject storage, with the

highest costs shaded darker. Each color shade represented a range of 0.2 %. In addition to percentage cost difference grids, scatter plots and 3-D topographical surface plots were created based on the grid data. The scatter plots helped to determine the ease of estimating the mathematical relationships of daily cost difference versus injected storage size based at different locations, while the 3-D plots allowed for better visualization of the overall cost trends.

4.1.1 Solar REG on a Fall Day

For the base case of solar REG on a fall day, the percent cost difference grid can be observed in Table 4-1 below.

Table 4-1: Percent Cost Difference Grid for 9-bus Single-Line Solar REG, Fall Day

Bus Distance/ Size (MW)	Bgen3 (0 Bus)	B9 (1 Bus)	B6 (2 Bus)	B8 (2 Bus)	B7 (3 Bus)	B4 (3 Bus)	B5 (4 Bus)	Bgen2 (4 Bus)
10	-0.037	-0.036	-0.008	-0.024	0.001	0.012	-0.013	0.001
20	-0.055	-0.054	0.011	-0.029	0.009	0.037	0.009	0.008
30	-0.058	-0.058	0.043	-0.022	0.025	0.067	0.040	0.023
40	-0.044	-0.045	0.090	-0.004	0.046	0.105	0.081	0.044
50	-0.016	-0.017	0.149	0.025	0.073	0.150	0.130	0.071
60	0.026	0.026	0.223	0.064	0.105	0.199	0.190	0.105
70	0.085	0.085	0.312	0.079	0.142	0.254	0.259	0.143
80	0.156	0.158	0.416	0.138	0.188	0.317	0.338	0.189
90	0.199	0.202	0.535	0.278	0.238	0.383	0.426	0.240
100	0.311	0.314	0.669	0.420	0.286	0.458	0.524	0.288
110	0.505	0.509	0.818	0.535	0.332	0.537	0.632	0.335
120	0.668	0.674	0.975	0.616	0.383	0.624	0.750	0.386
130	0.822	0.829	1.152	0.703	0.437	0.717	0.879	0.440

From this chart alone some initial conclusions can be drawn. First, for the 9-bus Single-Line Solar REG Fall cases, the most money was saved when injecting 30 MW of storage at either the REG bus (Bgen3) or at one bus away (B9). **Thus, the optimum size for this fall case set was 30 MW placed at or 1 bus away from the Solar Farm.** Secondly, as the injection size of storage increased, the overall costs

increased (with some exception) but at different rates depending on the bus. However, the actual relationships were hard to determine based on the numbers of the cost difference grid alone.

Looking at the scatter plot of Figure 4-1, below, the relationships for injected storage on buses B6, B5, and B4 (2, 3 and 3 buses away from REG respectively) were represented by 2nd order polynomials, suggesting that the percent cost difference depends on the size of storage squared, and is easy to quantify. However, the relationships for buses Bgen3, B9 and B8 (0, 1 and 2 buses away) were represented by 6th order polynomials, and on buses B7 and Bgen2 (3 and 4 buses away) by 3rd order polynomials suggesting that it would be harder to estimate the percent cost differences at those buses.
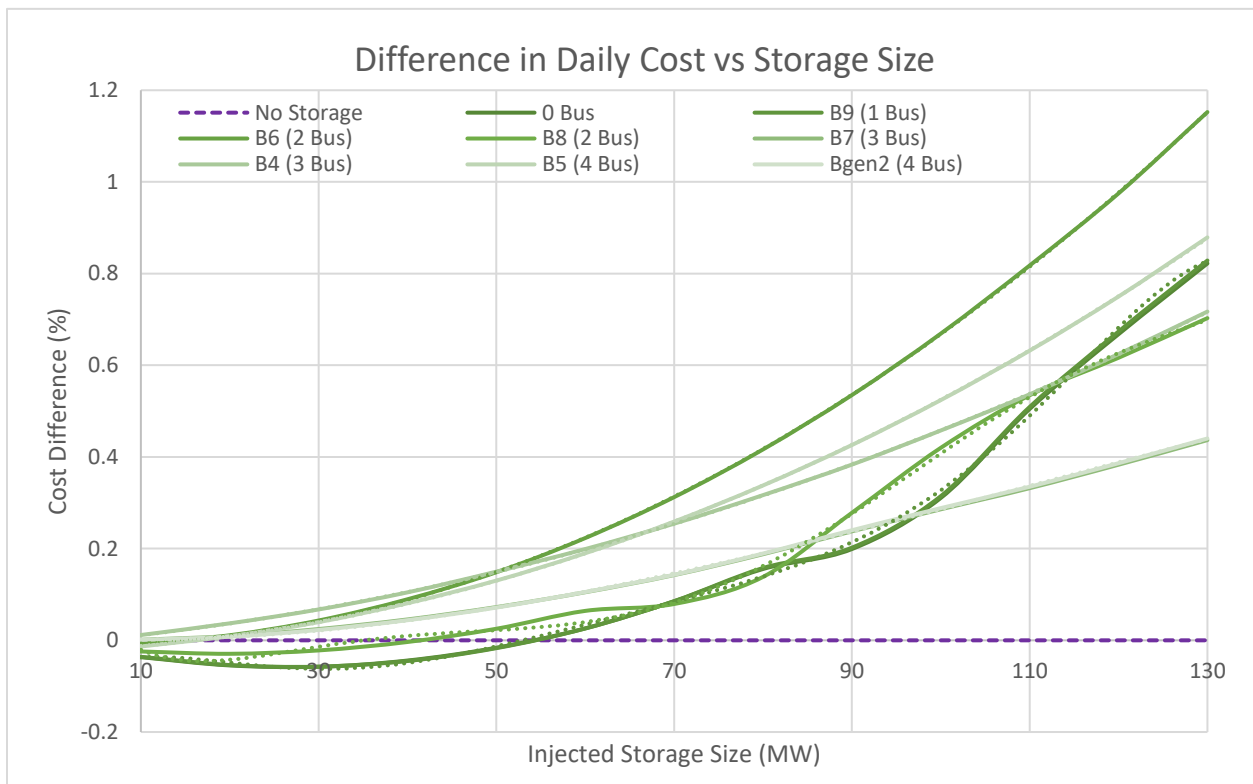
Figure 4-1: Percent Cost Difference Scatter Plot for 9-bus Single-Line Solar REG, Fall Day

Maintaining the same color-coding as displayed in the Cost Difference Grid from Table 4-1 the data was transposed into a 3-D Topographical Surface Plot. With each color representing a 0.2 % difference, this plot clearly indicates additional general trends, as well as verifying previously mentioned points. First, the

larger sizes of storage affected system cost more than smaller sizes of storage. In other words, the incremental cost decreased as size of storage decreased, as exemplified by the fact that more than half of the cases fell within the -0.2 to 0.2 % range despite only covering 2/7ths of the total range. Additionally, the local maximum for this data set occurred at 130 MW of injected storage at bus B6 (2 buses away), while the local minima occur at 30 MW of storage at either the REG bus (Bgen3) or at B9 (1 bus away).
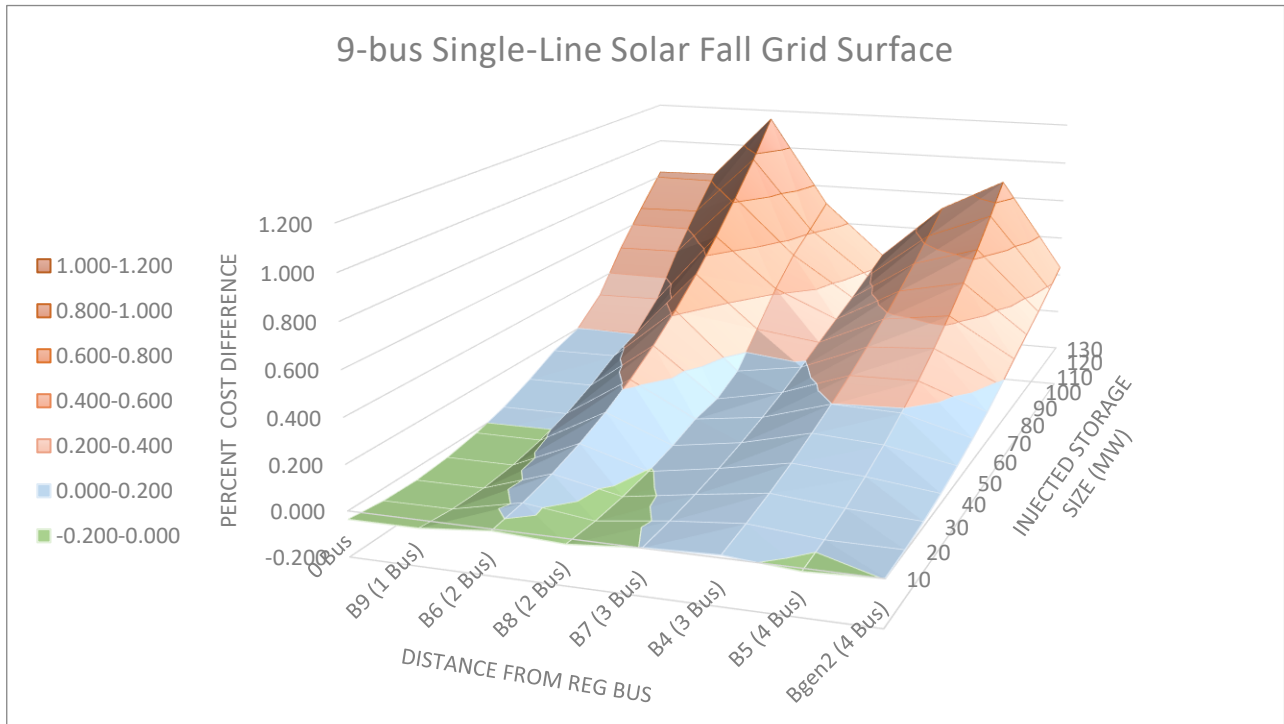
Figure 4-2: 3-D Surface Plot for 9-bus Single-Line Solar REG, Fall Day

This plot indicated that injecting storage on some buses yields overall higher costs than at other buses regardless of size. For example, buses B6, B4 and B5 (2, 3 and 4 buses away respectively) were the most expensive buses for storage injection in the system. On the other hand, bus B7 and bus Bgen2 (3 and 4 buses away respectively) appear to be the least expensive buses for storage injection, suggesting that both size and injection location affect the cost of the system, but in different ways.

4.1.2 Solar REG on a Summer Day

For the base case of solar REG on a summer day, the percent cost difference grid can be observed in Table 4-2 below.

Table 4-2: Percent Cost Difference Grid for 9-bus Single-Line Solar REG, Summer Day

Bus Distance/ Size (MW)	Bgen3 (0 Bus)	B9 (1 Bus)	B6 (2 Bus)	B8 (2 Bus)	B7 (3 Bus)	B4 (3 Bus)	B5 (4 Bus)	Bgen2 (4 Bus)
10	-0.010	-0.007	-0.005	-0.006	0.017	0.014	-0.013	0.016
20	-0.010	-0.008	0.011	0.001	0.032	0.035	0.003	0.032
30	0.009	0.012	0.046	0.019	0.054	0.063	0.028	0.055
40	0.043	0.046	0.094	0.049	0.087	0.096	0.069	0.088
50	0.094	0.097	0.156	0.089	0.124	0.136	0.116	0.126
60	0.167	0.170	0.234	0.142	0.167	0.183	0.174	0.170
70	0.252	0.255	0.326	0.209	0.211	0.242	0.241	0.215
80	0.353	0.355	0.435	0.193	0.267	0.304	0.318	0.272
90	0.449	0.451	0.561	0.184	0.308	0.372	0.406	0.314
100	0.491	0.493	0.680	0.363	0.355	0.446	0.504	0.361
110	0.753	0.754	0.807	0.652	0.405	0.527	0.614	0.413
120	1.074	1.073	0.967	1.013	0.464	0.615	0.730	0.472
130	1.334	1.334	1.131	1.272	0.525	0.711	0.836	0.535

As with the first case set, some initial conclusions can be drawn from this chart by itself. For the 9-bus Single-Line Solar REG Summer cases, the most money was saved when injecting 10 MW of storage at bus B5 (4 buses away). **Thus, the optimum size for this summer case set was 10 MW placed 4 buses away at B5 from the Solar Farm.** As with the previous case set, an increase in storage size generally increases overall costs (with some exception) but at different rates depending on the bus.

The scatter plot of Figure 4-3 revealed the mathematical relationships for injected storage on the buses. Buses B6, B5, and B4 (2, 3 and 3 buses away from REG respectively) were represented by 4th, 3rd and 2nd order polynomials, while buses Bgen3, B9, B8, B7 and Bgen2 (0, 1, 2, 3 and 4 buses away) were all represented by 6th order polynomials. These relationships differed from those of the Solar Fall case set, suggesting that storage will affect system costs differently in the summer than in the fall.
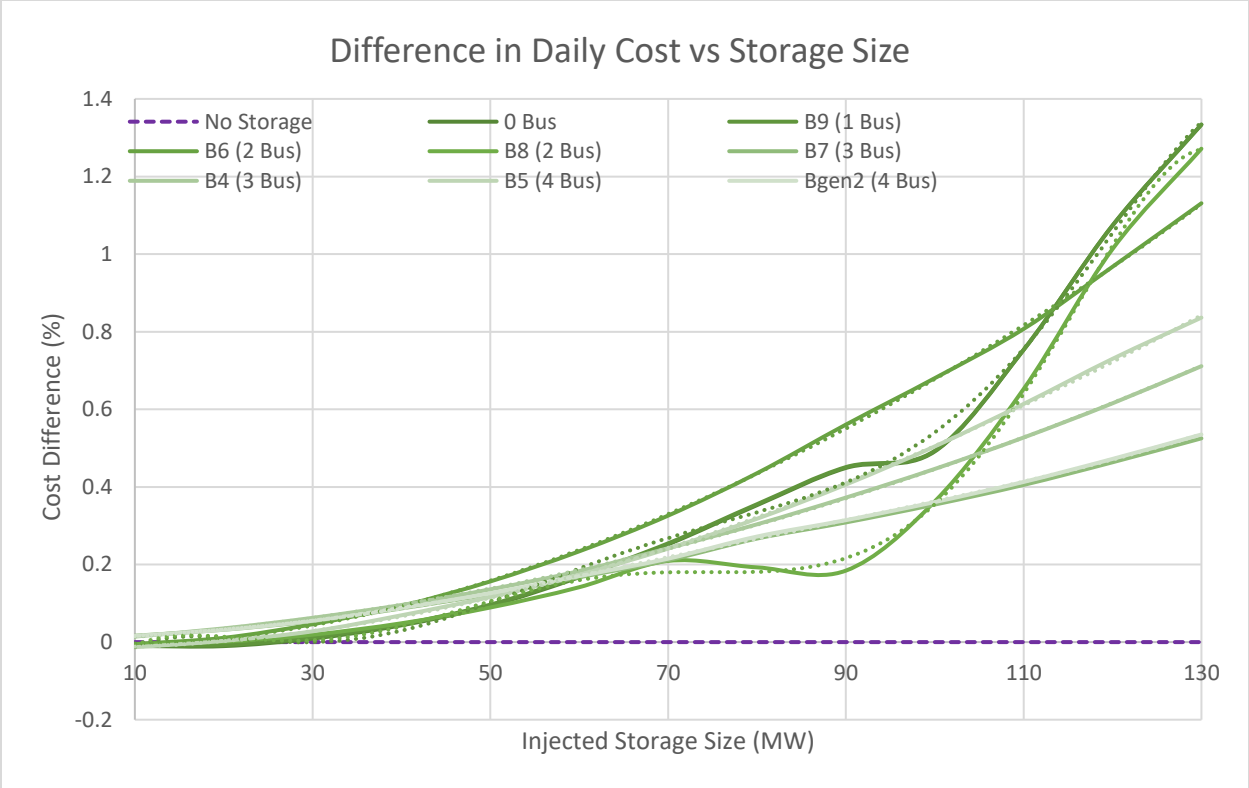
Figure 4-3: Percent Cost Difference Scatter Plot for 9-bus Single-Line Solar REG, Summer Day

Maintaining the same color-coding as displayed in the Cost Difference Grid from Table 4-2 the data can also be represented by a 3-D Topographical Surface Plot. As in Figure 4-4, the larger sizes of storage affect system cost more than smaller sizes of storage, however this trend is much better defined here. The local maxima in this set occur at 130 MW injected at or next to the REG bus.
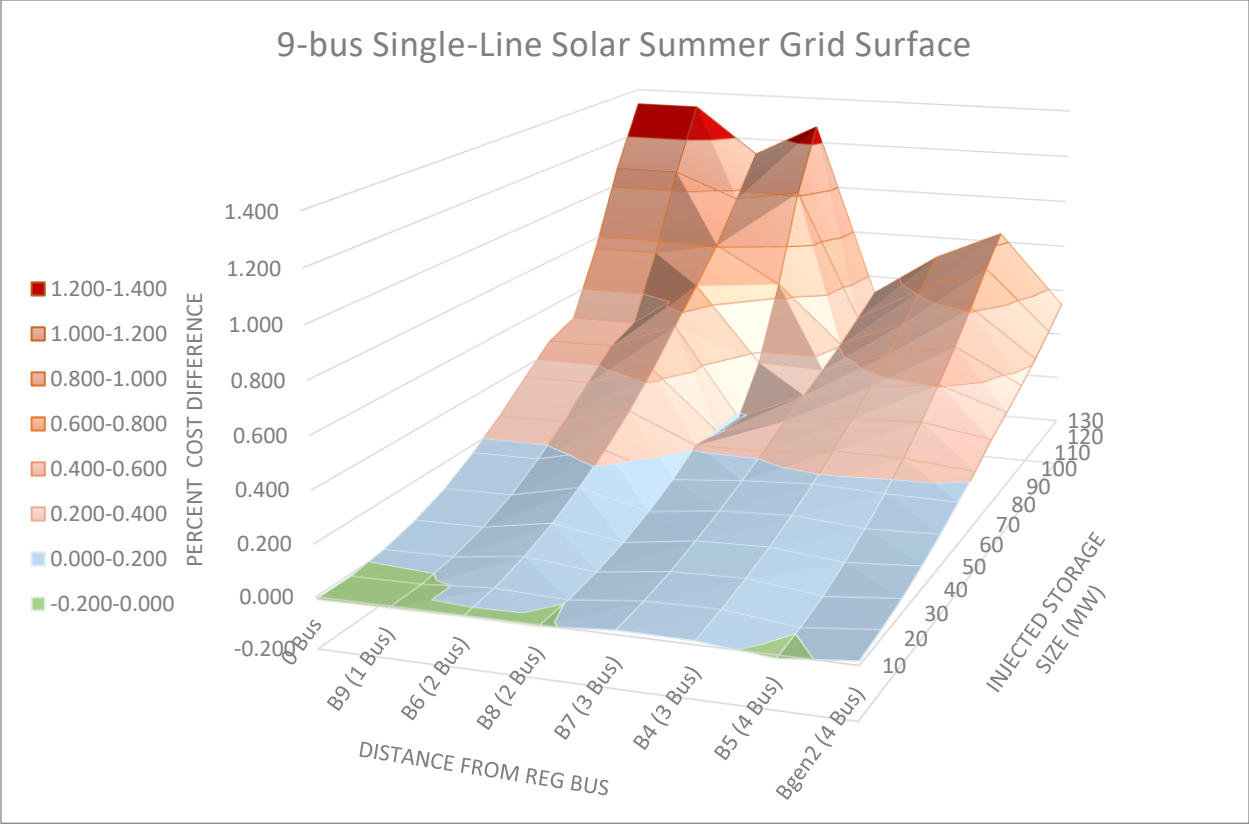
Figure 4-4: 3-D Surface Plot for 9-bus Single-Line Solar REG, Summer Day

However, the trend from the solar fall set that some buses yielding overall higher costs than others with injected storage is no longer as defined as before. At small sizes of storage, bus B6 and bus B4 (2 and 3 buses away respectively) appear to be the most expensive buses for storage injection in the system with bus B7 and bus Bgen3 (3 and 0 buses away respectively) appearing to be the least expensive buses for storage injection. However, at larger sizes of storage buses Bgen3 and B9 (0 and 1 buses away) overwhelmingly become the most expensive buses, with buses B7 and Bgen2 (3 and 4 buses away) becoming the least expensive. These observations lead to two general assumptions: 1) **Location of storage matters much less in the Solar Summer case set for smaller sizes of injected storage than for the Solar Fall case set**, and 2) **Injecting large amounts of storage farther away from the REG bus within the Solar Summer case set will generally lead to decreased incremental costs, albeit still more expensive than not utilizing storage.**

### 4.1.3   Wind REG on a Fall Day

For the base case of wind REG on a fall day, the percent cost difference grid can be observed in Table 4-3 below.

Table 4-3: Percent Cost Difference Grid for 9-bus Single-Line Wind REG, Fall Day

Bus Distance/ Size (MW)	Bgen3 (0 Bus)	B9 (1 Bus)	B6 (2 Bus)	B8 (2 Bus)	B7 (3 Bus)	B4 (3 Bus)	B5 (4 Bus)	Bgen2 (4 Bus)
10	-0.022	-0.020	-0.005	-0.016	0.008	0.010	-0.018	0.006
20	-0.027	-0.022	0.017	-0.008	0.025	0.037	0.006	0.021
30	-0.011	-0.008	0.049	0.009	0.047	0.068	0.033	0.045
40	0.022	0.025	0.102	0.041	0.077	0.108	0.076	0.076
50	0.073	0.076	0.172	0.085	0.113	0.156	0.129	0.112
60	0.143	0.146	0.260	0.142	0.166	0.209	0.194	0.165
70	0.231	0.234	0.365	0.213	0.217	0.271	0.271	0.216
80	0.340	0.343	0.486	0.296	0.278	0.341	0.359	0.277
90	0.467	0.469	0.627	0.392	0.347	0.417	0.458	0.347
100	0.622	0.624	0.786	0.501	0.422	0.503	0.570	0.423
110	0.821	0.822	0.963	0.510	0.504	0.595	0.695	0.506
120	1.035	1.035	1.153	0.505	0.595	0.695	0.830	0.598
130	1.357	1.357	1.350	0.620	0.693	0.802	0.979	0.697

For the 9-bus Single-Line Wind REG Fall cases, the most money was saved when injecting 20 MW of storage at the REG bus (Bgen3). **Thus, the optimum size for this fall case set was 20 MW placed at the Wind Farm bus.** As with the solar case sets, increasing injection size of storage lead to increased overall costs but at different rates depending on the bus. However, the actual relationships are hard to determine based on the numbers of the cost difference grid alone.

Looking at the scatter plot of Figure 4-5, below, the relationships for injected storage on buses B6, B5, B4 and Bgen2 (2, 3, 3 and 4 buses away from REG respectively) were determined to be represented by 2nd order polynomials, suggesting that the percent cost difference depends on the size of storage squared and is easy to quantify. However, the relationships for buses B8 and B7 (2 and 3 buses away) were

represented by 6th order polynomials, and on Bgen3 and B9 buses (0 and 1 buses) by 5th order

polynomials suggesting that it would be harder to estimate the percent cost differences at those buses.

These relationships differed from those of the solar case sets, suggesting that storage will affect system

costs differently for systems utilizing solar versus utilizing wind energy.
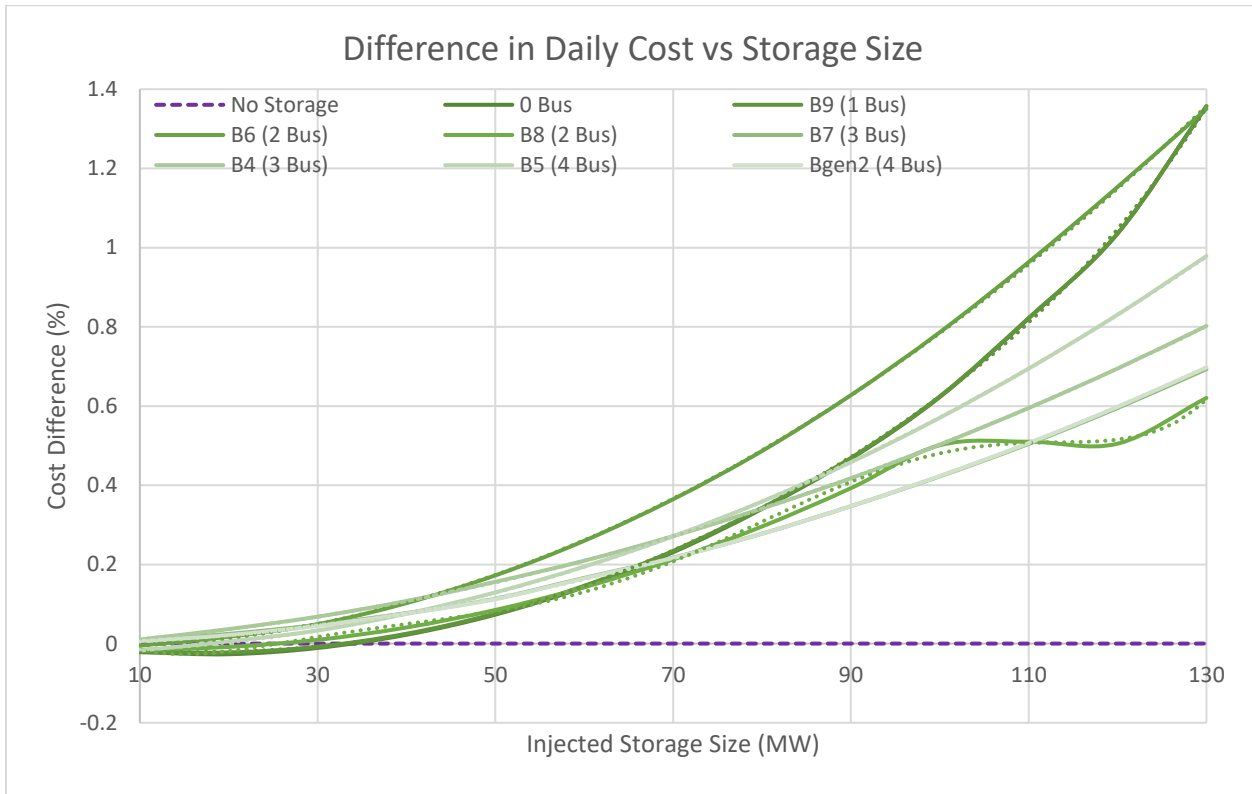
Figure 4-5: Percent Cost Difference Scatter Plot for 9-bus Single-Line Wind REG, Fall Day

Looking at the 3-D surface plot for this data set the larger sizes of storage affect system cost more than

smaller sizes of storage, as was previously determined in the solar case sets. The local maxima occur at

130 MW of injected storage at buses Bgen3, B9 and B6 (0, 1 and 3 buses away respectively).
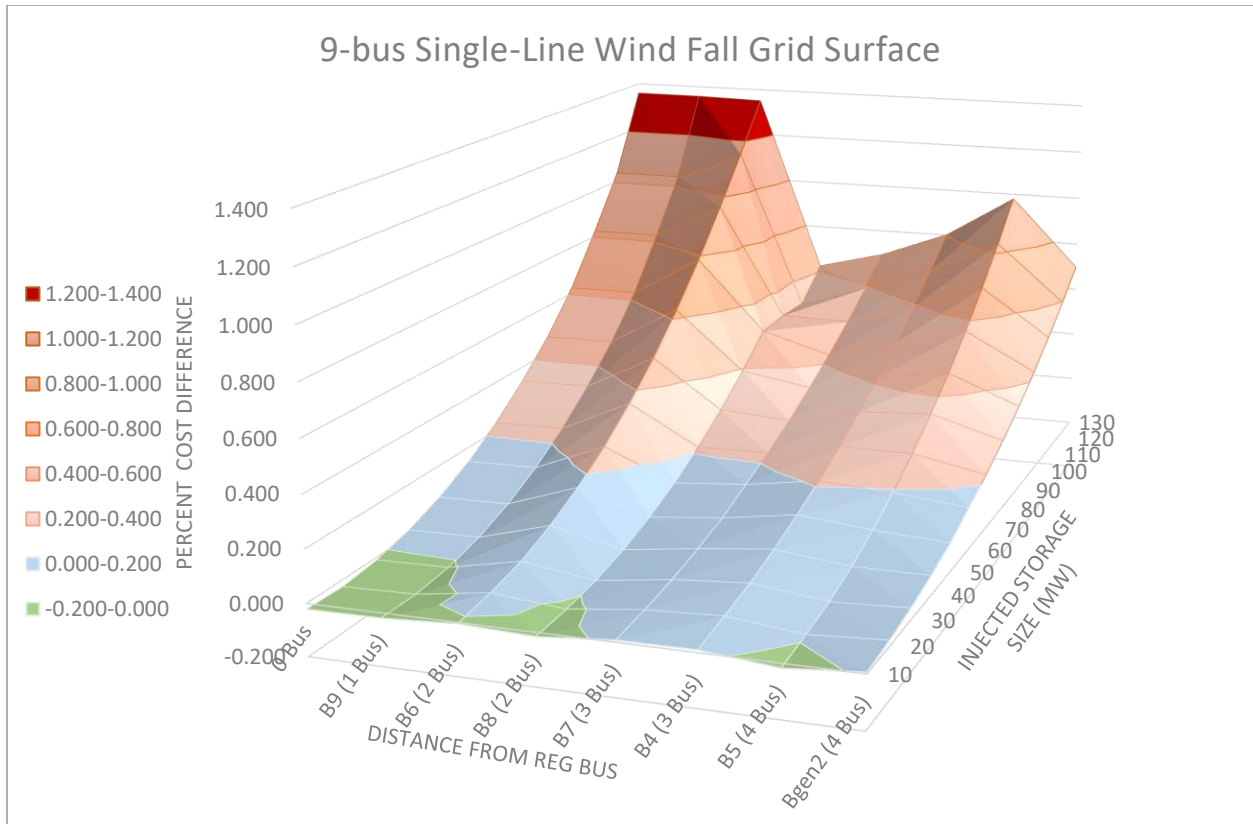
Figure 4-6: 3-D Surface Plot for 9-bus Single-Line Wind REG, Fall Day

This plot displayed two additional trends somewhat related to the previous sets. Firstly, the trend from the Solar Fall set reappeared, but only for one bus in the system: injecting storage on some buses yields overall higher costs than at other buses. Bus B6 (4 buses away) appeared to be the most expensive bus for storage injection in the system. On the other hand, bus B7 and B8 (3 and 2 buses away) were for the most part the least expensive buses for storage injection. Additionally, as with the Solar Summer case set, larger storage sizes on buses closer to the REG appeared to be more expensive than buses farther away. For example, buses Bgen3, B9 and B6 (0, 1 and 2 buses away) all yielded much higher system costs while being the closest buses to the REG. On the other hand, buses B4, B5 and Bgen2 (3, 4 and 4 buses away) yielded much lower costs while being farthest away from the REG.

4.1.4 Wind REG on a Summer Day

For the base case of wind REG on a summer day, the percent cost difference grid can be observed in Table 4-4 below.

Table 4-4: Percent Cost Difference Grid for 9-bus Single-Line Wind REG, Summer Day

Bus Distance/ Size (MW)	Bgen3 (0 Bus)	B9 (1 Bus)	B6 (2 Bus)	B8 (2 Bus)	B7 (3 Bus)	B4 (3 Bus)	B5 (4 Bus)	Bgen2 (4 Bus)
10	0.010	0.017	-0.003	0.006	0.027	0.014	-0.019	0.026
20	0.035	0.041	0.007	0.024	0.055	0.031	-0.013	0.053
30	0.074	0.080	0.039	0.057	0.085	0.056	0.007	0.084
40	0.141	0.147	0.089	0.101	0.131	0.091	0.041	0.132
50	0.223	0.228	0.157	0.158	0.182	0.134	0.086	0.183
60	0.324	0.331	0.242	0.231	0.240	0.184	0.144	0.242
70	0.439	0.445	0.347	0.317	0.306	0.242	0.213	0.310
80	0.580	0.584	0.469	0.417	0.380	0.308	0.294	0.385
90	0.740	0.743	0.611	0.538	0.463	0.382	0.388	0.470
100	0.901	0.904	0.739	0.665	0.551	0.464	0.494	0.560
110	1.121	1.123	0.887	0.626	0.649	0.554	0.612	0.660
120	1.342	1.341	1.072	0.730	0.755	0.652	0.733	0.769
130	1.589	1.585	1.293	1.076	0.869	0.758	0.847	0.884

For the 9-bus Single-Line Wind REG Summer cases, the most money was saved when injecting 10 MW of storage at bus B5 (4 buses away). **Thus, the optimum size for this summer case set was 10 MW placed 4 buses away from the Wind Farm at bus B5.**

Looking at the scatter plot of Figure 4-7, the relationships for injected storage on buses, B7, B4 and Bgen2 (3, 3 and 4 buses away from REG respectively) were determined to be represented by 2nd order polynomials, suggesting that the percent cost difference for these buses depend on the size of storage squared. However, the relationships for buses B6, B8 and B5 and (2, 2 and 4 buses away) were represented by 5th, 5th and 6th order polynomials, and on Bgen3 and B9 buses (0 and 1 buses) by 4th order polynomials suggesting that it would be harder to estimate the percent cost differences at those buses.
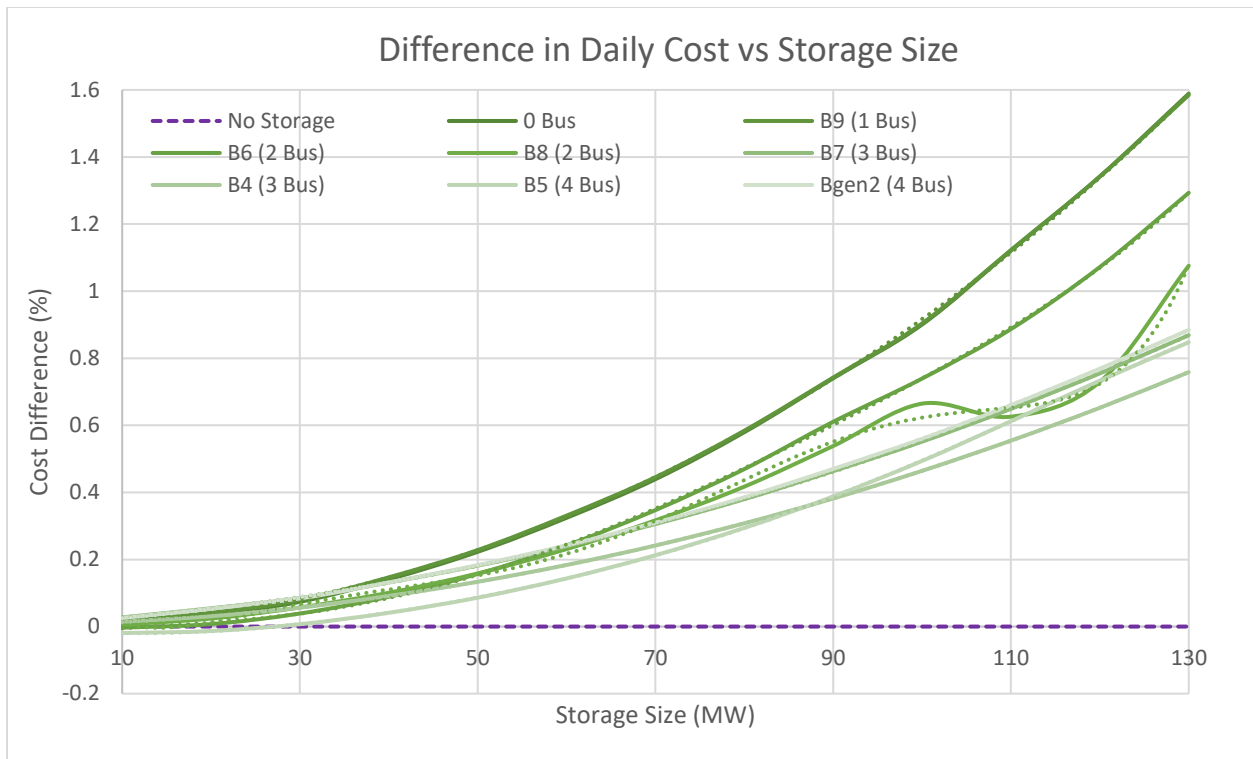
Figure 4-7: Percent Cost Difference Scatter Plot for 9-bus Single-Line Wind REG, Summer Day

As determined previously from the previous case sets, it is clear from the 3-D surface plot for the Wind Summer case set that the larger sizes of storage affect system cost more than smaller sizes of storage.
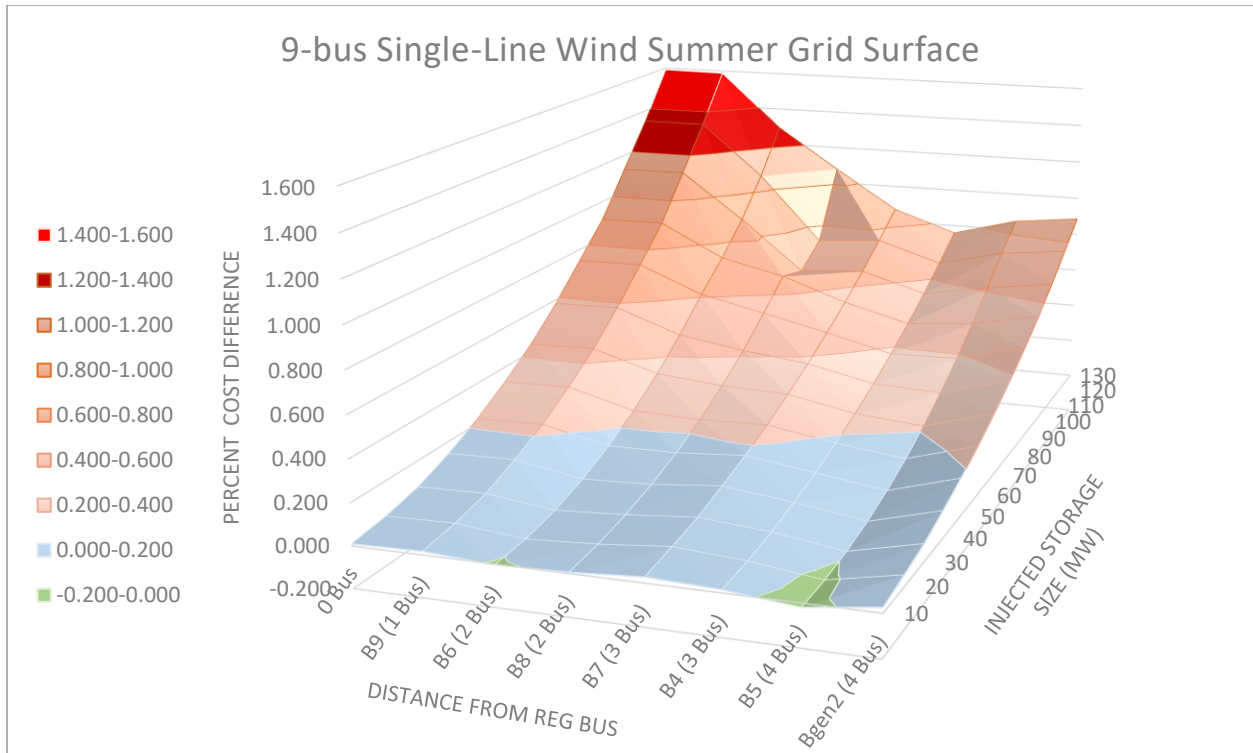
Figure 4-8: 3-D Surface Plot for 9-bus Single-Line Wind REG Summer Day

In addition, this plot was by far the smoothest out of the other four case sets studied. With a local

maximum occurring at 130 MW injected at the REG bus and a local minimum occurring between sizes of

10 to 20 MW injected at bus B5 (4 buses away), a new overall trend can be observed. It appears that for

the Wind Summer case set, **the overall system costs decrease as storage size decreases and injection**

location increases. **Conversely, the overall system costs increase as storage size increases and**

injection location decreases. Put another way, small amounts of storage injected farthest from the REG

reduced the overall system costs, while large amounts injected closest to the REG significantly increased

overall system costs.

4.1.5   9-bus Single-Line Cases Discussion

Considering all four case sets studied, some general conclusions can be made. First, the overall daily cost increased as storage sized increased, with different relationships for different injection buses. This was consistent across all cases, and makes sense as the capital costs are indeed larger for larger sizes of storage. Second, larger storage sizes relative to the size of the system (or more specifically the size of the REG) may not be economical. Every case that included injecting storage greater than 50 % of the built REG size was more expensive than the corresponding base case. While having the capacity to store large amounts of energy at a time would seem to be a reasonable approach, it would appear that the capital costs and thus overall system costs are just too high to justify installing amounts of storage that are well over 50 % of the size of REG.

When focusing on the economical cases themselves, there were far fewer cases in which injecting storage was cheaper than the base cases without storage. This was largely unexpected as previous reports seemed to suggest otherwise, proposing that EES could be a practical and economical solution to an increasingly relevant issue. For the cases that were economical, the injected size was also much smaller than expected, and the costs saved from utilizing storage were extremely small, never exceeding 0.06 %. For a cost savings of less than $1/10^{th}$ of a percent, it may be hard to justify going through the process of building and installing storage for systems like the 9-bus systems tested.

Additional observations can be made across all four cases when comparing their respective 3-D surface plots. For amounts of storage below roughly 50 % of the rated REG size, the overall daily costs are not only relatively small, but also fairly comparable to each other regardless of bus location and case set, with little variance. However, for amounts of storage above 50 % of the rated REG size the incremental costs are not only larger but much less predictable with larger variation in the values depending on the injection location and case set.

This can be further examined when looking at the Percent Cost Difference Scatter Plots of Figures 4-1, 4-3, 4-5 and 4-7. For each of these plots, the majority of the bus relationships are predictable, with increases

in cost difference as storage size increases. However, certain buses have much less predictable relationships when under heavy storage injection. For example, bus B8 consistently had dips in the cost differences for larger storage sizes. In Figure 4-7, the cost differences on bus B8 decreased significantly between 100 and 120 MW of storage with a local minimum at 110 MW, before increasing again at 130 MW. This suggests that line congestion may play a larger role in the high system costs of injecting large amounts of storage.

Since storage is either pulling or injecting large amounts of power at the installed location, the larger the storage, the higher the power flow. The higher the power flow, the more likely that the lines nearest to the storage will become overloaded due to the limited line capacity within the systems, creating congestion. Bus B8 is a particular point of interest in each case as the centrally located bus in the system reacted more heavily to increased storage sizes, suggesting that congestion affects certain buses more than others.

If line congestion does in fact play such a large role in the percent difference in overall system cost, then an increase in either system connectivity or line capacity should theoretically decrease the variability of the costs of large storage amounts, as well as decreasing the values themselves. An addition of line capacity would theoretically also decrease the incremental costs of the higher amounts of storage. This would all be theoretically possible as increasing line capacity decreases the likelihood of overloaded lines and power flow losses.

4.2   9-bus Redundant-Line Cases

The second data set to be discussed are the 9-bus redundant-line cases. This set consisted of all the cases that utilized the modified 9-bus test bed with double transmission lines connecting each bus as described in Section 3.5 to determine what effects ESS would have on a well-connected system with more line capacity. As with the single-line cases, there were four test beds in this set: two beds with solar REG and two beds with wind REG each on a fall and summer day respectively.

Percentage cost difference grids were created for each case set to observe the initial trends. The values within the grids were color-coded to better highlight the changes in cost at each bus. Grid values in green represented cases in which it was more economical to inject storage. Grid values in blue represented cases in which it was more expensive to inject storage, but cost difference was very little. Grid values in shades of orange represented cases in which it was significantly more expensive to inject storage, with the highest costs shaded darker. Each color shade represented a range of 0.2 %. In addition to percentage cost difference grids, scatter plots and 3-D topographical surface plots were created based on the grid data. The scatter plots helped to determine the estimated mathematical relationships of daily cost difference versus injected storage size based at different locations, while the 3-D plots allowed for better visualization of the overall cost trends.

Finally, these results were compared to those from the single-line cases to see the changes in trends and overall system costs for a system with line redundancy versus that without line redundancy. New percent cost difference grids were created to represent the percent cost differences between the original single-line base costs and the double-line costs. With the new grids, each shade of green represented a 0.2 % range of cost savings from the bases, with darker color leading to more cost savings. Values in blue represented a range of 0 to 0.2 % cost increase. In addition, the scatter plots were also re-evaluated and compared with the single-line case data obtained.

4.2.1 Solar REG on a Fall Day

For the base case of solar REG on a fall day, the percent cost difference grid can be observed in Table 4-5 below.

Table 4.5: Percent Cost Difference Grid for 9-bus Double-Line Solar REG, Fall Day

Bus Distance/ Size (MW)	Bgen3 (0 Bus)	B9 (1 Bus)	B6 (2 Bus)	B8 (2 Bus)	B7 (3 Bus)	B4 (3 Bus)	B5 (4 Bus)	Bgen2 (4 Bus)
10	-0.012	-0.012	-0.004	-0.001	0.008	0.014	0.011	0.005
30	-0.014	-0.014	0.026	0.009	0.028	0.049	0.044	0.025
50	0.013	0.013	0.084	0.040	0.058	0.095	0.095	0.056
70	0.068	0.068	0.168	0.091	0.101	0.153	0.162	0.098
90	0.154	0.155	0.278	0.161	0.154	0.222	0.245	0.152
110	0.269	0.269	0.415	0.253	0.219	0.302	0.345	0.217
130	0.412	0.413	0.578	0.365	0.294	0.395	0.461	0.293

For the 9-bus Double-Line Solar Fall case set, the most money was saved when injecting 30 MW of storage at either the REG bus (Bgen3) or at bus B9 (1 bus away). **Thus, the optimum size for this fall case set was 30 MW placed at or 1 bus away from the Solar Farm.** This is consistent with the 9-bus Single-Line Solar Fall case set. Also, consistent with the single-line case set is the fact that increasing injection size of storage leads to increased overall costs but at different rates depending on the bus.

Creating the scatter plot of Figure 4-9, below, the relationships for injected storage on buses B6, B5, and B4 (2, 3 and 3 buses away from REG respectively) were determined to be represented by 2nd order polynomials, suggesting that the percent cost difference depends on the size of storage squared. Again, this was consistent with the single-line case set. However, the relationships for buses Bgen3, B9, B8, B7 and Bgen2 (0, 1, 2, 3 and 4 buses away) were all represented by 2nd order polynomials as well, which was not consistent with the single-line case set. This suggests that **a congested system will create more complicated relationships between the percent cost difference and injected storage size**, whereas a system with added line capacity will likely yield relationships that are easier to model. Despite this new finding, the overarching trend remained the same: **overall daily cost increased as storage size increased, with different relationships for different injection buses.**
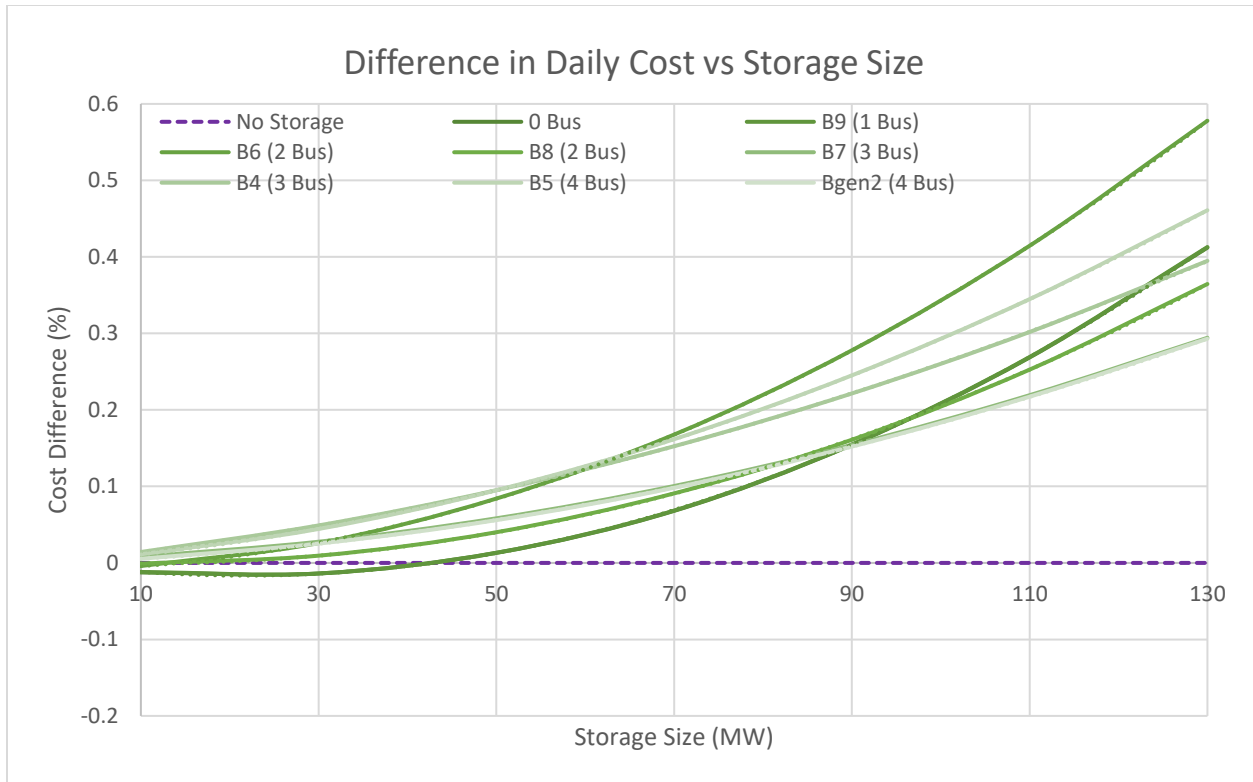
Figure 4-9: Percent Cost Difference Scatter Plot for 9-bus Double-Line Solar REG, Fall Day

Looking at the 3-D surface plot for this data set the local maximum occurred at 130 MW of injected storage at bus B6 (2 buses away), while the local minima occur at 30 MW of storage at either the REG bus (Bgen3) or at B9 (1 bus away). While larger sizes of storage affected the system costs of the single-line cases more than the smaller sizes, this trend appeared to be much less significant for the double-line cases. Whereas previously the maximum percent cost difference for the single-line case set exceeded 1.152 %, the maximum percent cost difference here was exactly half of that at 0.578 %. While not every case had percent cost differences half as much as their single-line counterparts, they were all significantly reduced.
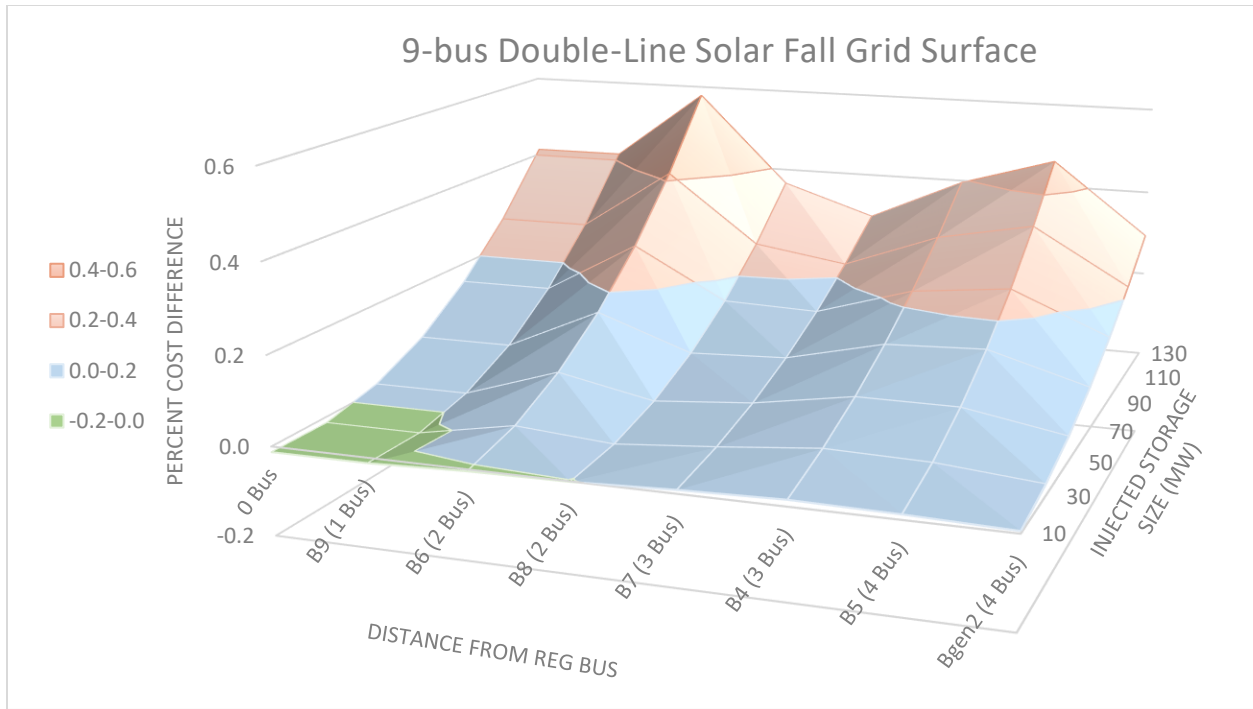
Figure 4-10: 3-D Surface Plot for 9-bus Double-Line Solar REG, Fall Day

Consistent with the single-line case set, this plot also indicated that injecting storage on some buses yields overall higher costs than at other buses regardless of size. For example, buses B6, B4 and B5 (2, 3 and 4 buses away respectively) were still the most expensive buses for storage injection in the system. On the other hand, buses Bgen3, B9, B7 and Bgen2 (0, 1, 3 and 4 buses away respectively) appeared to be the least expensive buses for storage injection, suggesting that both size and injection location still largely affect the cost of the system, but in different ways.

**Table 4-6:** Percent Cost Difference Grid between 9-bus Single and Double-Line Solar REG, Fall Day

Bus Distance/ Size (MW)	No Storage	Bgen3 (0 Bus)	B9 (1 Bus)	B6 (2 Bus)	B8 (2 Bus)	B7 (3 Bus)	B4 (3 Bus)	B5 (4 Bus)	Bgen2 (4 Bus)
10	-0.596	-0.609	-0.608	-0.600	-0.597	-0.588	-0.582	-0.585	-0.591
30	-0.596	-0.610	-0.610	-0.571	-0.587	-0.569	-0.548	-0.552	-0.571
50	-0.596	-0.583	-0.583	-0.513	-0.556	-0.538	-0.502	-0.502	-0.541
70	-0.596	-0.529	-0.528	-0.430	-0.506	-0.496	-0.445	-0.436	-0.499
90	-0.596	-0.443	-0.442	-0.320	-0.436	-0.443	-0.376	-0.353	-0.445
110	-0.596	-0.329	-0.329	-0.184	-0.345	-0.378	-0.296	-0.254	-0.380
130	-0.596	-0.187	-0.186	-0.022	-0.234	-0.304	-0.204	-0.138	-0.305

Notice that the new percent cost difference grid above in Table 4-6 includes the percent change in cost between the two base cases (the cases without storage). The change in overall system operating costs changed by -0.596 % just by adding line redundancy. In addition, while every case was cheaper than that of the single-line case, what is most interesting however is the fact that the line redundancy had the most impact between the 10-30 MW range at buses Bgen3, B9, B6 and B8 (0, 1, 2 and 2 buses away) which were all the closest buses to the REG. This would lead to the conclusion that all things equal, this system with redundant lines still benefits most from storage that is 30 MW closest to the REG bus. This was slightly unexpected, as the original prediction was that the addition of line redundancy and doubling capacity would affect the cases with larger storage more than those with smaller amounts of storage, since congestion was such a large factor at high amounts of storage.

Superimposing the comparison data onto the original scatter plot, this becomes easier to visualize. In blue is the original, change in costs for the single-line cases, while in green is the change in cost of the double-line compared to the single-line case data.
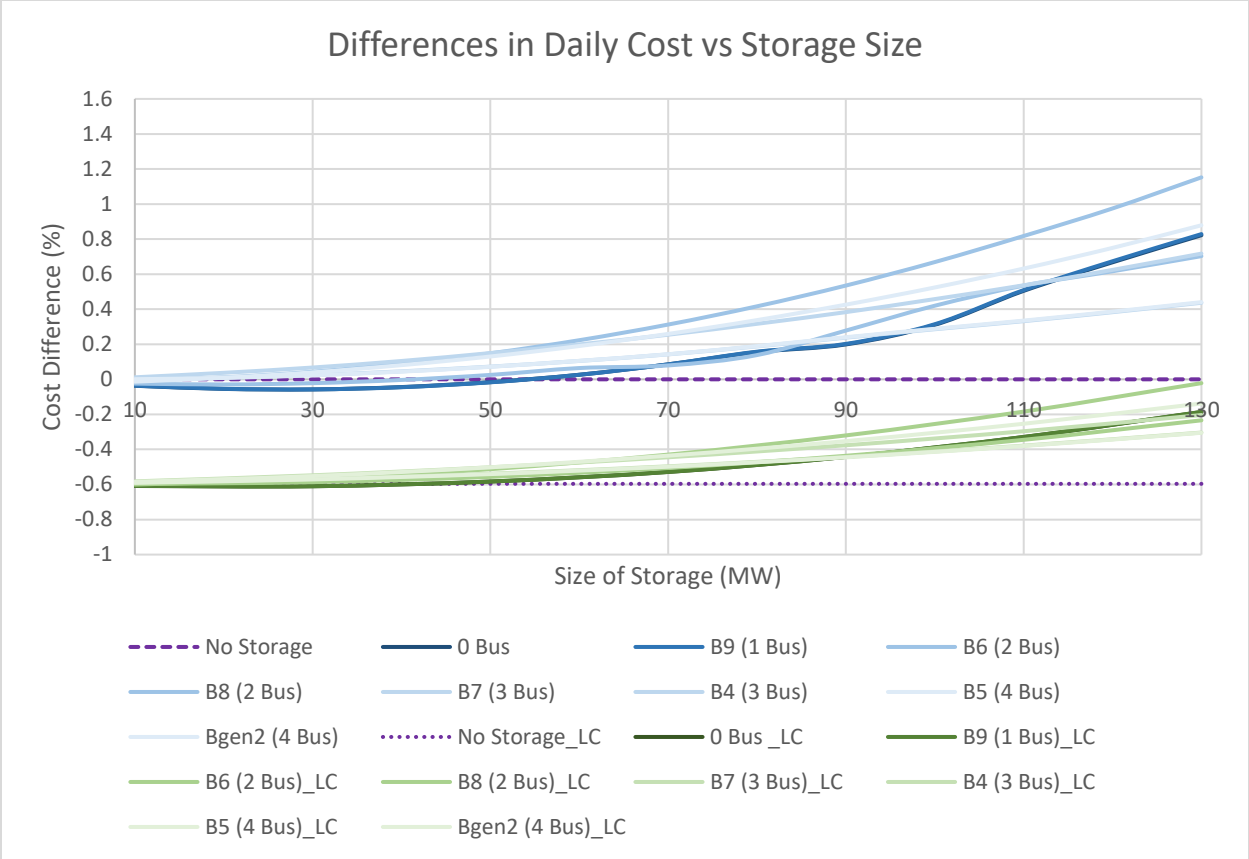
Figure 4-11: Percent Cost Difference Scatter Plot for 9-bus Single and Double-Line Solar REG, Fall Day

From Figure 4-11 alone, the double-line cases were much cheaper than the single-line cases. However, it is important to keep in mind that while this could be because more line capacity reduced the effects of congestion when adding storage, the reduction of overall system costs was still achieved by adding line capacity alone, challenging the usage of energy storage.

4.2.2   Solar REG on a Summer Day

For the base case of solar REG on a summer day, the percent cost difference grid can be observed in Table 4-7 below.
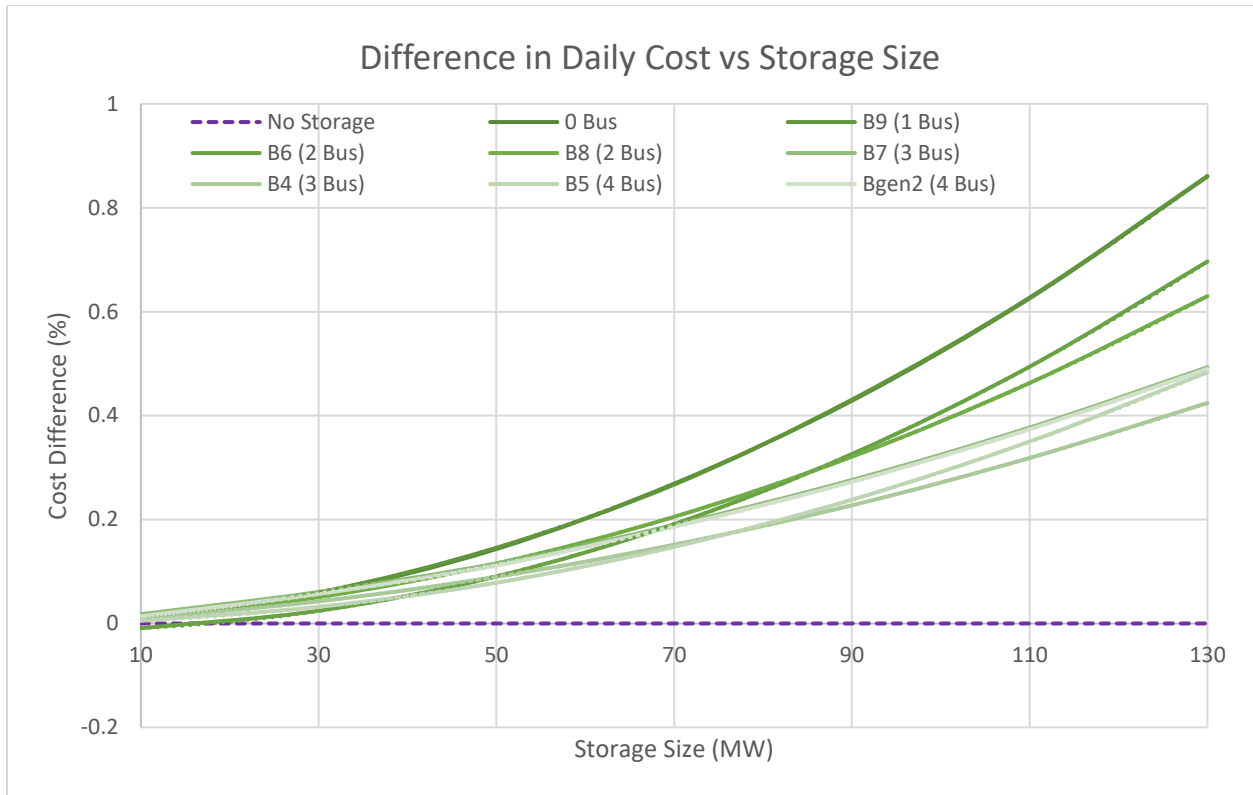
Table 4-7: Percent Cost Difference Grid for 9-bus Double-Line Solar REG, Summer Day

Bus Distance/ Size (MW)	0 Bus	B9 (1 Bus)	B6 (2 Bus)	B8 (2 Bus)	B7 (3 Bus)	B4 (3 Bus)	B5 (4 Bus)	Bgen2 (4 Bus)
10	-0.003	-0.001	-0.006	0.005	0.013	0.012	0.009	0.009
30	0.016	0.017	0.027	0.027	0.041	0.046	0.040	0.038
50	0.066	0.067	0.086	0.071	0.081	0.091	0.087	0.078
70	0.148	0.149	0.177	0.136	0.135	0.149	0.155	0.130
90	0.260	0.261	0.294	0.222	0.200	0.219	0.240	0.197
110	0.406	0.407	0.440	0.330	0.278	0.301	0.342	0.275
130	0.581	0.581	0.613	0.462	0.367	0.395	0.461	0.365

For the 9-bus Double-Line Solar Summer case set, the most money was saved when injecting 10 MW of storage at bus B6 (2 buses away). **Thus, the optimum size for this summer case set was 10 MW placed at B6, 2 buses away from the Solar Farm.** This was somewhat consistent with the 9-bus Single-Line Solar Summer case set. While the optimum size matched that of the summer, the location was closer than in the single-line set. Also consistent was the fact that increasing injection size of storage leads to increased overall costs but at different rates depending on the bus.

Creating the scatter plot of Figure 4-12, below, the relationships for injected storage on every bus could be represented by 2nd order polynomials, suggesting that the percent cost difference depends on the size of storage squared. This was not consistent with the single-line case set at all, as most bus relationships were represented by much more complex polynomials.
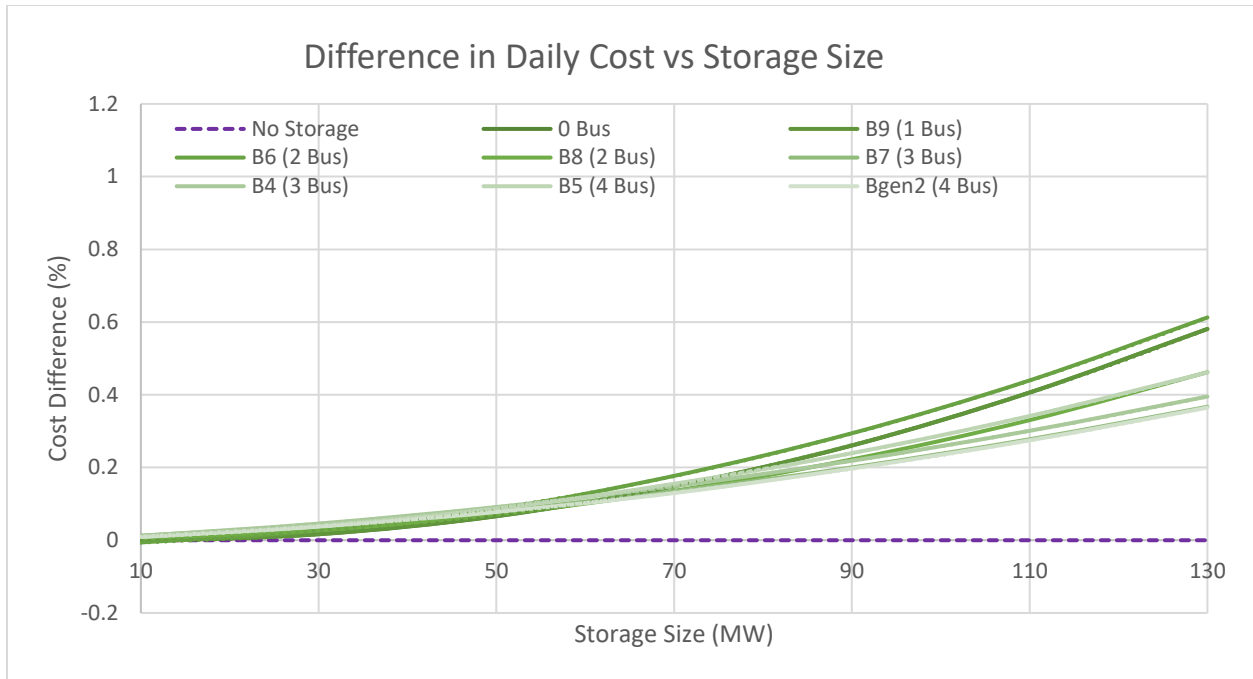
Figure 4-12: Percent Cost Difference Scatter Plot for 9-bus Double-Line Solar REG, Summer Day

Looking at the 3-D surface plot for this data set the local maximum occurred at 130 MW of injected storage at bus B6 (2 buses away), while the local minimum occurred at 10 MW also at bus B6. While larger sizes of storage affected the system costs of the 9-bus Single-Line Solar Summer cases more than that of smaller sizes, this trend appeared to be much less significant for the double-line cases. This remained consistent with the fall cases. Whereas previously the maximum percent cost difference for the single-line case set was 1.334 %, the maximum percent cost difference here was less than half of that at 0.613 %. Every case had percent cost differences reduced compared to their single-line counterparts, with some being more reduced than others.
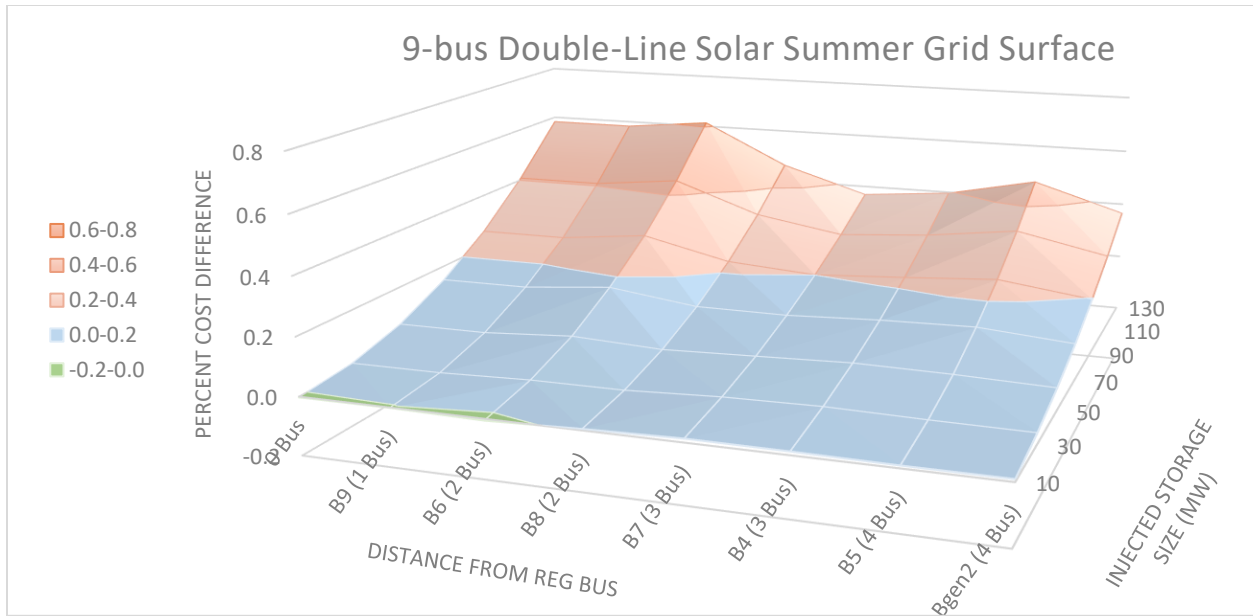
Figure 4-13: 3-D Surface Plot for 9-bus Double-Line Solar REG, Summer Day

Consistent with the single-line case set, this plot failed to define the trend from the fall sets that injecting

storage on some buses yields overall higher costs than at other buses regardless of size. Instead, it

appeared that there was hardly any variance between each bus. While at higher amounts of storage B6 and

B5 buses still proved to be more expensive than other buses, for the most part the values were consistent

across all buses.

Table 4-8: Percent Cost Difference Grid between 9-bus Single and Double-Line Solar REG, Summer Day

Bus Distance/ Size (MW)	No Storage	0 Bus	B9 (1 Bus)	B6 (2 Bus)	B8 (2 Bus)	B7 (3 Bus)	B4 (3 Bus)	B5 (4 Bus)	Bgen2 (4 Bus)
10	-0.682	-0.685	-0.684	-0.688	-0.677	-0.670	-0.671	-0.674	-0.673
30	-0.682	-0.666	-0.665	-0.656	-0.655	-0.642	-0.637	-0.643	-0.645
50	-0.682	-0.617	-0.616	-0.597	-0.612	-0.602	-0.592	-0.596	-0.605
70	-0.682	-0.535	-0.534	-0.507	-0.547	-0.548	-0.535	-0.528	-0.553
90	-0.682	-0.424	-0.423	-0.390	-0.462	-0.483	-0.465	-0.445	-0.486
110	-0.682	-0.279	-0.279	-0.246	-0.354	-0.407	-0.383	-0.343	-0.409
130	-0.682	-0.105	-0.105	-0.074	-0.223	-0.318	-0.290	-0.224	-0.320

From the new percent cost difference grid above in Table 4-8, the change in overall system operating costs changed by -0.682 % just by adding line redundancy. In addition, while every case was cheaper than that of the single-line case, the line redundancy had the most impact within the 10-30 MW range at every bus. This would lead to the conclusion that all things equal, this system with redundant lines still benefitted most from the smaller sizes of storage. This was again unexpected, as the original prediction was that the addition of line redundancy and doubling capacity would affect the cases with larger storage more than those with smaller amounts of storage, since congestion was such a large factor at high amounts of storage.

The superimposed scatterplot (Figure 4-14) for this data again revealed that the double-line cases were much cheaper than the single-line cases. In blue is the original, change in costs for the single-line cases, while in green is the change in cost of the double-line compared to the single-line case data. While this could be due to the fact that more line capacity in this system reduced the effects of congestion when adding storage, the reduction of overall system costs was still achieved by adding line capacity alone, challenging the usage of energy storage.
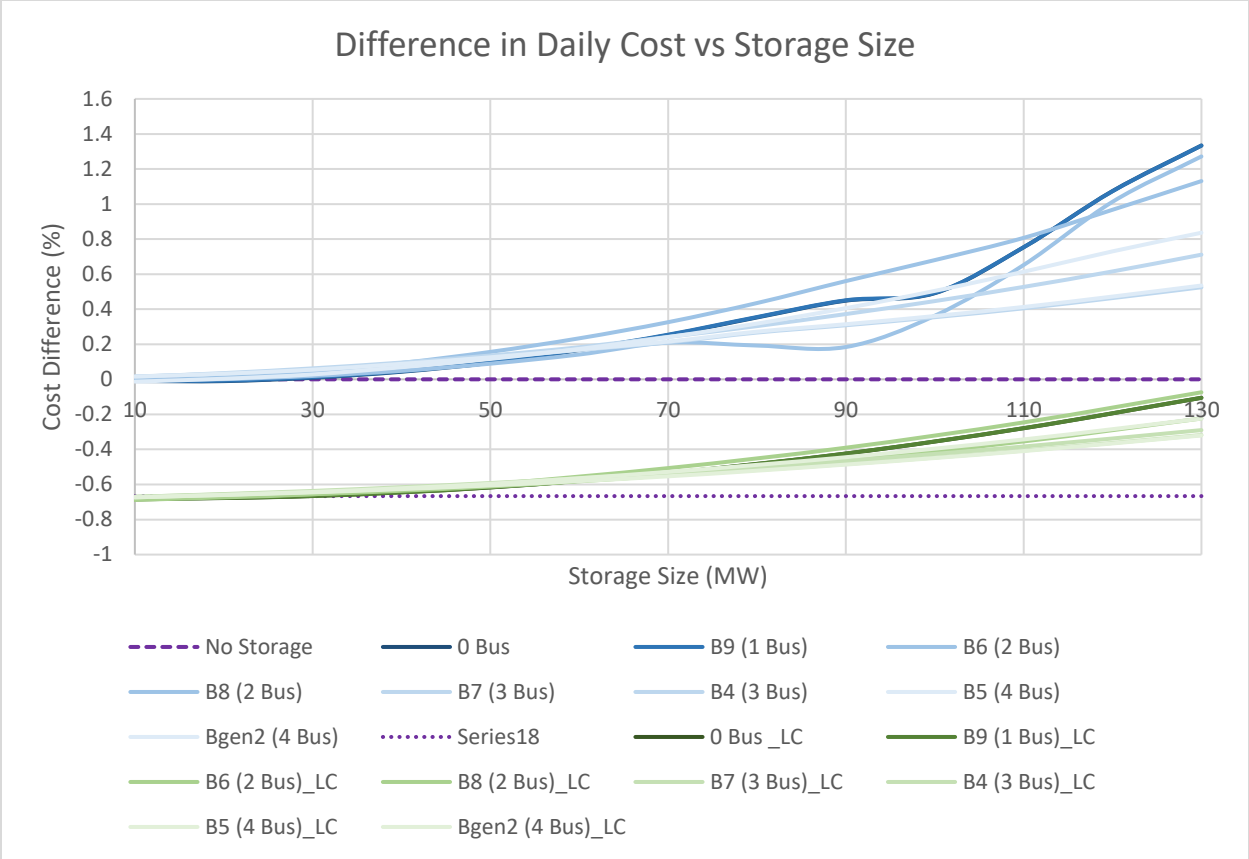
Figure 4-14: Percent Cost Difference Scatter Plot for 9-bus Single and Double-Line Solar REG, Summer Day

4.2.3 Wind REG on a Fall Day

For the base case of wind REG on a fall day, the percent cost difference grid can be observed in Table 4-9 below.

Table 4-9: Percent Cost Difference Grid for 9-bus Double-Line Wind REG, Fall Day

Bus Distance/ Size (MW)	0 Bus	B9 (1 Bus)	B6 (2 Bus)	B8 (2 Bus)	B7 (3 Bus)	B4 (3 Bus)	B5 (4 Bus)	Bgen2 (4 Bus)
10	-0.005	-0.004	-0.007	0.003	0.012	0.013	0.011	0.008
30	0.011	0.012	0.030	0.025	0.040	0.051	0.046	0.037
50	0.061	0.062	0.097	0.071	0.082	0.102	0.100	0.079
70	0.147	0.147	0.197	0.141	0.138	0.167	0.175	0.134
90	0.266	0.267	0.328	0.236	0.208	0.247	0.271	0.205
110	0.422	0.422	0.492	0.355	0.290	0.339	0.387	0.288
130	0.612	0.612	0.688	0.498	0.393	0.445	0.522	0.390

For the 9-bus Double-Line Wind Fall case set, the most money was saved when injecting 10 MW of storage at bus B6 (2 buses away). **Thus, the optimum size for this fall case set was 10 MW placed at bus B6, 2 buses away from the Wind Farm.** This was not consistent with the 9-bus Single-Line Wind Fall case set. However, as with every case set so far, increasing injection size of storage led to increased overall costs but at different rates depending on the bus.

Creating the scatter plot of Figure 4-15, below, the relationships for injected storage on every bus could be represented by 2nd order polynomials. This was not consistent with the single-line case set at all, as most bus relationships were represented by much more complex polynomials.
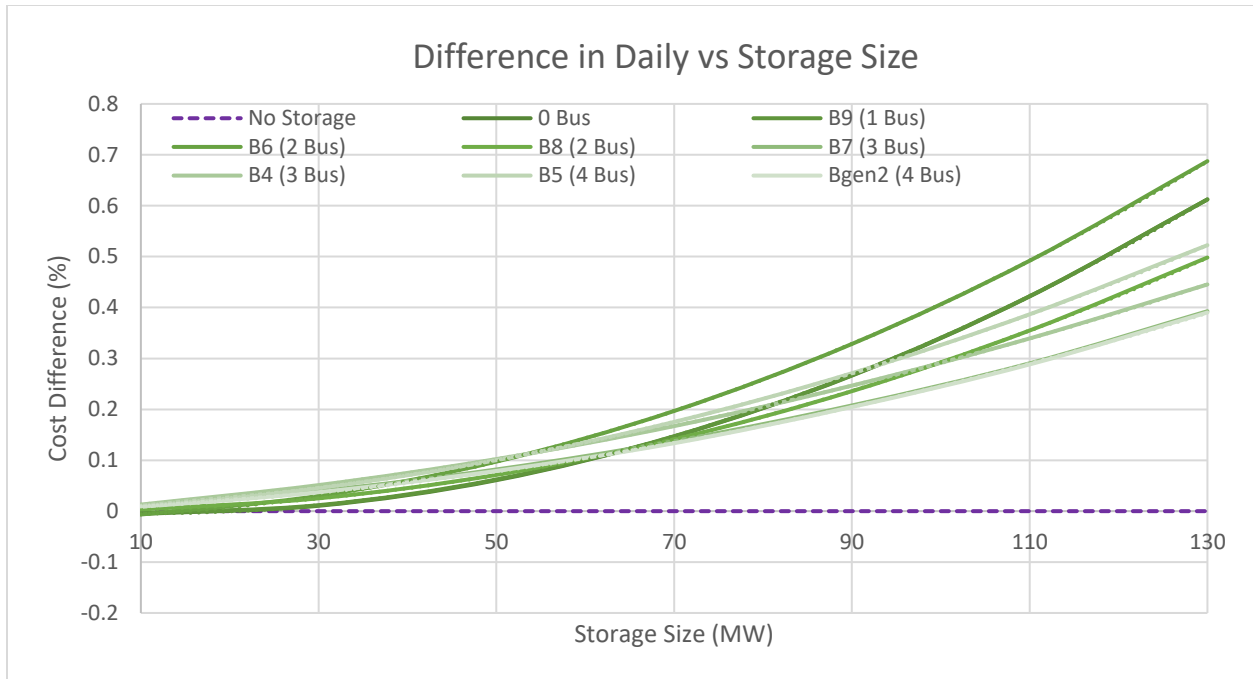
Figure 4-15: Percent Cost Difference Scatter Plot for 9-bus Double-Line Wind REG, Fall Day

Looking at the 3-D surface plot for this data set the local maximum occurred at 130 MW of injected storage at bus B6 (2 buses away), while the local minimum occurred at 30 MW of storage also at B6. As with the previous double-line case sets, larger sizes of storage had less of an effect on the system costs, despite having had a bigger impact on system costs in the single-line cases. Whereas previously the maximum percent cost difference for the single-line case set was 1.357 %, the maximum percent cost difference here was almost exactly half of that at 0.688 %. While not every case had percent cost differences half as much as their single-line counterparts, they were all significantly reduced.
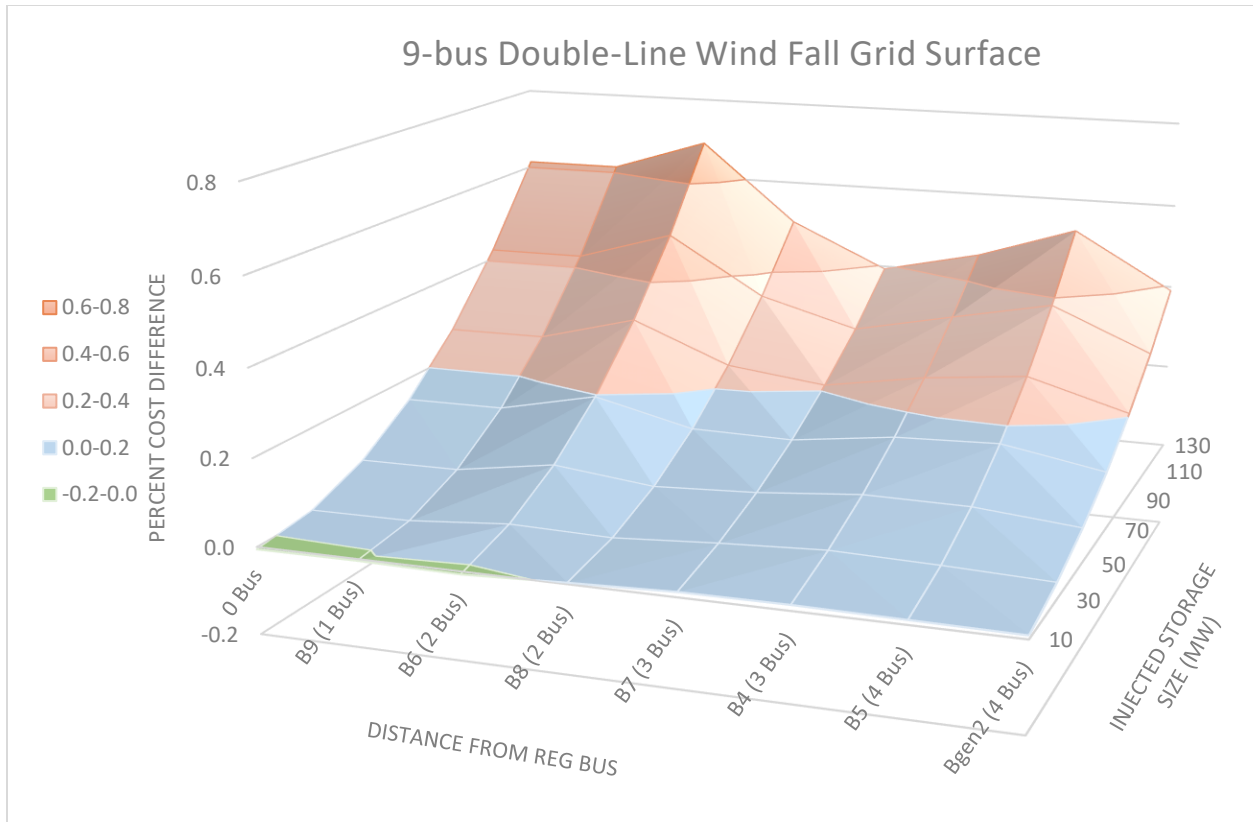
Figure 4-16: 3-D Surface Plot for 9-bus Double-Line Wind REG, Fall Day

Inconsistent with the corresponding single-line case set, this plot indicated for the most part **injecting storage on some buses yields overall higher costs than at other buses regardless of size**. Buses B6 and B5 (2 and 4 buses away) were for the most part the most expensive buses for storage injection in the system. On the other hand, buses B8 and B7 (2 and 3 buses away) were for the most part the least expensive buses for storage injection in the system.

Table 4-10: Percent Cost Difference Grid between 9-bus Single and Double-Line Wind REG, Fall Day

Bus Distance/ Size (MW)	No Storage	0 Bus	B9 (1 Bus)	B6 (2 Bus)	B8 (2 Bus)	B7 (3 Bus)	B4 (3 Bus)	B5 (4 Bus)	Bgen2 (4 Bus)
10	-0.666	-0.672	-0.670	-0.673	-0.663	-0.655	-0.654	-0.656	-0.658
30	-0.666	-0.656	-0.655	-0.637	-0.641	-0.627	-0.615	-0.621	-0.629
50	-0.666	-0.606	-0.605	-0.570	-0.596	-0.585	-0.565	-0.567	-0.588
70	-0.666	-0.521	-0.520	-0.471	-0.526	-0.530	-0.500	-0.492	-0.534
90	-0.666	-0.402	-0.401	-0.340	-0.432	-0.460	-0.421	-0.397	-0.463
110	-0.666	-0.247	-0.247	-0.178	-0.314	-0.378	-0.329	-0.282	-0.380
130	-0.666	-0.058	-0.058	0.017	-0.171	-0.276	-0.224	-0.147	-0.279

Observing the new percent cost difference grid above in Table 4-10, the change in overall system operating costs changed by -0.666 % just by adding line redundancy. In addition, this was the first case set in which there existed a case that had more expensive operating costs than the single-line base case. The 130 MW case on bus B6 was slightly more expensive than the no-storage single-line base case, suggesting that congestion can still be a factor on certain buses, even for systems with added capacity.

On the other hand, while **the line redundancy had great impact between 10 and 30 MW on every bus, the greatest impact occurred at 10 MW on bus B6**. This would support the conclusion that bus B6 represents an area in the system in which congestion could occur more easily given higher load flows. While a small amount of storage in a single-line system would benefit the system if placed at bus B6, it would benefit the system even more in a double-line system. Conversely, larger amounts of storage would eventually not become uneconomical as they would begin to add to the increased load flows, adding to the congestion overall.

Superimposing the comparison data onto the original scatter plot, this becomes easier to visualize. In blue is the original, change in costs for the single-line cases, while in green is the change in cost of the double-line compared to the single-line case data.
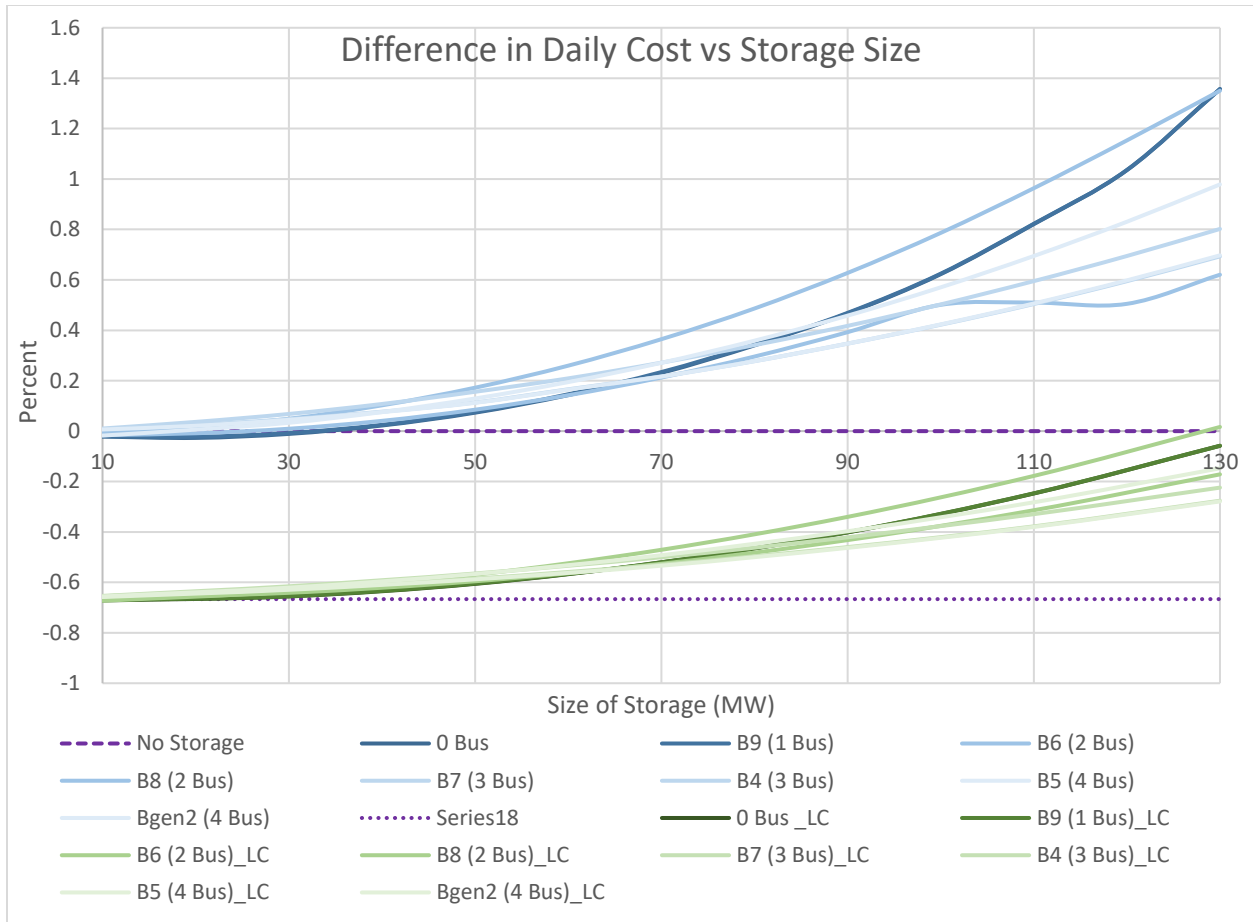
Figure 4-17: Percent Cost Difference Scatter Plot for 9-bus Single and Double-Line Wind REG, Fall Day

From Figure 4-17 alone, the double-line cases were much cheaper than the single-line base case, except for the 130 MW case at bus B6. Again, while this could be because more line capacity reduced the effects of congestion when adding storage, the reduction of overall system costs was still achieved by adding line capacity alone, challenging the usage of energy storage.

4.2.4   Wind REG on a Summer Day

For the base case of wind REG on a summer day, the percent cost difference grid can be observed in Table 4-11 below.

Table 4-11: Percent Cost Difference Grid for 9-bus Double-Line Wind REG, Summer Day

Bus Distance/ Size (MW)	Bgen3 (0 Bus)	B9 (1 Bus)	B6 (2 Bus)	B8 (2 Bus)	B7 (3 Bus)	B4 (3 Bus)	B5 (4 Bus)	Bgen2 (4 Bus)
10	0.010	0.012	-0.009	0.012	0.018	0.010	0.005	0.014
30	0.058	0.060	0.025	0.051	0.061	0.043	0.032	0.057
50	0.143	0.146	0.090	0.115	0.116	0.090	0.078	0.112
70	0.269	0.267	0.191	0.205	0.190	0.152	0.147	0.186
90	0.429	0.431	0.326	0.321	0.276	0.227	0.238	0.273
110	0.626	0.627	0.494	0.463	0.377	0.319	0.350	0.374
130	0.860	0.861	0.697	0.630	0.493	0.424	0.484	0.490

For the 9-bus Double-Line Wind Summer case set, the most money was saved again when injecting 10 MW of storage at bus B6 (2 buses away). **Thus, the optimum size for this summer case set was 10 MW placed at bus B6, 2 buses away from the Wind Farm.** This was not consistent with the 9-bus Single-Line Wind Summer case set.

Creating the scatter plot of Figure 4-18, below, the relationships for injected storage on every bus again could be represented by 2nd order polynomials. This was not consistent with the single-line case set at all, as most bus relationships were represented by much more complex polynomials.

Figure 4-18: Percent Cost Difference Scatter Plot for 9-bus Double-Line Wind REG, Summer Day

Looking at the 3-D surface plot for this data set the local maximum occurred at 130 MW of injected storage at buses Bgen3 or B9 (0 and 1 buses away) while the local minimum occurred at 30 MW of storage at B6. As with the previous double-line case sets, larger sizes of storage had less of an effect on the system costs, despite having had a bigger impact on system costs in the single-line cases. Whereas previously the maximum percent cost difference for the single-line case set was 1.589 %, the maximum percent cost difference here was a bit over half of that at 0.861 %. While not every case had percent cost differences as drastic compared to their single-line counterparts, they were all significantly reduced.
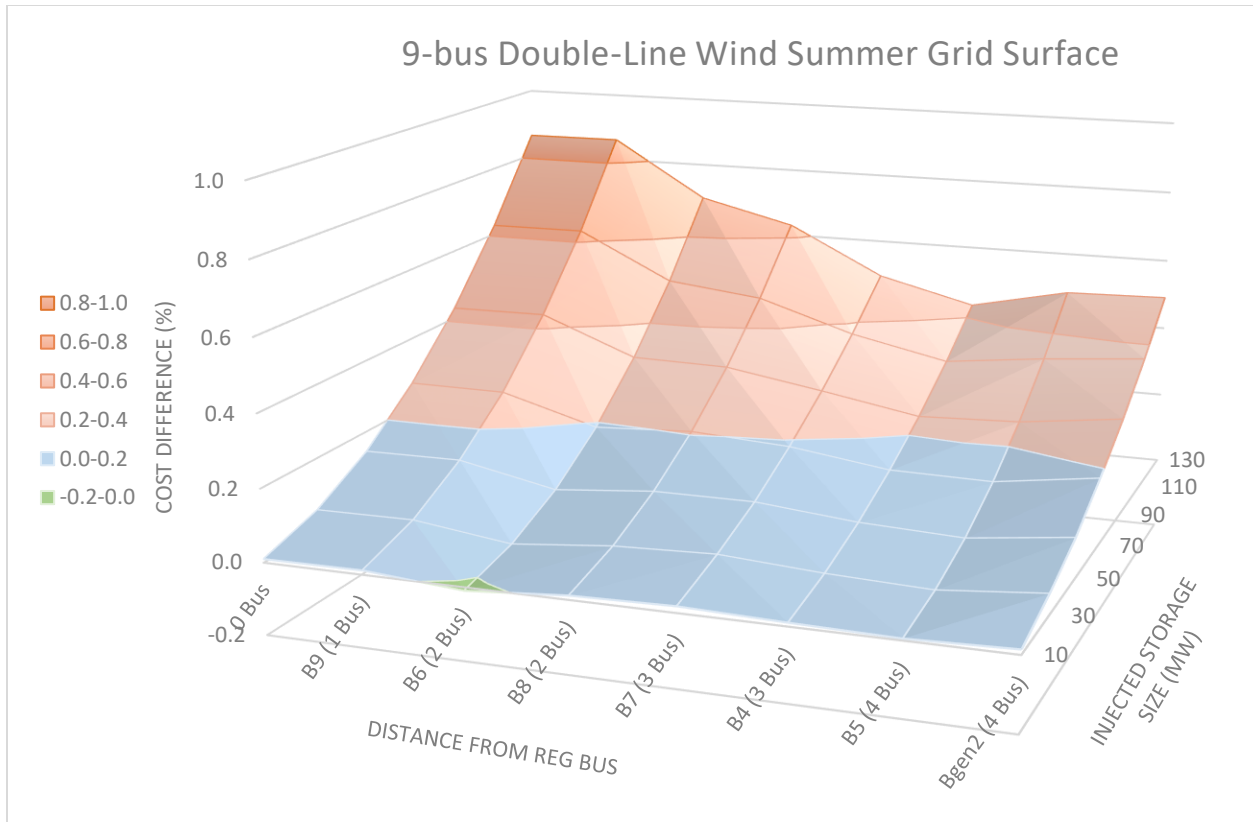
Figure 4-19: 3-D Surface Plot for 9-bus Double-Line Wind REG, Summer Day

Consistent with the corresponding single-line set, this plot was by far the smoothest out of the other four case sets studied. With a local maximum occurring at 130 MW injected at the REG bus and a local minimum occurring at 10 MW injected at bus B6 (2 buses away), the overarching trend discussed in the single-line set that **overall system costs decrease as storage size decreases and injection location increases** was less defined, but still present.

Table 4-12: Percent Cost Difference Grid between 9-bus Single and Double-Line Wind REG, Summer Day

Bus Distance/ Size (MW)	No Storage	0 Bus	B9 (1 Bus)	B6 (2 Bus)	B8 (2 Bus)	B7 (3 Bus)	B4 (3 Bus)	B5 (4 Bus)	Bgen2 (4 Bus)
10	-0.805	-0.795	-0.793	-0.814	-0.793	-0.787	-0.795	-0.800	-0.791
30	-0.805	-0.748	-0.746	-0.781	-0.755	-0.745	-0.763	-0.773	-0.749
50	-0.805	-0.663	-0.661	-0.715	-0.691	-0.690	-0.716	-0.727	-0.694
70	-0.805	-0.538	-0.540	-0.615	-0.601	-0.617	-0.655	-0.659	-0.620
90	-0.805	-0.380	-0.378	-0.482	-0.487	-0.531	-0.579	-0.569	-0.535
110	-0.805	-0.184	-0.183	-0.315	-0.346	-0.431	-0.489	-0.458	-0.434
130	-0.805	0.048	0.049	-0.114	-0.180	-0.316	-0.384	-0.325	-0.319

Observing the new percent cost difference grid above in Table 4-12, the change in overall system operating costs changed by -0.805 % just by adding line redundancy. This was by far the cheapest base case. As with the previous double-line wind set, this set also contained cases that were more expensive than the single-line base. The 130 MW case on buses Bgen3 and B9 were slightly more expensive than the no-storage single-line base case. On the other hand, while **the line redundancy had great impact between 10 and 30 MW on every bus, the greatest impact occurred at 10 MW on bus B6**.

Superimposing the comparison data onto the original scatter plot, this becomes easier to visualize. In blue is the original, change in costs for the single-line cases, while in green is the change in cost of the double-line compared to the single-line case data.
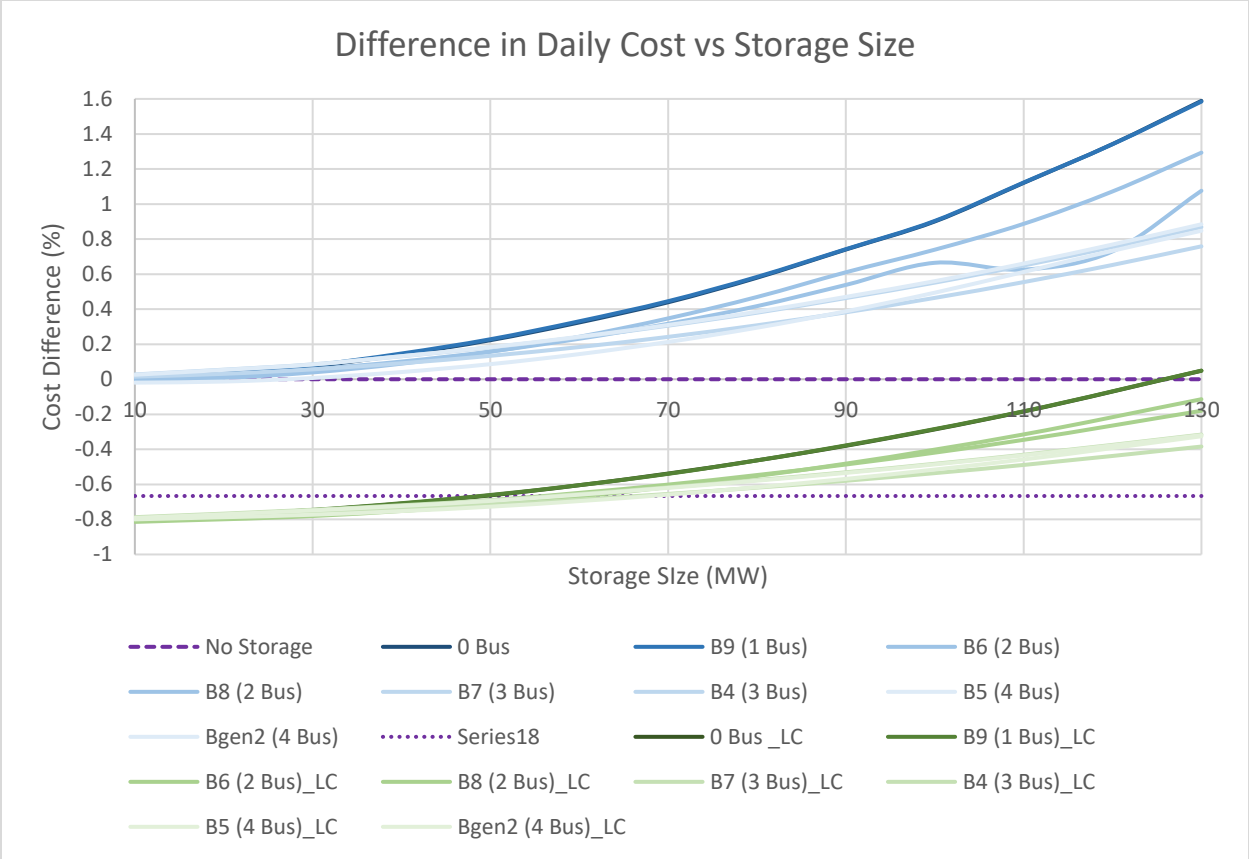
Figure 4-20: Percent Cost Difference Scatter Plot for 9-bus Single and Double-Line Wind REG, Summer Day

From Figure 4-20 alone, the double-line cases were much cheaper than the single-line base case, except for the two 130 MW cases at buses Bgen3 and B9. Again, while this could be because more line capacity reduced the effects of congestion when adding storage, the reduction of overall system costs was still achieved by adding line capacity alone, challenging the usage of energy storage.

4.2.5   9-bus Double-Line Cases Discussion

Considering all four double-line case sets studied, some general conclusions can be made. First, the overall daily cost increased as storage sized increased with different relationships for different injection buses. This was consistent across all cases, including the single-line cases. This makes sense as the capital

costs are indeed larger for larger sizes of storage. These relationships were much easier to model than the relationships in the single-line cases. Thus, a congested system will create more complicated relationships between the percent cost difference and injected storage size, whereas a system with added line capacity and less congestion will likely yield relationships that are easier to model.

Second, when comparing the four double-line 3-D surface plots, two new patterns could be observed. Looking at the two fall plots, both buses B6 and B5 appear to be consistently the two most expensive buses regardless of storage size, although this is certainly more pronounced for larger sizes of storage. Similarly, bus B7 consistently appears to be the least expensive bus for either system regardless of size. The only exception appears at 10 MW of storage, where B6 is for both sets the cheapest bus. This suggests that the fall load profile creates a scenario within 9-bus double-line system in which the areas surrounding buses B6 and B5 become more congested, and that of bus B7 becomes less congested, regardless of the renewable source. In addition, when comparing the Percent Cost Difference Scatter Plots, there was no longer dips in the cost differences at bus B8 under heavy storage injection. Instead, the relationships at bus B8 were like the other buses, suggesting that congestion was significantly reduced at bus B8. This further reinforces the idea that congestion creates less predictable cost difference relationships.

When observing the two summer case sets, apart from the 10 MW range there is a clear indication that overall system costs decrease as storage size decreases and injection location increases. Conversely, the system costs increase as storage size increases and injection location decreases. This suggests that the summer load profile creates a scenario within the 9-bus double-line system in which small amounts of storage injected farthest from the REG resulted in reduced system costs, while large amounts injected closest to the REG resulted in significantly increased system costs, regardless of renewable source.

Third, larger storage sizes relative to the size of the system (or more specifically the size of the REG) may not be economical, even for the double-line cases. While they were much more economical than in the single-line cases, they were still more expensive then not including storage at all.

When focusing on the economical cases themselves, there were hardly any cases in which injecting storage was cheaper than the cases without storage. The fact that there were fewer cost-effective cases for the double-line case sets than the single-line case sets was unanticipated as the prediction was that the addition of line redundancy (keeping all else equal) would create more opportunities for cost savings, not less. For the cases that were economical, the injected size was also much smaller than expected, and the costs saved from utilizing storage were extremely small, never exceeding 0.014 %. For such a tiny cost savings, it may be hard to justify going through the process of building and installing storage for systems like the double-line 9-bus systems tested.

It is important to note that this is only comparing double-line scenarios to the double-line bases. Looking at it from a different perspective, the double-line scenarios can be compared to the respective single-line bases. If the single-line bases are used to compare the overall costs instead of the double-line bases, very different results are obtained. Every double-line base was significantly more economical than their respective single-line bases, with savings ranging from 0.596 % to 0.805 % of the original system cost. Because the savings on the double-line base cases were so high, almost every scenario with added energy storage also had high savings.

However, the results from this perspective should be considered carefully, and with hesitation. First, while almost every scenario had high cost savings, any scenario with less cost savings than the respective base case is an indication that the storage is adversely affecting the system costs, negating the cost savings created by the additional line capacity. This implies that again there are far fewer cases in which storage is beneficial within a double-line system, even when comparing the results to the single-line base case. Thus, in a double-line system small amounts of storage can still create more economical scenarios, but larger storage sizes reduce the cost savings, confirming that large storage sizes in relation to the size of REG are still not economical, nor practical.

Additionally, these comparisons do not consider the capital costs of adding additional lines to the systems. Powerworld has a powerful cost model for the operation of generators and thus storage, but it

cannot easily model the fixed costs of installing transmission lines. While the double-line cases had significant cost savings both with and without storage, it would be interesting to verify whether the cost savings existed when adjusting for the capital costs of installing additional lines.

4.3   13-bus Single-Line Cases

At this point, there are some interesting trends appearing with the 9-bus models, and it would be interesting to see if these trends held true within other test beds. While ideally both single- and double-line models could be tested, only single-line models were tested further because of the drawback of not being able to accurately include the capital costs of installing redundant lines within an original test system. Moreover, due to limitations of the Powerworld software used, any additional test system still needed to be under 13 buses or modified to fit within the 13-bus constraint. Conveniently, the IEEE resources contained a 14-bus test system with a different configuration than the 9-bus, allowing for potentially different results. Since the system was 14 buses, it needed to be modified, but the modifications were simple as there was only a need to combine two buses into one. The new 13-bus system was much more interconnected than the 9-bus, but also much less balanced. There were more loads than the 9-bus system, but they were individually smaller and more distributed throughout the system, with some loads more than one bus away from a generator. In addition, there were more generators, and while interconnected to other buses, three of them were clumped together, each being no more than one bus away from the other.

Thus, the final data set to be discussed are the 13-bus single-line cases. This set consisted of all the cases that utilized the modified 14-bus test bed with only single transmission lines connecting each bus as described in Section 3.6. There were four test beds in this set: two beds with solar REG and two beds with wind REG each on a fall and summer day respectively.

102

For each case set, percentage cost difference grids were created to observe the initial trends. The values within the grids were color-coded to better highlight the changes in cost at each bus. Grid values in green represented cases in which it was more economical to inject storage. Grid values in blue represented cases in which it was more expensive to inject storage, but cost difference was very little. Grid values in shades of orange represented cases in which it was significantly more expensive to inject storage, with the highest costs shaded darker. Each color shade represented a range of 1.0 %. In addition to percentage cost difference grids, scatter plots and 3-D topographical surface plots were created based on the grid data. The scatter plots helped to determine the ease of estimating the mathematical relationships of daily cost difference versus injected storage size based at different locations, while the 3-D plots allowed for better visualization of the overall cost trends.

4.3.1 Solar REG on a Fall Day

For the base case of solar REG on a fall day, the percent cost difference grid can be observed in Table 4-13 below.
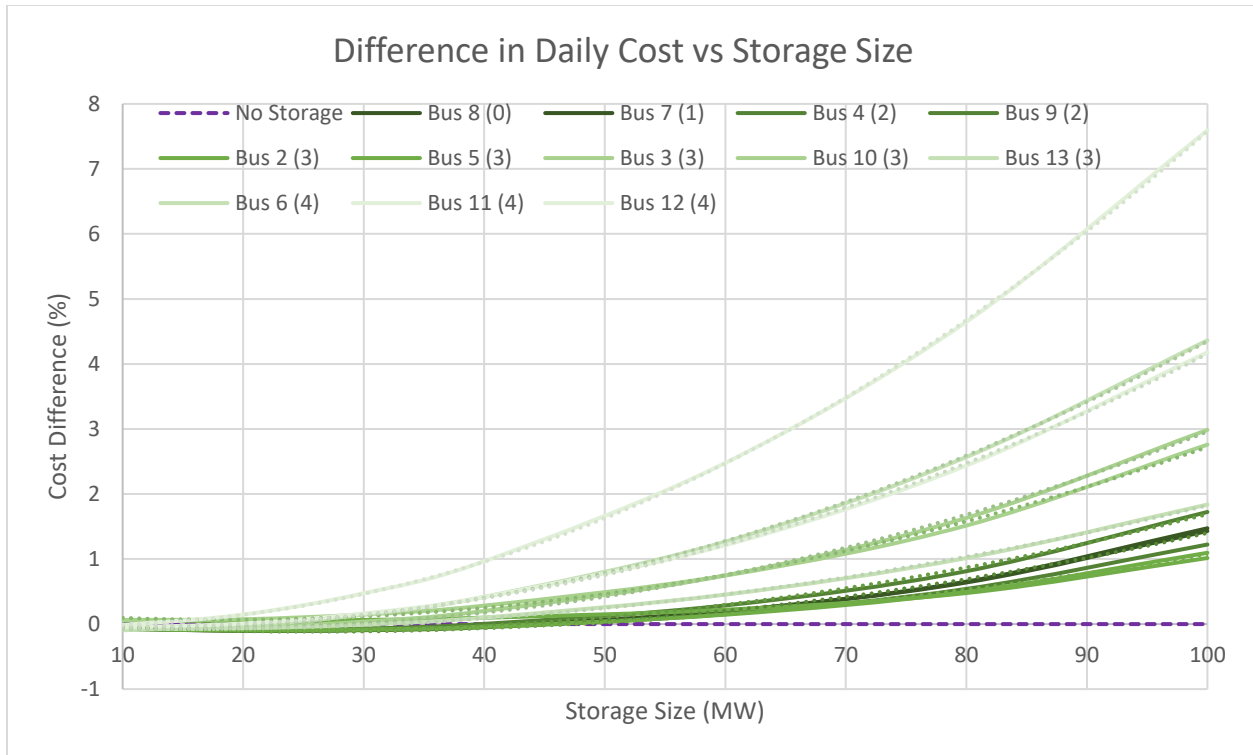
Table 4-13: Percent Cost Difference Grid for 13-bus Solar REG, Fall Day

Bus Dis./ Size (MW)	Bus 8 (0)	Bus 7 (1)	Bus 4 (2)	Bus 9 (2)	Bus 2 (3)	Bus 5 (3)	Bus 3 (3)	Bus 10 (3)	Bus 13 (3)	Bus 6 (4)	Bus 11 (4)	Bus 12 (4)
10	-0.069	0.171	0.185	0.244	-0.025	0.258	-0.037	0.355	0.409	0.220	0.407	0.450
20	-0.110	0.131	0.148	0.205	-0.033	0.239	-0.025	0.355	0.473	0.236	0.457	0.615
30	-0.118	0.124	0.136	0.202	-0.023	0.243	0.039	0.417	0.624	0.290	0.591	0.921
40	-0.090	0.143	0.163	0.244	0.002	0.269	0.157	0.540	0.862	0.385	0.805	1.371
50	-0.028	0.206	0.227	0.326	0.044	0.328	0.328	0.725	1.187	0.526	1.103	1.976
60	0.069	0.304	0.324	0.447	0.108	0.422	0.573	0.973	1.605	0.709	1.487	2.735
70	0.201	0.439	0.450	0.608	0.183	0.537	0.834	1.285	2.112	0.941	1.952	3.658
80	0.368	0.616	0.604	0.811	0.275	0.697	1.169	1.660	2.712	1.215	2.507	4.749
90	0.569	0.823	0.789	1.057	0.384	0.859	1.558	2.100	3.405	1.530	3.150	6.018
100	0.808	1.067	1.005	1.345	0.510	1.049	2.001	2.606	4.195	1.892	3.885	7.480

From this chart alone some initial conclusions can be drawn. First, for the 13-bus Solar REG Fall cases, the most money was saved when injecting 30 MW of storage at the REG bus (Bus 8). **Thus, the optimum size for this fall case set was 30 MW placed at the Solar Farm bus.** Secondly, as the injection size of storage increased, the overall costs increased, but at different rates depending on the bus. However, the actual relationships were hard to determine based on the numbers of the cost difference grid alone.

Looking at the scatter plot of Figure 4-21, below, the relationships for injected storage on every bus could be represented by 2nd order polynomials, suggesting that the percent cost difference depends on the size of storage squared, and is easy to quantify.
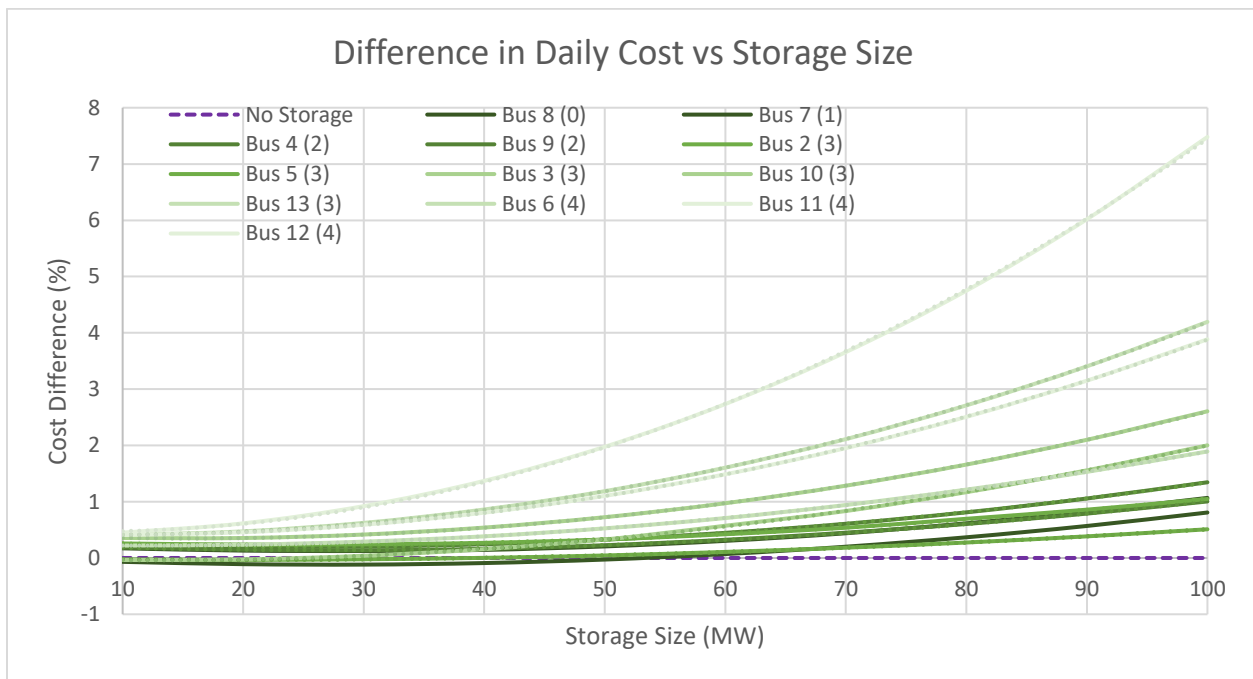
Figure 4-21: Percent Cost Difference Scatter Plot for 13-bus Solar REG, Fall Day

Maintaining the same color-coding as displayed in the Cost Difference Grid from Table 4-13 the data was transposed into a 3-D Topographical Surface Plot. With each color representing a 1.0 % difference, this plot clearly indicates additional general trends, as well as verifying previously mentioned points. As was

made clear in the grid from Table 4-13, the local maximum for this data set occurred at 100 MW of injected storage at bus 12 (4 buses away), while the local minimum occurred at 30 MW of storage at the REG bus (Bus 8).
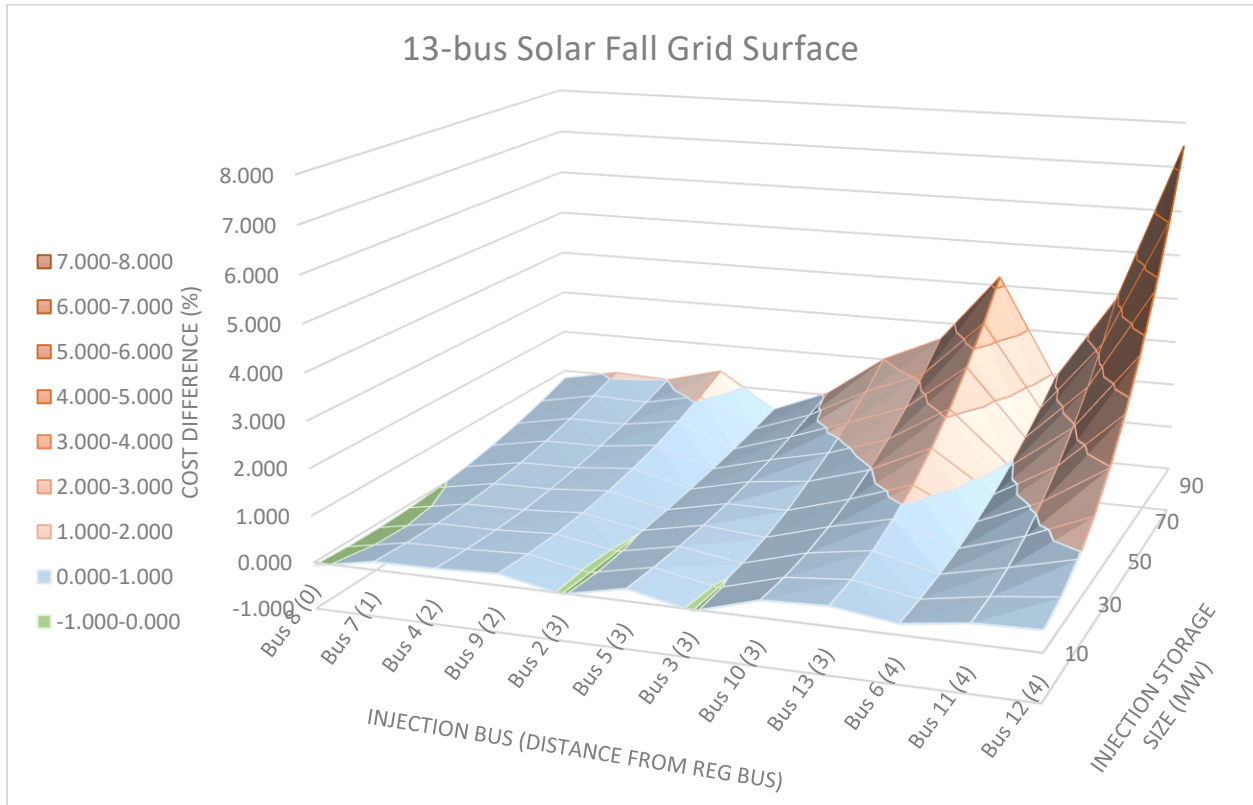
Figure 4-22: 3-D Surface Plot for 13-bus Solar REG, Fall Day

This plot indicated three clear patterns:

1) Injecting storage on some buses yields overall higher costs than at other buses regardless of size, while injection at other buses yields overall lower costs.

For example, buses 10, 13, 11 and 12 (3, 3, 4 and 4 buses away respectively) were the most expensive buses, with higher costs than any other bus at a given storage size. On the other hand, buses 8, 4, 2 and 6 (0, 2, 3, and 4 buses away) were the least expensive buses with lower costs than any other bus at a given storage size.

2) As storage size increased and distance from REG bus increased, the cost generally increased.

While there was some exception to this rule (with certain buses breaking the trend), for the most part as the injection location of the storage moved farther away from the REG bus, and as the storage size increased, the percentage cost difference increased as well. In addition, generally the incremental cost difference increased as the size increased and the storage location moved farther away. For example, the costs at bus 8 (the REG bus) were minimized for the smaller storage sizes, but even at larger sizes the cost differences never exceeded 1.0 %. Compare that to bus 12 (4 buses away) at the opposite end of the plot where the costs were minimized for the smaller storage sizes, and maximized for the largest storage sizes. Here the percent cost difference for 100 MW at bus 12 was nearly 7 times as large as that at bus 8, despite it being the only bus to reach that magnitude. Buses 2 and 6 were the only buses to go against this trend. Their behavior can be explained by the first observation, since different buses represent different areas of the system each with different properties affecting the cost differently.

3) Generally, buses closer to the REG were overall less expensive with more comparable costs than buses farther from the REG.

Buses 8, 7, 4, 9, 2 and 5 (0, 1, 2, 2, 3 and 3 buses away) yielded costs that were all well under 1.5 %, with most of cases under 0.5 %. While increasing the storage size did increase the costs, the difference was not nearly as significant for these buses as compared to the buses farther away. Buses 8 and 2 were the cheapest out of the group mentioned, while buses 7, 4 and 9 were comparable to each other, but more expensive than the rest.

4.3.2   Solar REG on a Summer Day

For the base case of solar REG on a summer day, the percent cost difference can be observed in Table 4.1 below.
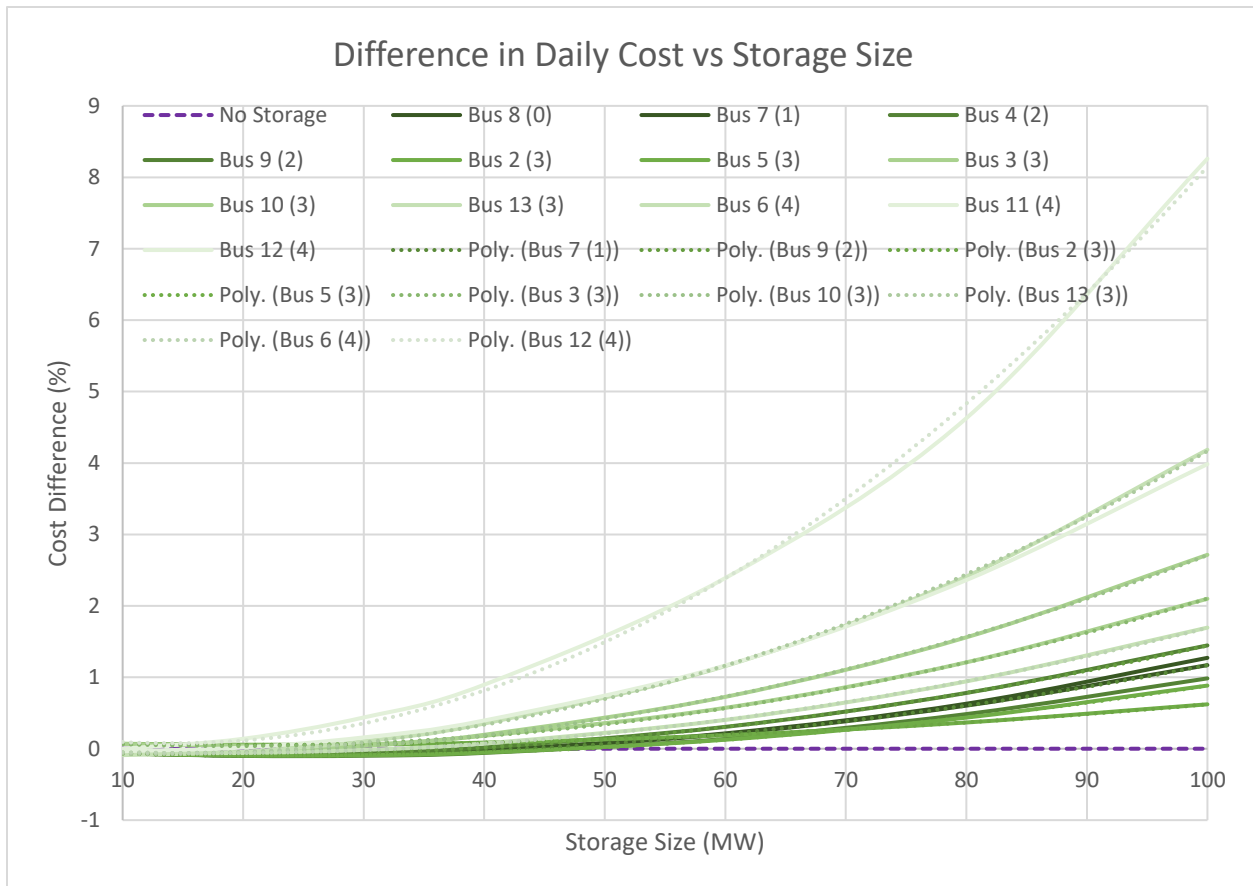
Table 4-14: Percent Cost Difference Grid for 13-bus Solar REG, Summer Day

Bus/ Size (MW)	Bus 8 (0)	Bus 7 (1)	Bus 4 (2)	Bus 9 (2)	Bus 2 (3)	Bus 5 (3)	Bus 3 (3)	Bus 10 (3)	Bus 13 (3)	Bus 6 (4)	Bus 11 (4)	Bus 12 (4)
10	-0.061	-0.058	-0.052	-0.056	0.056	-0.057	0.079	-0.049	-0.056	-0.034	-0.023	0.016
20	-0.087	-0.084	-0.080	-0.076	0.050	-0.073	0.085	-0.035	-0.005	-0.025	0.028	0.147
30	-0.073	-0.073	-0.072	-0.055	0.060	-0.062	0.142	0.037	0.151	0.028	0.154	0.426
40	-0.025	-0.027	-0.032	0.007	0.087	-0.021	0.251	0.169	0.383	0.122	0.373	0.846
50	0.058	0.056	0.040	0.113	0.130	0.048	0.415	0.370	0.702	0.258	0.667	1.424
60	0.177	0.173	0.146	0.248	0.189	0.145	0.633	0.631	1.115	0.437	1.051	2.159
70	0.335	0.327	0.286	0.432	0.264	0.270	0.903	0.956	1.627	0.659	1.525	3.059
80	0.532	0.517	0.459	0.656	0.349	0.426	1.227	1.350	2.246	0.931	2.092	4.150
90	0.770	0.743	0.663	0.923	0.457	0.610	1.608	1.817	2.982	1.243	2.752	5.535
100	1.056	1.008	0.900	1.232	0.578	0.822	2.044	2.357	3.872	1.604	3.521	7.539

From this chart alone some initial conclusions can be drawn. First, for the 13-bus Solar REG Summer cases, the most money was saved when injecting 20 MW of storage at the REG bus (Bus 8). **Thus, the optimum size for this fall case set was 20 MW placed at the Solar Farm bus.** Secondly, as the injection size of storage increased, the overall costs increased, but at different rates depending on the bus. However, the actual relationships were hard to determine based on the numbers of the cost difference grid alone.

Looking at the scatter plot of Figure 4-23, below, the relationships for injected storage on every bus could be represented by 2nd order polynomials, suggesting that the percent cost difference depends on the size of storage squared, and is easy to quantify.
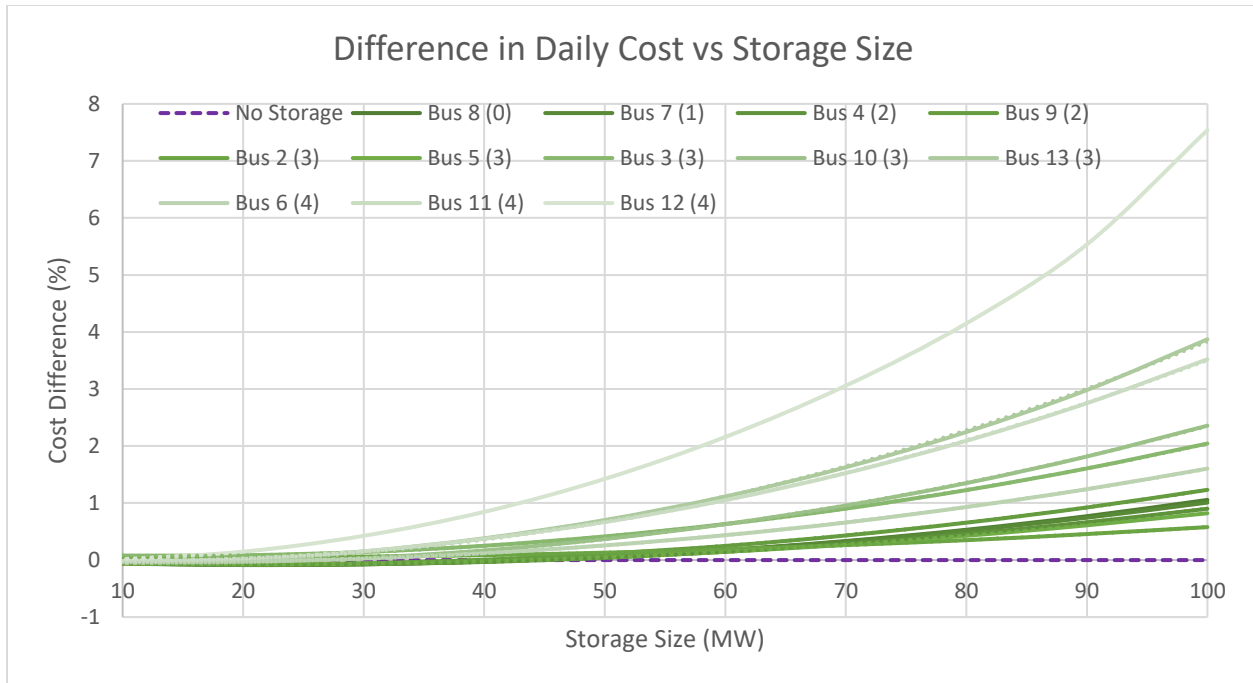
Figure 4-23: Percent Cost Difference Scatter Plot for 13-bus Solar REG, Summer Day

Maintaining the same color-coding as displayed in the Cost Difference Grid from Table 4-14 the data was transposed into a 3-D Topographical Surface Plot. With each color representing a 1.0 % difference, this plot clearly indicates additional general trends, as well as verifying previously mentioned points. As was made clear in the grid from Table 4-14, the local maximum for this data set occurred at 100 MW of injected storage at bus 12 (4 buses away), while the local minimum occurred at 20 MW of storage at the REG bus (Bus 8).
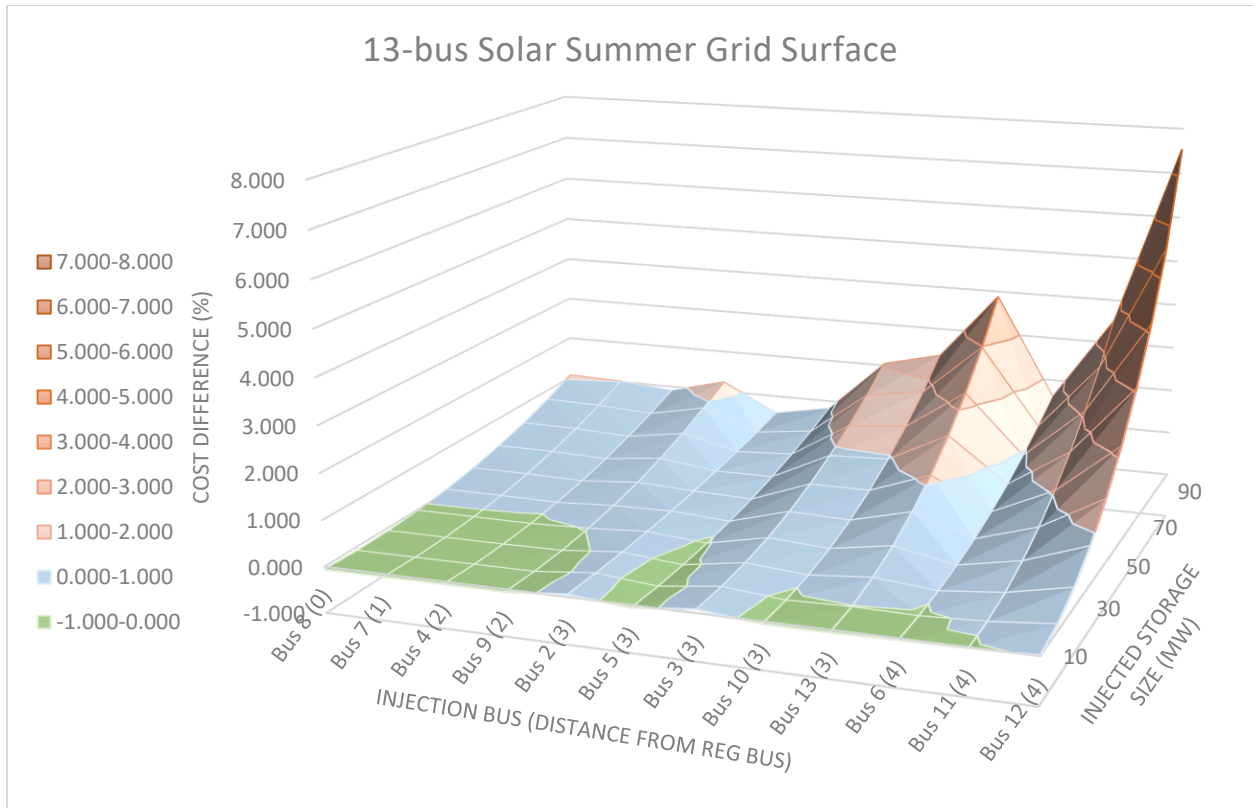
Figure 4-24: 3-D Surface Plot for 13-bus Solar REG, Summer Day

This plot indicated three clear patterns:

1) Injecting small amounts of storage on most buses yielded cost savings.

For example, almost every bus except buses 2, 3 and 12 had at least one case in which the cost difference was negative. Most buses however had cost savings between 10 and 20 MW of injected storage.

2) As storage size increased and distance from REG bus increased, the cost generally increased.

While there was more exception to this rule than in the fall case set (with certain buses breaking the trend), for the most part as the injection location of the storage moved farther away from the REG bus, and as the storage size increased, the percentage cost difference increased as well. In addition, generally the incremental cost difference increased as the size increased and the storage location moved farther away. For example, the costs at bus 8 (the REG bus) were minimized for the smaller storage sizes, but

109

even at larger sizes the cost differences barely exceeded 1.0 %. Compare that to bus 12 (4 buses away) at the opposite end of the plot where the costs were minimized for the smaller storage sizes, and maximized for the largest storage sizes. Here the percent cost difference for 100 MW at bus 12 was over 7 times as large as that at bus 8, despite it being the only bus to reach that magnitude. There were a few more buses here than in the fall case set that went against this trend, suggesting that the summer load profile affects the system costs differently at certain buses than the fall load profile.

3) Generally, buses closer to the REG were overall less expensive with more comparable costs than buses farther from the REG.

This trend was much more noticeable than in the fall set. Buses 8, 7, 4, 9, 2 and 5 (0, 1, 2, 2, 3 and 3 buses away) all yielded costs that were well under 1.5 %, with the clear majority of cases under 0.5 %. While increasing the storage size did increase the costs, the difference was not nearly as significant for these buses as compared to the buses farther away. In addition, these buses had the most cases with cost savings, with buses 8, 7, 4, 9 and 5 all yielding negative cost differences for storage sizes between 10 and 30 MW.

4.3.3 Wind REG on a Fall Day

For the base case of wind REG on a fall day, the percent cost difference can be observed in Table 4.1 below. Note that for the wind case sets, storage sizes 50, 70 and 90 MW were not tested and thus omitted in these results to increase computing speed.

Table 4-15: Percent Cost Difference Grid for 13-bus Wind REG, Fall Day

Bus/ Size (MW)	Bus 8 (0)	Bus 7 (1)	Bus 4 (2)	Bus 9 (2)	Bus 2 (3)	Bus 5 (3)	Bus 3 (3)	Bus 10 (3)	Bus 13 (3)	Bus 6 (4)	Bus 11 (4)	Bus 12 (4)
10	-0.074	-0.074	-0.072	-0.071	0.054	-0.077	0.063	-0.068	-0.095	-0.080	-0.052	-0.015
20	-0.101	-0.100	-0.101	-0.092	0.050	-0.096	0.074	-0.051	-0.024	-0.066	0.009	0.146
30	-0.089	-0.088	-0.094	-0.068	0.064	-0.083	0.148	0.038	0.146	-0.006	0.164	0.474
40	-0.035	-0.033	-0.049	0.004	0.098	-0.038	0.284	0.202	0.419	0.100	0.418	0.966
60	0.198	0.195	0.153	0.287	0.221	0.145	0.747	0.749	1.267	0.453	1.214	2.479
80	0.653	0.640	0.541	0.814	0.478	0.493	1.515	1.633	2.569	1.015	2.438	4.648
100	1.473	1.432	1.223	1.724	1.016	1.096	2.760	2.987	4.363	1.838	4.178	7.592

From this chart alone some initial conclusions can be drawn. First, for the 13-bus Wind REG Fall cases, the most money was saved when injecting 20 MW of storage at either the REG bus (Bus 8) or 2 buses away (Bus 4). **Thus, the optimum size for this fall case set was 20 MW placed either at the Wind Farm bus or 2 buses away.** Secondly, as the injection size of storage increased, the overall costs increased, but at different rates depending on the bus. However, the actual relationships were hard to determine based on the numbers of the cost difference grid alone.

Looking at the scatter plot of Figure 4-25, below, the relationships for injected storage on every bus could be represented by 2nd order polynomials, suggesting that the percent cost difference depends on the size of storage squared, and is fairly easy to quantify.

Figure 4-25: Percent Cost Difference Scatter Plot for 13-bus Wind REG, Fall Day

Maintaining the same color-coding as displayed in the Cost Difference Grid from Table 4-15 the data was transposed into a 3-D Topographical Surface Plot. With each color representing a 1.0 % difference, this plot clearly indicates additional general trends, as well as verifying previously mentioned points. However, the plot appeared rougher for the larger sizes of storage, likely because not all values of the larger storage range were tested. As was made clear in the grid from Table 4-15, the local maximum for this data set occurred at 100 MW of injected storage at bus 12 (4 buses away), while the local minima occurred at 20 MW of storage at either the REG bus (Bus 8) or at Bus 4.

112
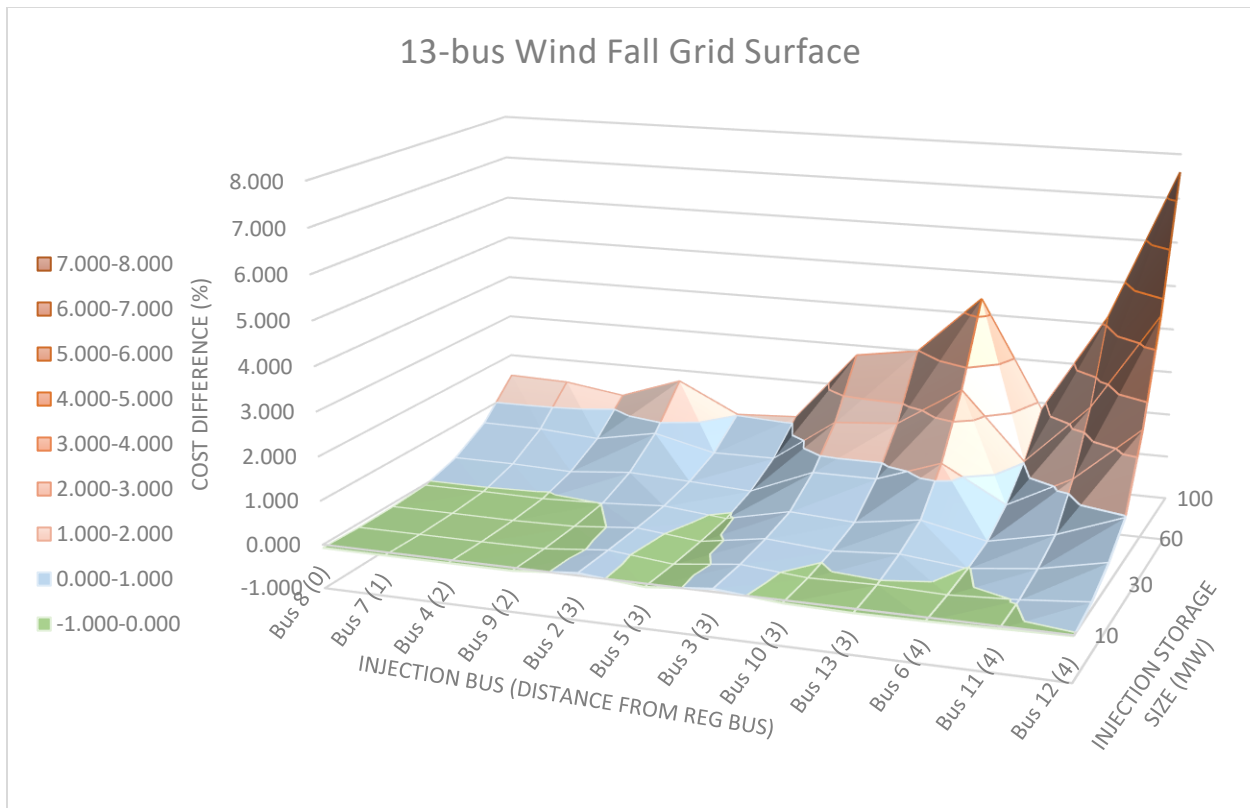
Figure 4-26: 3-D Surface Plot for 13-bus Wind REG, Fall Day

This plot indicated three clear patterns:

1) Injecting small amounts of storage on most buses yielded cost savings.

For example, almost every bus except buses 2 and 3 had at least one case in which the cost difference was negative. Most buses however had cost savings between 10 and 20 MW of injected storage.

2) As storage size increased and distance from REG bus increased, the cost generally increased.

While there was more exception to this rule than in the solar case sets (with certain buses breaking the trend), for the most part as the injection location of the storage moved farther away from the REG bus, and as the storage size increased, the percentage cost difference tended to increase as well. In addition, generally the incremental cost difference increased as the size increased and the storage location moved farther away.

3) Generally, buses closer to the REG were overall less expensive with more comparable costs than buses farther from the REG.

Buses 8, 7, 4, 9, 2 and 5 (0, 1, 2, 2, 3 and 3 buses away) all yielded costs that were well under 2.0 %, with most of cases under 0.5 %. While increasing the storage size did increase the costs, the difference was not nearly as significant for these buses as compared to the buses farther away. In addition, these buses had the most cases with cost savings, with buses 8, 7, 4, 9 and 5 all yielding negative cost differences for storage sizes between 10 and 30 MW.

4.3.4 Wind REG on a Summer Day

For the base case of solar REG on a summer day, the percent cost difference can be observed in Table 4-16 below. Note that for the wind case sets, storage sizes 50, 70 and 90 MW were not tested and thus omitted in these results to increase computing speed.

Table 4-16: Percent Cost Difference Grid for 13-bus Wind REG, Summer Day

Bus/ Size (MW)	Bus 8 (0)	Bus 7 (1)	Bus 4 (2)	Bus 9 (2)	Bus 2 (3)	Bus 5 (3)	Bus 3 (3)	Bus 10 (3)	Bus 13 (3)	Bus 6 (4)	Bus 11 (4)	Bus 12 (4)
10	-0.067	-0.067	-0.066	-0.064	0.069	-0.069	0.067	-0.059	-0.089	-0.053	-0.035	-0.001
20	-0.095	-0.096	-0.100	-0.081	0.056	-0.096	0.045	-0.045	-0.043	-0.059	0.016	0.140
30	-0.080	-0.082	-0.098	-0.055	0.061	-0.091	0.058	0.040	0.105	-0.017	0.159	0.437
40	-0.023	-0.027	-0.058	0.017	0.086	-0.052	0.181	0.195	0.352	0.074	0.395	0.897
60	0.215	0.205	0.137	0.306	0.189	0.126	0.572	0.726	1.157	0.403	1.165	2.390
80	0.630	0.603	0.485	0.781	0.367	0.436	1.210	1.560	2.411	0.943	2.361	4.628
100	1.272	1.170	0.985	1.446	0.622	0.884	2.099	2.715	4.186	1.695	3.985	8.260

From this chart alone some initial conclusions can be drawn. First, for the 13-bus Wind REG Summer cases, the most money was saved when injecting 20 MW of storage 2 buses away from the REG at bus 4. **Thus, the optimum size for this summer case set was 20 MW placed 2 buses away.** Secondly, as the injection size of storage increased, the overall costs increased, but at different rates depending on the bus.

However, the actual relationships were hard to determine based on the numbers of the cost difference grid alone.

Looking at the scatter plot of Figure 4-27, below, the relationships for injected storage on every bus could be represented by 2nd order polynomials, suggesting that the percent cost difference depends on the size of storage squared, and is easy to quantify.

Figure 4-27: Percent Cost Difference Scatter Plot for 13-bus Wind REG, Summer Day

Maintaining the same color-coding as displayed in the Cost Difference Grid from Table 4-16 the data was transposed into a 3-D Topographical Surface Plot. With each color representing a 1.0 % difference, this plot clearly indicates additional general trends, as well as verifying previously mentioned points. However, the plot appeared rougher for the larger sizes of storage, likely due to the fact that not all values

of the larger storage range were tested. As was made clear in the grid from Table 4-16, the local

maximum for this data set occurred at 100 MW of injected storage at bus 12 (4 buses away), while the

local minimum occurred at 20 MW of storage at bus 4.
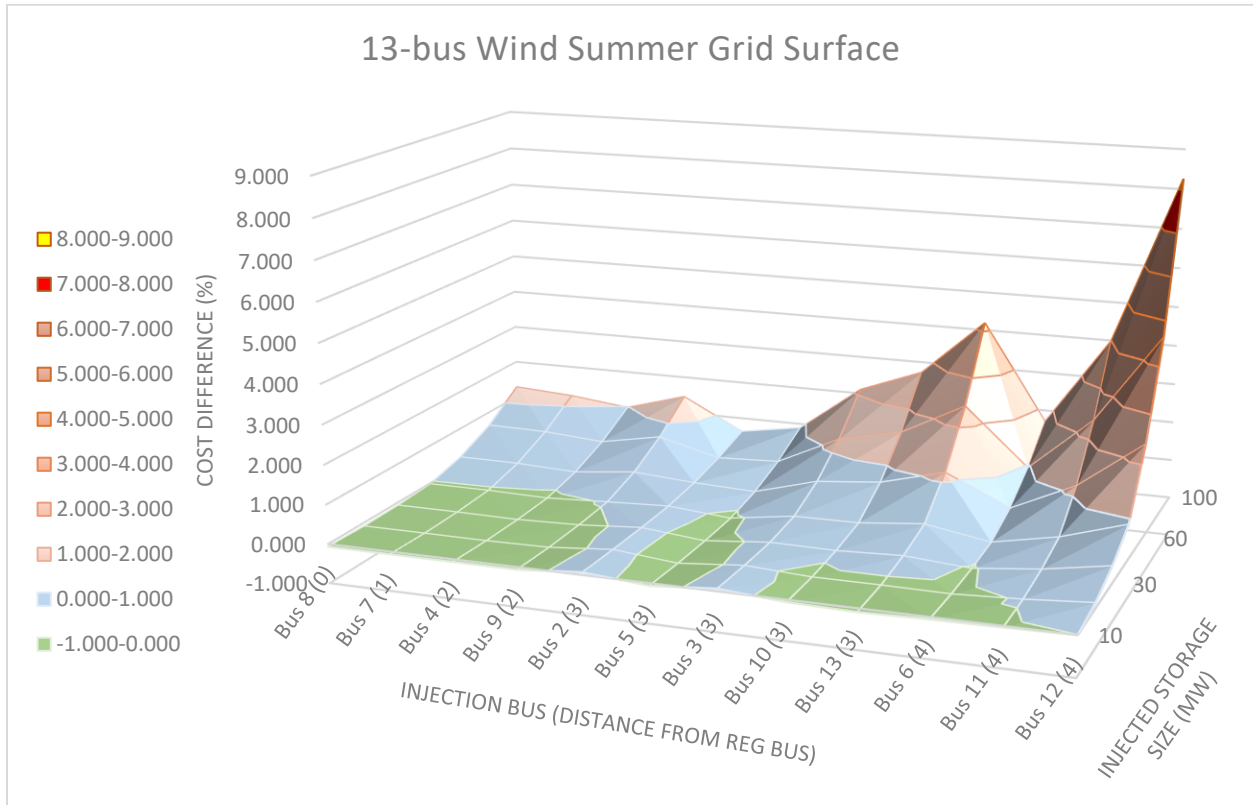
Figure 4-28: 3-D Surface Plot for 13-bus Wind REG, Fall Day

This plot indicated three clear patterns:

1) Injecting small amounts of storage on most buses yielded cost savings.

For example, almost every bus except buses 2 and 3 had at least one case in which the cost difference was

negative. Most buses however had cost savings between at least 10 and 20 MW of injected storage.

2) As storage size increased and distance from REG bus increased, the cost generally increased.

While there was more exception to this rule than in the solar case sets (with certain buses breaking the trend), for the most part as the injection location of the storage moved farther away from the REG bus, and as the storage size increased, the percentage cost difference tended to increase as well. In addition, generally the incremental cost difference increased as the size increased and the storage location moved farther away.

3) Generally, buses closer to the REG were overall less expensive with more comparable costs than buses farther from the REG.

Buses 8, 7, 4, 9, 2 and 5 (0, 1, 2, 2, 3 and 3 buses away) all yielded costs that were well under 1.5 %, with the majority of cases under 0.5 %. While increasing the storage size did increase the costs, the difference was not nearly as significant for these buses as compared to the buses farther away. In addition, these buses had the most cases with cost savings, with buses 8, 7, 4, 9 and 5 all yielding negative cost differences for storage sizes between 10 and 30 MW.

4.3.5 13-bus Cases Discussion

Considering all four case sets studied, some general conclusions can be made. First, as anticipated, the overall daily cost increased as storage size increased, with different relationships for different injection buses. This was consistent across all cases, and makes sense as the capital costs are indeed larger for larger sizes of storage. Second, larger storage sizes relative to the size of the system (or more specifically the size of the REG) may not be economical. Apart from a single test, every case that included injecting storage greater than 50 % of the built REG size was more expensive than the corresponding base case. While having the capacity to store large amounts of energy at a time would seem to be a reasonable approach, the capital costs and thus overall system costs are just too high to justify installing amounts of storage that are well over 50 % of the size of REG.

When focusing on the economical cases themselves, there were less cases in which injecting storage was cheaper than the base cases without storage. This was largely unexpected as previous reports seemed to suggest otherwise, proposing that EES could be a practical and economical solution to an increasingly relevant issue. For the cases that were economical, the injected size was also much smaller than expected, and the costs saved from utilizing storage were fairly small, never exceeding 0.118 %. For a cost savings of just over $1/10^{th}$ of a percent, it may be hard to justify going through the process of building and installing storage for systems similar to the 9-bus systems tested.

Additional observations can be made across all four cases when comparing their respective 3-D surface plots. For amounts of storage below roughly 50 % of the rated REG size and closer to the REG location, the overall daily costs were for the most part comparable to each other regardless of bus location and case set, with little variance. However, for amounts of storage above 50 % of the rated REG size and farther from the REG location, the incremental costs were much larger depending on the injection location and case set. This suggests that line congestion may play a larger role in the high system costs of injecting large amounts of storage, especially for buses farther away from the REG bus.

4.4   Overall Assessment

Comparing the 13-bus results to the 9-bus result revealed the following conclusions:

   1) **As the size of ESS increased, the overall daily cost of the system increases.**
This was true regardless of test bed, REG utilized or load profile.

   2) **The optimum size of storage that typically made most economic sense was between 10-30 MW.**
The size differed depending on the system properties, load profile etc. For the single-line 9-bus cases, most scenarios varied between 10-30 MW. For the double-line 9-bus cases, most scenarios were closer to 10 MW, but within the fall set 30 MW was still cheapest. While many scenarios in the 13-bus test bed

118

had negative percent cost differences past 30 MW, the most economical cases were still within the 10-30 MW range. Cases in which storage sizes exceeded 50 MW were always more expensive than their respective base cases. In other words, utilizing bulk storage amounts exceeding 50 % of the size of REG will be uneconomical and will only add to line congestion, not reduce it.

3) The optimum location of storage tended to be closer to the REG bus.

This was only the case for smaller amounts of storage. The one case in which this was not true was for the 9-bus Single-Line Wind Summer case set, in which the optimum location was actually 4 buses away from the REG.

4) The worst location of storage varied depending on test system.

While the optimum location was closer to the REG bus for almost every case set and test bed, the worst location of storage in which the costs were the most expensive varied depending on the test bed utilized. For the 9-bus systems (both single- and double-line systems), the worst location for large amounts of storage was almost always at or near the REG bus, suggesting that for the 9-bus systems, congestion was the largest factor near the REG bus. For the 13-bus systems, the worst location for large amounts of storage was at the farthest bus away from the REG bus, suggesting that congestion was the largest factor at the buses farthest from the REG bus. These results agree with the findings of [26] for an uncongested system. While the optimum size of storage can be determined, the optimum or least optimum location of storage depends on the system properties, and cannot always be easily determined based on one or two variables.

5) Seasonal load profiles will affect the economics of injected energy storage within a system.

While only a single fall day and a single summer day were tested, it was quite clear that the different load profiles affected the system costs significantly depending on the test bed. The fall and summer profiles each tended to affect different buses more heavily than others on the 9-bus sets. On the other hand, the different profiles appeared to affect the 13-bus network much less, with less variation between each set.

6) Fewer economical scenarios existed than expected.

Across every set of network tests, there were not that many economical scenarios. The 9-bus Single-Line cases had few economical scenarios, but the Double-Line cases had even less. The 13-bus cases had the most economical scenarios by far, with savings occurring for small amounts of storage at almost every bus.

7) Cost reductions were smaller than expected.

Despite some case sets containing more economical scenarios than others, the cost reductions that existed barely surpassed 0.01 % of the overall system cost, if at all. Thus, it would be very difficult to justify the installation of storage under the assumed conditions for the economic benefit alone. This result agrees with [28] in which the costs of installing storage negatively outweigh the economic benefit for relatively small wind penetration. For high RE penetration, the economic benefit may certainly outweigh the costs, but since this thesis focused on relatively small RE penetration, it would make sense that this was not the case.

8) Congestion affects the economics of injected storage.

First, when comparing the scenarios with small amounts of storage to those with large amounts of storage in the 9-bus Single-Line cases, it was clear that congestion affected the cost relationships. The percent cost increases became less comparable and less predictable across the various bus locations for larger storage amounts, despite the same, static Powerworld costs models. Second, when comparing the 9-bus Single-Line cases to the 9-bus Double-Line less congested cases, this trend can further be verified. The Double-Line cases had double the line capacity, leading to very comparable cost relationships between each bus location. In other words, the bus location mattered much less in the Double-Line cases than in the single-line cases. This suggests that adding line capacity does increases storage effectiveness and reduces overall system costs, but it is unclear in these results whether the storage helped or dampened the reduction in overall system costs. It is also important to reiterate that the fixed costs of adding the transmission lines could not be accounted for in Powerworld, so any comparison between the 9-bus Single-Line cases and the Double-line cases should be carefully considered.

Taking all of this into account, it appears that the test beds successfully allowed for the observation of the economic effects of injecting storage into isolated power networks with renewable and conventional generation sources. By varying the size of storage and the injection location, many general trends appeared. There were clear relationships between storage size and location and the overall daily system costs. In addition, these tests made it easier to determine how the system properties affect the system costs. Overall the case studies proved to be useful for the determination of the optimum size and location of storage within each test bed such that future projects may be able to test systems in a similar fashion.

4.4.1 Results Compared to Similar Economic Studies of Storage

The results and conclusions from the previously mentioned reports in the Literature Review of Section 1.2 can be discussed alongside the results of this thesis to create a more complete analysis of the economics of storage. Since most of these reports had techniques that are quite different from each other and from that of this thesis, the bulk of their findings cannot be completely compared to the previously discussed results here. Note that only the reports from the Literature Review that had the most similar methodologies to this thesis will be discussed further, as they will be most relevant.

The first comparison can be made from the results of [26] and [27]. Using a complex, three-stage algorithm to determine the best locations and parameters of distributed storage within a large transmission test network, the methodology of [26] certainly differed from that used in [27] and in this thesis in which OPF studies were completed on test systems. However, all three methods had low computational burden allowing for straightforward testing that could be completed easily without additional computational resources. The most similar trend revealed that when the test network in question was not congested, the methods utilized could determine the optimal capacity of storage for the system, but the location of storage was not as easily determined based on the algorithm from [26] alone. This is similar to findings 3 and 4 of this thesis; while the optimal storage sizing was straightforward, the optimal and least optimal

locations of storage depended heavily on various network properties, and could not be predicted without fully considering the networks in question, nor could it be predicted as easily within congested networks.

The results from [28] indicated that wind power can be efficiently utilized in a network with proper placement of storage. By carefully distributing the storage within a network, transmission upgrades or expansions could be avoided, reducing costs and increasing the economic benefit and effectiveness of storage. This was especially true for systems with limited power flow capacities and high wind penetration. In other words, storage becomes less useful and less economical for lower wind energy penetration.

While only bulk storage with one size of RE was tested for either solar or wind energy in this thesis, this is an interesting finding from [28] and could likely be observed or tested by modifying the Methodology of Section 3 to include networks with more and less RE penetration respectfully. This agrees with the notion discussed in this thesis that added storage capacity challenges the necessity of adding transmission line capacity, while the opposite is also true. In a heavily congested network, properly installed storage can certainly be useful, but for a well-connected network, the effectiveness of storage may increase while the usefulness of storage for economic benefit may decrease.

The findings from [22] suggest similar trends as well. While completing Mixed-Integer Linear Programming methods to reduce the operating and investment costs of installing storage within a given network, the authors identified the optimum locations of storage in a large 240 bus system modeled after the WECC interconnection. They determined that for optimum storage locations, storage tended to reduce the RE "spillage", but not always. Put another way, storage placement based on the most economical scenario generally increased the effective usage of the installed RE capacity. However, operating storage to minimize the total operating cost did not guarantee that RE penetration would be used most efficiently, nor did it guarantee that investments in storage for RE penetration applications would be profitable.

In addition, [22] found that as the energy rating of the installed storage increased, the overall usefulness of storage increased, but profitability generally decreased. This was consistent with the very first finding across every case study in this thesis: as the size of bulk installed storage increased, the overall daily cost of the system increased. This relationship eventually leads to uneconomical scenarios in which installing large amounts of storage becomes costlier than not adding storage at all.

Finally, like the findings of [28], the authors of [22] determined that as RE penetration increased, the installed power capacity became more saturated, suggesting that adding storage capacity to a network is most useful when the network is under high RE penetration. For smaller amounts of installed RE penetration, storage may not necessarily be useful. Again, this is something that was not directly determined in this thesis since the testing methods differed from these reports, but by allowing for slight adjustments to the techniques utilized in Section 3, these results could be confirmed or rejected.

5. Conclusion

Using Powerworld Simulator, case studies were built using modified test beds to determine and observe the economic effects of injecting energy storage into an isolated power network with conventional and renewable generation sources. Ultimately there were fewer economical scenarios involving the injection of energy storage than originally anticipated. Additionally, the optimum size of injected storage was much smaller than expected, and the actual cost savings of installing said storage was quite small compared to the overall system costs. Nevertheless, there were still scenarios in which installing energy storage was cost effective.

There are many reasons why so few economical scenarios existed, and why those scenarios involved such small cost savings overall. It is important to keep in mind that this thesis aimed to observe and analyze overall economic trends within the test systems created. Assumptions were made to limit the scope and create realistic scenarios, but these are still only a small representation of the many scenarios that could occur when installing ESS.

For example, one large assumption made at the beginning for all case sets was that the charging and discharging hours of the ESS would be based off the cheapest and most expensive hours respectively of the base system in question. While this initially seems intuitive, it would be interesting to observe the effects of storage that can only charge or discharge for 12 consecutive hours, instead of being more flexible as was the case here. There is a possibility that since the power flow would potentially be changing less often, there would be reduced overall congestion and thus reduced overall system costs.

Another set of assumptions made at the beginning for all case sets was regarding the cost models of the ESS. PHS was chosen as it was the most developed in industry. PHS has high capital costs due to the high land capital required. While BES is still much more expensive overall for smaller capacity, it would be interesting to observe the economic effects of BES with a cost model based off future projections.

124

Moreover, one of the most fundamental original assumptions made could have also been the most limiting on the results: that the ESS had to be installed and injected into the system in bulk. Since congestion was such a large factor, it would be interesting to determine the effects of injecting small amounts of storage distributed more evenly within a network, such as was the case in [26]. While the capital costs of having large amounts of storage would be high regardless of whether or not that storage is distributed, allowing for distributed storage such as in [28, 26] could potentially create a more balanced network, eliminating the need for additional transmission line capacity. Distributed storage could also be the solution in an already congested network, as the costs of installing the storage could be cheaper than the costs of installing additional lines.

Regardless, there are still many scenarios in which ESS could be economical, and there are many variables which affect the overall value ESS adds to a power network. Currently it may not make practical sense to install ESS given the high costs, low RE penetration and few economical scenarios. However, the industry is progressing rapidly, and that could change in the near future as energy storage continues to develop and RE capacity within global power networks continues to increase. Despite the focused results discussed in this thesis, ESS still has great potential to solve many problems in the power industry.

References

[1]   D. V. H. L. M. R. B. Stijn Cole, "Energy Storage on Production and Trasmission Level: A SWOT Analysis," 2009. [Online]. Available: http://www.leonardo-energy.info/sites/leonardo-energy/files/root/Documents/2009/pub_1515.pdf. [Accessed 01 June 2016].

[2]   Sino Voltaics, "Base Load and Peak Load: Understanding both concepts," 9 6 2015. [Online]. Available: http://sinovoltaics.com/learning-center/basics/base-load-peak-load/. [Accessed 12 6 2017].

[3]   National Wind Watch INC, "FAQ- The Grid," 2017. [Online]. Available: https://www.wind-watch.org/faq-electricity.php. [Accessed 12 6 2017].

[4]   EnergyVortex.com, "Energy Dictionary," Association of Energy Engineers, 2017. [Online]. Available: http://www.energyvortex.com/energydictionary/baseload_plant.html. [Accessed 12 6 2017].

[5]   J. W. M. D. J. C. Xing Luo, "Overview of Current Development in Electrical Energy Storage Technologies and the Application in Power System Operation," 16 October 2014. [Online]. Available: http://www.sciencedirect.com/science/article/pii/S0306261914010290?np=y. [Accessed 01 June 2016].

[6]   R. Fares, "Scientific American: Study Indicates Bulk Energy Storage Would Increase Total US Electricity System Emissions," 17 August 2015. [Online]. Available: http://blogs.scientificamerican.com/plugged-in/study-indicates-bulk-energy-storage-would-increase-total-u-s-electricity-system-emissions/. [Accessed 01 June 2016].

[7]   Rocky Mountain Institute, "Power and Duration of Electricity Bulk Storage Technologies," 01 November 2011. [Online]. Available: http://www.rmi.org/RFGraph-power_duration_electricity_bulk_storage_technologies. [Accessed 01 June 2016].

[8]   Z. H. Y. S. Fang Zhang, "Mixed-integer linear model for transmission expansion planning with line losses and energy storage systems," 15 7 2013. [Online]. Available: http://au4sb9ax7m.search.serialssolutions.com/?ctx_ver=Z39.88-2004&ctx_enc=info%3Aofi%2Fenc%3AUTF-8&rfr_id=info%3Asid%2Fsummon.serialssolutions.com&rft_val_fmt=info%3Aofi%2Ffmt%3Akev%3Amtx%3Ajournal&rft.genre=article&rft.atitle=Mixed-integer+linear+model+. [Accessed 12 6 2017].

[9]   H. A. K. A. Zach, "Bulk energy storage versus transmission grid investments: Bringing flexibility into future electricty systems with high penetration of variable RES-electricity," 10 5 2012. [Online]. Available: http://au4sb9ax7m.search.serialssolutions.com/?ctx_ver=Z39.88-2004&ctx_enc=info%3Aofi%2Fenc%3AUTF-8&rfr_id=info%3Asid%2Fsummon.serialssolutions.com&rft_val_fmt=info%3Aofi%2Ffmt%3Akev%3Amtx%3Ajournal&rft.genre=article&rft.atitle=Mixed-integer+linear+model+. [Accessed 12 6 2017].

[10]   G. T. H. John R. Ruggiero, "Making the economic case for bulk energy storage in electric power systems," 25 11 2013. [Online]. Available: http://ieeexplore.ieee.org.ezproxy.wpi.edu/document/6666839/. [Accessed 12 6 2017].

[11]   M. O. H. K. Robby Orvis, "Debunking 4 Myths About the Clean Energy Transition, Part 1: The "Duck Curve"," Clean Technica, 13 5 2016. [Online]. Available: https://cleantechnica.com/2016/05/13/duck-curve-debunking-renewable-energy-myths-1/. [Accessed 12 6 2017].

[12]   A. Reinhold, "File:Duck Curve CA-ISO 2016-10-22.agr.png," 16 October 2016. [Online]. Available: https://commons.wikimedia.org/wiki/File:Duck_Curve_CA-ISO_2016-10-22.agr.png. [Accessed 1 May 2017].

[13]   University of Manchester School of Electrical and Electronic Engineering, "Improving the stability of power systems using high voltage direct current power lines," 2017. [Online]. Available: http://www.eee.manchester.ac.uk/our-research/research-groups/eeps/projects/improving-stability/. [Accessed 12 6 2017].

[14]   Enviromental and Energy Study Institute, "Energy Stoage Issue Brief," Environmental and Energy Study Institute, Washington, DC, 2013.

[15]   E. E. J. I. e. a. Andris Abele, "2020 Strategic Analysis of Energy Storage in California," November 2011. [Online]. Available: http://www.energy.ca.gov/2011publications/CEC-500-2011-047/CEC-500-2011-047.pdf. [Accessed 01 June 2016].

[16]   US Department of Energy, "Sandia.gov," 2013. [Online]. Available: http://www.sandia.gov/ess/docs/other/Grid_Energy_Storage_Dec_2013.pdf. [Accessed 12 6 2017].

[17]   D. Khastieva, *Energy Storage Impact On Systems With High Wind Energy Penetration,* Cleveland: Case Western Reserve University, 2014.

[18]   M. A. D. P. e. a. Goran Strbac, "Strategic Assessment of the Role and Value of Energy Storage Systems in the UK Low Carbon Energy Future," June 2012. [Online]. Available: https://www.carbontrust.com/media/129310/energy-storage-systems-role-value-strategic-assessment.pdf. [Accessed 01 June 2016].

[19]   T. Zhang, *The Economic Benefits of Battery Energy Storage System in Electric Distribution System,* Worcester, MA: Worcester Polytechnic Institute, 2013.

[20]   P. S. G. N. D. H. T. C. D. S. Matija Zidar, "Review of energy storage allocation in power distribution networks: applications, methods and future research," 3 3 2016. [Online]. Available: http://ieeexplore.ieee.org.ezproxy.wpi.edu/stamp/stamp.jsp?tp=&arnumber=7422904. [Accessed 13 6 2017].

[21]   D. X. Srinivas Bhaskar Karanki, "Optimal capacity and placement of battery energy storage systems for integrating renewable energy sources in distribution system," 19 12 2016. [Online]. Available: http://ieeexplore.ieee.org.ezproxy.wpi.edu/document/7858983/. [Accessed 12 6 2017].

[22]   Y. D. B. X. Y. W. D. S. K. Ricardo Fernandez-Blanco, "Optimal Energy Storage Siting and Sizing: A WECC Case Study," 11 10 2016. [Online]. Available: http://ieeexplore.ieee.org.ezproxy.wpi.edu/document/7587806/. [Accessed 13 6 2017].

[23]   P. D. M. C. W. K.-M. C. J. H. F. I. Yuri V. Makarov, "Sizing Energy Storage to Accomodate High Penetration of Variable Energy Resources," 5 12 2011. [Online]. Available: http://ieeexplore.ieee.org.ezproxy.wpi.edu/document/6095383/. [Accessed 13 6 2017].

[24]   D. M. K. D. C. A. A. Solomon, "The role of large-scale energy storage design and dispatch in the power grid," *Applied Energy,* vol. 134, no. C, pp. 75-89, 2014.

[25]   A. T. H. R. H. Magnis Korpaas, "Operation and sizing of energy storage for wind power plants in a market system," *Electrical Power and Energy Systems,* vol. 25, pp. 599-606, 2003.

[26]   Y. W. T. Q. Y. D. D. S. K. Hrvoje Pandzic, "Near-Optimal Method for Siting and Sizing of Distributed Storage in a Transmission Network," *IEEE Transactions on Power Systems,* vol. 30, no. 5, pp. 2280-2300, 2015.

[27]   D. F. G. Sonja Wogrin, "Optimizing Storage Siting, Sizing, and Technology Portfolios in Transmission-Constrained Networks," *IEEE Transactions on Power Systems,* vol. 30, no. 6, pp. 3304-3313, 2015.

[28]   A. A. M. E.-A. M. S. F. Mahmoud Ghofrani, "A Framework for Optimal Placement of Energy Storage Units Within a Power System With High Wind Penetration," *IEEE Transactions on Sustainable Energy,* vol. 4, no. 2, pp. 434-442, 2013.

[29]   N. Ivanova, "Lithium-Ion Costs to Fall by up to 50 % Within Five Years," 30 July 2015. [Online]. Available: http://analysis.newenergyupdate.com/energy-storage/lithium-ion-costs-fall-50-within-five-years. [Accessed 15 March 2017].

[30]   I. Cowie, "All About Batteries, Part 9: Sodium Sulfur," 14 7 2014. [Online]. Available: http://www.eetimes.com/author.asp?section_id=36&doc_id=1323091. [Accessed 15 March 2017].

[31]   T. N. C. W. Y. C. T. Y. L. Y. D. Haisheng Chen, "Progress in Electrical Energy Storage System: A Critical Review," *Progress in Natural Science,* vol. 19, no. 2, pp. 291-312, 2008.

[32]   J. H. Kopera, "Inside the Nickel Metal Hydride Battery," Cobasys, 2004.

[33]   PowerStream, "NiMH Battery Charging Basics," PowerStream Technology, 12 12 2016. [Online]. Available: http://www.powerstream.com/NiMH.htm. [Accessed 15 March 2017].

[34]   Y. Z. Z. D. B. J. T. Wenhua H. Zhu, "Energy efficiency and capacity retention of Ni–MH batteries for storage applications," *Applied Energy,* vol. 106, pp. 307-313, 2013.

[35]   Meridian International Research, "The Sodium Nickel Chloride "Zebra" Battery," Meridian International Research, 2005.

[36]   International Electrotechnical Comission, "Electrical Energy Storage," IEC, Geneva, 2011.

[37]   National Renewable Energy Laboratory, "NREL Energy Storage Projects: FY2014 Annual Report," NREL, Denver, 2015.

[38] A. S. O. G.-B. e. a. Francisco Diaz-Gonzalez, "A Review of Energy Storage Technologies for Wind Power Applications," 18 February 2012. [Online]. Available: http://ac.els-cdn.com/S1364032112000305/1-s2.0-S1364032112000305-main.pdf?_tid=2080c736-267b-11e6-968e-00000aab0f6c&acdnat=1464622275_8dbe2488396271bdafcdd52f1b21b08a . [Accessed 01 June 3016].

[39] Sandia National Laboratories, "DOE/EPRI 2013 Electricity Storage Handbook in Collaboration with NRECA," Sandia National Laboratories, Albuquerque, 2013.

[40] E. E. B. K. M. M. Paul Denholm, "The Role of Energy Storage with Renewable Electricity Generation," National Renewable Energy Laboratory, Denver, 2010.

[41] S. N. Jim Skea, "Policies and Practices for a Low-Carbon Society," 2008. [Online]. Available: http://www.fao.org/fileadmin/user_upload/rome2007/docs/Policies%20and%20practices%20for%20a%20low-carbon%20society.pdf . [Accessed 01 June 2016].

[42] Sandia National Laboratories, "DOE Global Energy Storage Database," United States Department of Energy, 2017. [Online]. Available: https://www.energystorageexchange.org/projects?utf8=%E2%9C%93&technology_type_sort_eqs=&technology_type_sort_eqs_category=&country_sort_eq=United+States&state_sort_eq=&kW=&kWh=&service_use_case_inf=&ownership_model_eq=&status_eq=&siting_eq=&order_by=&sort. [Accessed 15 March 2017].

[43] J. Geinzer, "AES Laurel Mountain Overview," AES Energy Storage, 2012.

[44] North American Electric Reliability Corporation, "Regional Entities," 2016. [Online]. Available: http://www.nerc.com/AboutNERC/keyplayers/Pages/Regional-Entities.aspx. [Accessed 15 March 2017].

[45] Western Electric Coordinating Council, "WECC Home," 2016. [Online]. Available: https://www.wecc.biz/Pages/home.aspx. [Accessed 15 March 2017].

[46] A. A. F. P. M. Anderson, Power System Control and Stability, New York: John Wiley & Sons, 2003.

[47] M. A. P. P. W. Sauer, Power System Dynamics and Stability, Upper Saddle River, NJ: Prentice Hall, 1998.

[48] Dynamic IEEE Test Systems, "IEEE 9-bus modified test system," 2016. [Online]. Available: http://www.kios.ucy.ac.cy/testsystems/index.php/dynamic-ieee-test-systems/ieee-9-bus-modified-test-system. [Accessed 15 Dec 2017].

[49] ISONE, "ISO Express Real Time Maps and Charts," 15 Mar 2017. [Online]. Available: https://www.iso-ne.com/isoexpress/web/charts/guest-hub?p_p_id=fuelmixgraph_WAR_isoneportlet_INSTANCE_WQKSMAX9RozI&p_p_lifecycle=0&p_p_state=normal&p_p_state_rcv=1. [Accessed 15 Jan 2017].

[50] ISO New England, "Resource Mix," August 2016. [Online]. Available: https://www.iso-ne.com/about/key-stats/resource-mix. [Accessed 15 Jan 2017].

[51] US Energy Information Administration, "Assumptions to the Annual Energy Outlook: Electricy Market Module," US EIA, 2015.

[52]   Investing.com, "Natural Gas Futures," 2016. [Online]. Available:
         https://www.investing.com/commodities/natural-gas-historical-data. [Accessed 15 Jan 2017].

[53]   Coinnews Media Group LLC, "US Inflation Calculator," 2015. [Online]. Available:
         http://www.usinflationcalculator.com/. [Accessed 15 Jan 2017].

[54]   National Centers for Environmental Information, "Quality Controlled Local Climatological
         Data," NOAA, 2016. [Online]. Available: https://www.ncdc.noaa.gov/data-access/land-based-
         station-data/land-based-datasets/quality-controlled-local-climatological-data-qclcd. [Accessed 15
         Dec 2016].

[55]   G. M. Masters, "Chapter 7," in *Renewable and Efficient Electric Power Systems*, Hoboken, NJ,
         John Wiley & Sons, 2004, pp. 385-439.

[56]   Pacific Northwest National Laboratory, "National Assessment of Energy Storage for Grid
         Balancing and Aribtrage Phase II Vol 2: Cost and Performance Characterization," US
         Department of Energy, 2013.

[57]   R. Christie, "Power Systems Test Case Archive: 14 Bus Power Flow Test Case," 1993. [Online].
         Available: http://www2.ee.washington.edu/research/pstca/pf14/pg_tca14bus.htm. [Accessed 15
         Dec 2016].

[58]   cdf2matp, "Power Flow Data for IEEE 14 Bus test case," 10 3 2010. [Online]. Available:
         http://www.ece.ubc.ca/~hameda/download_files/case14.m. [Accessed 15 Dec 2016].

[59]   I. C. f. a. S. E. Grid, "IEEE 14-Bus System," Information Trust Institute, 2016. [Online].
         Available: http://icseg.iti.illinois.edu/ieee-14-bus-system/. [Accessed 15 Dec 2016].

[60]   S. B. B. K. Muhsin Abdurrahman, "Energy Storage as a Transmission Asset," 2012. [Online].
         Available: https://www.pjm.com/~/media/markets-ops/advanced-tech-pilots/xtreme-power-
         storage-as-transmission.ashx . [Accessed 01 June 2016].

Appendix A: 9-bus Parameters

Transmission Line Parameters:

	Series Z [pu]		Shunt Y [pu]
Bus to bus	R	X	B
Trans. 1-4	0.0	0.0576	
Trans. 3-9	0.0	0.0586	
Trans. 2-7	0.0	0.0625	
Line 4-5	0.01	0.085	0.176
Line 4-6	0.017	0.092	0.158
Line 5-7	0.032	0.161	0.306
Line 6-9	0.039	0.170	0.358
Line 7-8	0.0085	0.072	0.149
Line 8-9	0.0119	0.1008	0.209

Generator Parameters:

Parameter	M/C1	M/C2	M/C3
rated power [MVA]	247.5	192	128
H [sec.]	23.64	6.4	3.01
X_d [pu]	0.146	0.8958	1.3125
X_d' [pu]	0.0608	0.1198	0.1813
X_q [pu]	0.0969	0.8645	1.2578
X_q' [pu]	0.0969	0.1969	0.25
T_{d0}' [sec]	8.96	6.0	5.89
T_{q0}' [sec]	0	0.535	0.6

Appendix B: 9-bus Scaled Load Calculations

Summer Load Profile:

Hour	Actual Load [MW]	Total Scaled [MW]	Total Scaled [MVar]	Load 1 MW	Load 2 MW	Load 3 MW	Load 1 MVAR	Load 2 MVAR	Load 3 MVAR
0	15425	211.826	77.333	67.2	84.1	60.5	23.5	33.6	20.2
1	14366	197.284	72.024	62.6	78.3	56.4	21.9	31.3	18.8
2	13728	188.522	68.826	59.8	74.8	53.9	20.9	29.9	18.0
3	13324	182.974	66.800	58.1	72.6	52.3	20.3	29.0	17.4
4	13238	181.793	66.369	57.7	72.1	51.9	20.2	28.9	17.3
5	13546	186.023	67.913	59.1	73.8	53.1	20.7	29.5	17.7
6	14460	198.574	72.495	63.0	78.8	56.7	22.1	31.5	18.9
7	16342	224.419	81.931	71.2	89.1	64.1	24.9	35.6	21.4
8	18017	247.422	90.328	78.5	98.2	70.7	27.5	39.3	23.6
9	19400	266.414	97.262	84.6	105.7	76.1	29.6	42.3	25.4
10	20638	283.415	103.469	90.0	112.5	81.0	31.5	45.0	27.0
11	21477	294.937	107.675	93.6	117.0	84.3	32.8	46.8	28.1
12	22075	303.149	110.673	96.2	120.3	86.6	33.7	48.1	28.9
13	22594	310.276	113.275	98.5	123.1	88.7	34.5	49.3	29.6
14	22781	312.844	114.213	99.3	124.1	89.4	34.8	49.7	29.8
15	22938	315.000	115.000	100.0	125.0	90.0	35.0	50.0	30.0
16	22876	314.149	114.689	99.7	124.7	89.8	34.9	49.9	29.9
17	22916	314.698	114.890	99.9	124.9	89.9	35.0	50.0	30.0
18	22791	312.981	114.263	99.4	124.2	89.4	34.8	49.7	29.8

19	22304	306.293	111.821	97.2	121.5	87.5	34.0	48.6	29.2
20	21440	294.428	107.490	93.5	116.8	84.1	32.7	46.7	28.0
21	21051	289.086	105.539	91.8	114.7	82.6	32.1	45.9	27.5
22	19710	270.671	98.816	85.9	107.4	77.3	30.1	43.0	25.8
23	17819	244.702	89.336	77.7	97.1	69.9	27.2	38.8	23.3

Fall Load Profile:

Hour	Actual Load [MW]	Total Scaled [MW]	Total Scaled [MVar]	Load 1 MW	Load 2 MW	Load 3 MW	Load 1 MVAR	Load 2 MVAR	Load 3 MVAR
0	10613	244.915	89.414	77.8	97.2	70.0	27.2	38.9	23.3
1	10006	230.908	84.300	73.3	91.6	66.0	25.7	36.7	22.0
2	9716	224.215	81.856	71.2	89.0	64.1	24.9	35.6	21.4
3	9556	220.523	80.508	70.0	87.5	63.0	24.5	35.0	21.0
4	9603	221.608	80.904	70.4	87.9	63.3	24.6	35.2	21.1
5	9814	226.477	82.682	71.9	89.9	64.7	25.2	35.9	21.6
6	10416	240.369	87.754	76.3	95.4	68.7	26.7	38.2	22.9
7	11260	259.846	94.864	82.5	103.1	74.2	28.9	41.2	24.7
8	12066	278.446	101.655	88.4	110.5	79.6	30.9	44.2	26.5
9	12367	285.392	104.191	90.6	113.3	81.5	31.7	45.3	27.2
10	12285	283.500	103.500	90.0	112.5	81.0	31.5	45.0	27.0
11	12082	278.815	101.790	88.5	110.6	79.7	31.0	44.3	26.6
12	11827	272.931	99.641	86.6	108.3	78.0	30.3	43.3	26.0
13	11610	267.923	97.813	85.1	106.3	76.5	29.8	42.5	25.5

14	11418	263.492	96.196	83.6	104.6	75.3	29.3	41.8	25.1
15	11499	265.362	96.878	84.2	105.3	75.8	29.5	42.1	25.3
16	11792	272.123	99.347	86.4	108.0	77.7	30.2	43.2	25.9
17	12328	284.492	103.862	90.3	112.9	81.3	31.6	45.2	27.1
18	13044	301.015	109.895	95.6	119.5	86.0	33.4	47.8	28.7
19	13650	315.000	115.000	100.0	125.0	90.0	35.0	50.0	30.0
20	13293	306.762	111.992	97.4	121.7	87.6	34.1	48.7	29.2
21	12761	294.485	107.510	93.5	116.9	84.1	32.7	46.7	28.0
22	12050	278.077	101.520	88.3	110.3	79.5	30.9	44.1	26.5
23	11118	256.569	93.668	81.5	101.8	73.3	28.5	40.7	24.4

Appendix C: 9-bus Generation Cost Model Summary

Gen ID	Season	Fuel Source/ Gen Type	Gen Size (MW)	Capacity Factor (C)	Unit Fuel Cost ($/MMBTU)	Variable O&M Costs ($/MWh)	Fixed Cost Independent Value ($/hr)	Cubic Cost Model B (BTU/kWh)
1	Summer	NatGas (Conv CCGT)	247.5	8760	$2.76	$16.00	$12.42	10,783
2	Summer	NatGas (Conv CCGT)	192	8760	$2.76	$16.00	$9.63	10,783
3	Summer	Solar (PV)	128	8760	$0.00	$0.00	$21.75	9,516
3	Summer	Wind	128	8760	$0.00	$0.00	$13.13	9,516
1	Fall	NatGas (Conv CCGT)	247.5	8760	$3.28	$16.00	$12.42	10,783
2	Fall	NatGas (Conv CCGT)	192	8760	$3.28	$16.00	$9.63	10,783
3	Fall	Solar (PV)	128	8760	$0.00	$0.00	$21.75	9,516
3	Fall	Wind	128	8760	$0.00	$0.00	$13.13	9,516
4	F/S_4.1	Pumped Hydro Storage (PHS)	10	8760	$0.00	$4.30	$0.94	9,516
	F/S_4.2		20	8760	$0.00	$4.30	$1.88	9,516
	F/S_4.3		30	8760	$0.00	$4.30	$2.82	9,516
	F/S_4.4		40	8760	$0.00	$4.30	$3.76	9,516
	F/S_4.5		50	8760	$0.00	$4.30	$4.70	9,516
	F/S_4.6		60	8760	$0.00	$4.30	$5.64	9,516
	F/S_4.7		70	8760	$0.00	$4.30	$6.58	9,516
	F/S_4.8		80	8760	$0.00	$4.30	$7.53	9,516
	F/S_4.9		90	8760	$0.00	$4.30	$8.47	9,516
	F/S_4.10		100	8760	$0.00	$4.30	$9.41	9,516
	F/S_4.11		110	8760	$0.00	$4.30	$10.35	9,516
	F/S_4.12		120	8760	$0.00	$4.30	$11.29	9,516
	F/S_4.13		130	8760	$0.00	$4.30	$12.23	9,516

Appendix D: 9-bus Solar Generation Calculations

General Variables Assumed for Summer Data:

Worcester Airport/Central MA Lat 42.2680° N, Long 71.8735° W	
L, Latitude	42.268
Lo, Longitude	71.8735
Fall Date	15-Jul
n, Day num of Year	196
Local Standard Meridian Time (EST)	75
B angle [deg]	113.7362637
δ, solar declination angle [deg]	21.51733603
Apparent Solar Time adj, ASTj [min]	6.890188866
ET, Equation of Time [min]	-5.615811134
Weather Data	
Condition:	Sunny
Max Temp	88 F
Min Temp	69 F
Sunrise	5:25 AM
Sunset	8:22 PM
Length of visible light	16 H
Length of Day	15 H
deg to rad conv	0.017453293
rad to deg conv	57.29577951
Solar Constant [kW/m^2]	1.377
Hsr, Hour Angle at Sunrise/Sunset	110.9986972
Q, refraction adjustment	5.394316821
Sunrise Hour (geometric)	4.600086851
Geometric Sunrise (solar time)	4:36:00 AM
Adj Geo Sunrise	4:31:23 AM
Actual Sunrise (LST)	4:24:00 AM
Sunset Hour (geometric)	19.39991315
Geometric Sunset (solar time)	7:24:00 PM
Adj Geo Sunset	7:29:23 PM
Actual Sunset (LST)	7:22:00 PM
I0 [kW/m^2], Extraterrestrial Solar Insolation	1.331440546
k, Optical Depth Constant	0.208883062
A, Apparent ET Flux Constant	1086.661374
C, Sky Diffuse Factor Constant	0.134866356
ρ, ground reflectance	0.2

Summer Solar Data Calculations:

Local Time (EDT)	LST, Local Standard Time	Hour of Day	AST, Apparent Solar Time	H, Hour Angle	β [deg], Solar Altitude Angle	Φs [deg], Solar Azimuth Angle	m, Air Mass Ratio	IC, Total Insolation	Scaled Energy Prod, [MW]
1:00	0:00	0	0:07	180	-26.21466397	7.27905E-15	-2.26379825	672.8524	0.0
2:00	1:00	1	1:07	165	-24.72589803	15.37195631	-2.39075629	697.4313	0.0
3:00	2:00	2	2:07	150	-20.45691362	29.76624154	-2.86120654	790.4614	0.0
4:00	3:00	3	3:07	135	-13.89232655	42.66014183	-4.16496536	1081.787	0.0
5:00	4:00	4	4:07	120	-5.596311614	54.04980673	-10.2544296	4063.828	0.0
6:00	5:00	5	5:07	105	3.928880017	64.25340057	14.59466965	23.95463	3.3
7:00	6:00	6	6:07	90	14.28219143	73.7351241	4.053542216	229.4364	31.4
8:00	7:00	7	7:07	75	25.14290728	83.05418579	2.353619794	345.5627	47.3
9:00	8:00	8	8:07	60	36.22192784	87.05555253	1.69229232	458.8889	62.8
10:00	9:00	9	9:07	45	47.18008526	75.4260384	1.363338298	652.0432	89.3
11:00	10:00	10	10:07	30	57.44747513	59.82345758	1.18638242	804.4004	110.2
12:00	11:00	11	11:07	15	65.7376243	35.87098719	1.096884148	901.4373	123.4
13:00	12:00	12	12:07	0	69.24933603	0	1.069368772	934.7142	128.0
14:00	13:00	13	13:07	-15	65.7376243	-35.87098719	1.096884148	901.4373	123.4
15:00	14:00	14	14:07	-30	57.44747513	-59.82345758	1.18638242	804.4004	110.2
16:00	15:00	15	15:07	-45	47.18008526	-75.4260384	1.363338298	652.0432	89.3
17:00	16:00	16	16:07	-60	36.22192784	-87.05555253	1.69229232	458.8889	62.8
18:00	17:00	17	17:07	-75	25.14290728	-83.05418579	2.353619794	345.5627	47.3
19:00	18:00	18	18:07	-90	14.28219143	-73.7351241	4.053542216	229.4364	31.4
20:00	19:00	19	19:07	-105	3.928880017	-64.25340057	14.59466965	23.95463	3.3
21:00	20:00	20	20:07	-120	-5.596311614	-54.04980673	-10.2544296	4063.828	0.0
22:00	21:00	21	21:07	-135	-13.89232655	-42.66014183	-4.16496536	1081.787	0.0
23:00	22:00	22	22:07	-150	-20.45691362	-29.76624154	-2.86120654	790.4614	0.0
0:00	23:00	23	23:07	-165	-24.72589803	-15.37195631	-2.39075629	697.4313	0.0

General Variables Assumed for Fall Data:

Worcester Airport/Central MA Lat 42.2680° N, Long 71.8735° W	
L, Latitude	42.268
Lo, Longitude	71.8735
Fall Date	15-Oct
n, Day num of Year	288
Local Standard Meridian Time (EST)	75
B angle [deg]	204.72527
δ, solar declination angle [deg]	-9.5993972
Apparent Solar Time adj, ASTj [min]	27.472751
ET, Equation of Time [min]	14.966751
Weather Data	
Condition:	Sunny
Max Temp	57 F
Min Temp	38 F
Sunrise	7:01 AM
Sunset	6:05 PM
Length of visible light	12 H
Length of Day	11 H
deg to rad conv	0.0174533
rad to deg conv	57.29578
Solar Constant [kW/m^2]	1.377
Hsr, Hour Angle at Sunrise/Sunset	81.157391
Q, refraction adjustment	4.8087805
Sunrise Hour (geometric)	6.5895073
Geometric Sunrise (solar time)	6:35:24 AM
Adj Geo Sunrise	6:31:36 AM
Actual Sunrise (LST)	6:02:30 AM
Sunset Hour (geometric)	17.410493
Geometric Sunset (solar time)	5:24:38 PM
Adj Geo Sunset	5:29:26 PM
Actual Sunset (LST)	5:01:58 PM
I0 [kW/m^2], Extraterrestrial Solar Insolation	1.3883697
k, Optical Depth Constant	0.1706912
A, Apparent ET Flux Constant	1176.6441
C, Sky Diffuse Factor Constant	0.0912185
ρ, ground reflectance	0.2

Fall Solar Data Calculations:

Local Time (EDT)	LST, Local Standard Time	Hour of Day	AST, Apparent Solar Time	H, Hour Angle	β [deg], Solar Altitude Angle	Φs [deg], Solar Azimuth Angle	m, Air Mass Ratio	IC, Total Insolation	Scaled Energy Prod, [MW]
1:00	0:00	0	0:27	180	-57.33139723	1.28225E-14	-1.1879212	-288.288454	0.0
2:00	1:00	1	1:27	165	-54.7801002	26.26329372	-1.2240731	-284.496698	0.0
3:00	2:00	2	2:27	150	-48.07780494	47.55188481	-1.3439907	-273.693255	0.0
4:00	3:00	3	3:27	135	-38.90997874	63.63681325	-1.5921067	-257.840278	0.0
5:00	4:00	4	4:27	120	-28.4886156	76.29808664	-2.0965058	-241.687682	0.0
6:00	5:00	5	5:27	105	-17.51813345	87.10029356	-3.322175	-241.46305	0.0
7:00	6:00	6	6:27	90	-6.439935597	82.86625178	-8.9157098	424.7984705	0.0
8:00	7:00	7	7:27	75	4.39801509	72.78742605	13.0404472	43.05778825	5.7
9:00	8:00	8	8:27	60	14.63503228	61.94944825	3.95787246	348.0545668	46.1
10:00	9:00	9	9:27	45	23.81441331	49.64894057	2.47662407	608.6520667	80.5
11:00	10:00	10	10:27	30	31.31411868	35.24392247	1.92407726	804.1643394	106.4
12:00	11:00	11	11:27	15	36.34325978	18.47090767	1.68741767	925.8820115	122.5
13:00	12:00	12	12:27	0	38.13260277	0	1.61947631	967.2431699	128.0
14:00	13:00	13	13:27	-15	36.34325978	-18.47090767	1.68741767	925.8820115	122.5
15:00	14:00	14	14:27	-30	31.31411868	-35.24392247	1.92407726	804.1643394	106.4
16:00	15:00	15	15:27	-45	23.81441331	-49.64894057	2.47662407	608.6520667	80.5
17:00	16:00	16	16:27	-60	14.63503228	-61.94944825	3.95787246	348.0545668	46.1
18:00	17:00	17	17:27	-75	4.39801509	-72.78742605	13.0404472	43.05778825	5.7
19:00	18:00	18	18:27	-90	-6.439935597	-82.86625178	-8.9157098	424.7984705	0.0
20:00	19:00	19	19:27	-105	-17.51813345	-87.10029356	-3.322175	-241.46305	0.0
21:00	20:00	20	20:27	-120	-28.4886156	-76.29808664	-2.0965058	-241.687682	0.0
22:00	21:00	21	21:27	-135	-38.90997874	-63.63681325	-1.5921067	-257.840278	0.0
23:00	22:00	22	22:27	-150	-48.07780494	-47.55188481	-1.3439907	-273.693255	0.0
0:00	23:00	23	23:27	-165	-54.7801002	-26.26329372	-1.2240731	-284.496698	0.0

Appendix E: 9-bus Results Summary

Fall Solar Congested								
Storage Size (MW)	No Storage	BGen3 (0 Bus)	B9 (1 Bus)	B6 (2 Bus)	B8 (2 Bus)	B7 (3 Bus)	B4 (3 Bus)	B5 (4 Bus)	Bgen2 (4 Bus)
0	287940.57	287940.57	287940.57	287940.57	287940.57	287940.57	287940.57	287940.57	287940.57
10	287940.57	287834.8	287836.91	287918.03	287870.48	287944.17	287973.81	287901.88	287942.94
20	287940.57	287782.93	287785.32	287972.4	287856	287967.33	288047.24	287966.5	287963.58
30	287940.57	287774.52	287774.98	288065.04	287877.3	288011.38	288134.52	288054.95	288005.88
40	287940.57	287813.53	287810.76	288198.33	287930.15	288071.94	288241.86	288173.54	288067.03
50	287940.57	287894.18	287891.51	288368.35	288013.27	288149.47	288372.03	288315.98	288146.25
60	287940.57	288015.66	288014.96	288583.16	288125.55	288242.53	288514.01	288487.62	288244.01
70	287940.57	288186.02	288186.58	288840.12	288168.79	288350.45	288673.31	288686.46	288352.32
80	287940.57	288388.64	288394.88	289139.76	288339.1	288481.39	288852.62	288913.4	288485.71
90	287940.57	288513.86	288522.72	289481.13	288741.59	288625.07	289044.36	289167.39	288632.08
100	287940.57	288834.85	288846.04	289867.01	289149.71	288763.58	289258.58	289449.54	288770.99
110	287940.57	289393.91	289406.42	290295.07	289480.01	288896.12	289485.82	289760.19	288905.22
120	287940.57	289863.46	289880.23	290747.97	289715.52	289043.53	289738.58	290099.98	289053.21
130	287940.57	290307.92	290326.35	291258.82	289964.31	289198.23	290005.62	290471.46	289208.4
Fall Solar Less Congested								
Storage Size (MW)	No Storage	BGen3 (0 Bus)	B9 (1 Bus)	B6 (2 Bus)	B8 (2 Bus)	B7 (3 Bus)	B4 (3 Bus)	B5 (4 Bus)	Bgen2 (4 Bus)
0	286223.46	286223.46	286223.46	286223.46	286223.46	286223.46	286223.46	286223.46	286223.46
10	286223.46	286187.75	286189.58	286211.83	286221.06	286246.99	286264.31	286255.63	286239.01
30	286223.46	286183.81	286183.94	286297.82	286250.57	286302.76	286363.75	286350.53	286295.76
50	286223.46	286261.03	286261.5	286464.24	286338.24	286390.39	286495.53	286495.26	286383.58
70	286223.46	286418.32	286419.34	286703.6	286483.66	286511.19	286660.02	286686.43	286504.62
90	286223.46	286665.16	286666.57	287018.93	286684.33	286664.99	286857.53	286925.17	286658.88
110	286223.46	286992.25	286993.98	287410.12	286946.69	286851	287087.46	287210.35	286845.37
130	286223.46	287403.03	287405.35	287877.75	287266.98	287065.77	287353.59	287542.85	287062.13
Difference Between Congested and Less Congested								
Size (MW)	No Storage	0 Bus	B9 (1 Bus)	B6 (2 Bus)	B8 (2 Bus)	B7 (3 Bus)	B4 (3 Bus)	B5 (4 Bus)	Bgen2 (4 Bus)
0	-1717.11	-1717.11	-1717.11	-1717.11	-1717.11	-1717.11	-1717.11	-1717.11	-1717.11
10	-1717.11	-1647.05	-1647.33	-1706.2	-1649.42	-1697.18	-1709.5	-1646.25	-1703.93
30	-1717.11	-1590.71	-1591.04	-1767.22	-1626.73	-1708.62	-1770.77	-1704.42	-1710.12
50	-1717.11	-1633.15	-1630.01	-1904.11	-1675.03	-1759.08	-1876.5	-1820.72	-1762.67
70	-1717.11	-1767.7	-1767.24	-2136.52	-1685.13	-1839.26	-2013.29	-2000.03	-1847.7
90	-1717.11	-1848.7	-1856.15	-2462.2	-2057.26	-1960.08	-2186.83	-2242.22	-1973.2
110	-1717.11	-2401.66	-2412.44	-2884.95	-2533.32	-2045.12	-2398.36	-2549.84	-2059.85
130	-1717.11	-2904.89	-2921	-3381.07	-2697.33	-2132.46	-2652.03	-2928.61	-2146.27
Fall Wind Congested								
Storage Size (MW)	No Storage	BGen3 (0 Bus)	B9 (1 Bus)	B6 (2 Bus)	B8 (2 Bus)	B7 (3 Bus)	B4 (3 Bus)	B5 (4 Bus)	Bgen2 (4 Bus)

	No Storage	BGen3 (0 Bus)	B9 (1 Bus)	B6 (2 Bus)	B8 (2 Bus)	B7 (3 Bus)	B4 (3 Bus)	B5 (4 Bus)	Bgen2 (4 Bus)
0	237997.92	237997.92	237997.92	237997.92	237997.92	237997.92	237997.92	237997.92	237997.92
10	237997.92	237946.11	237950.74	237985.82	237960.16	238017.28	238022.47	237955.93	238013.26
20	237997.92	237933.94	237944.78	238039.38	237977.76	238056.41	238085.15	238011.72	238048.52
30	237997.92	237971.7	237979.4	238114.85	238020.31	238110.64	238159.75	238076.47	238104.56
40	237997.92	238051.12	238057.24	238241.42	238094.96	238181.42	238254.01	238177.69	238177.69
50	237997.92	238172.08	238178.6	238407.86	238200.21	238267.72	238369.24	238305.72	238264.99
60	237997.92	238337.9	238345.49	238615.76	238336.64	238392.67	238495.99	238460.69	238389.76
70	237997.92	238546.9	238554.94	238865.46	238503.7	238514.27	238643.94	238642.77	238512.58
80	237997.92	238807.39	238813.89	239155.31	238701.74	238658.53	238809.81	238851.67	238658.26
90	237997.92	239108.71	239113.97	239491.01	238931.98	238823.79	238991.33	239088.06	238823.8
100	237997.92	239479.36	239483.84	239868.95	239190.09	239002.77	239194.06	239355.13	239005.41
110	237997.92	239951.87	239955.1	240290.88	239211.38	239197.85	239413.94	239650.96	239202.91
120	237997.92	240462.3	240462.23	240742.11	239199.47	239413.57	239651.12	239974.45	239421.02
130	237997.92	241228.28	241226.86	241211.64	239474.38	239647.28	239906.75	240326.97	239657.47

Fall Wind Less Congested

Storage Size (MW)	No Storage	BGen3 (0 Bus)	B9 (1 Bus)	B6 (2 Bus)	B8 (2 Bus)	B7 (3 Bus)	B4 (3 Bus)	B5 (4 Bus)	Bgen2 (4 Bus)
0	236411.95	236411.95	236411.95	236411.95	236411.95	236411.95	236411.95	236411.95	236411.95
10	236411.95	236399.28	236402.49	236396.39	236419.65	236439.66	236442.46	236437.03	236431.82
30	236411.95	236437.07	236439.9	236482.99	236471.65	236506.43	236533.05	236520.17	236500.02
50	236411.95	236555.84	236559.06	236642.09	236580.28	236605.68	236653.78	236648.87	236598.82
70	236411.95	236758.62	236760.05	236877.31	236746.11	236737.5	236807.06	236826.42	236727.66
90	236411.95	237041.58	237043.48	237188.41	236969.23	236902.83	236995.04	237052.43	236895.89
110	236411.95	237409.22	237410.52	237574.92	237251.05	237098.66	237214.04	237326.14	237093.5
130	236411.95	237859.5	237859.85	238037.32	237589.82	237340.56	237464.7	237647.18	237334.6

Difference Between Congested and Less Congested

Size (MW)	No Storage	0 Bus	B9 (1 Bus)	B6 (2 Bus)	B8 (2 Bus)	B7 (3 Bus)	B4 (3 Bus)	B5 (4 Bus)	Bgen2 (4 Bus)
0	-1585.97	-1585.97	-1585.97	-1585.97	-1585.97	-1585.97	-1585.97	-1585.97	-1585.97
10	-1585.97	-1546.83	-1548.25	-1589.43	-1540.51	-1577.62	-1580.01	-1518.9	-1581.44
30	-1585.97	-1534.63	-1539.5	-1631.86	-1548.66	-1604.21	-1626.7	-1556.3	-1604.54
50	-1585.97	-1616.24	-1619.54	-1765.77	-1619.93	-1662.04	-1715.46	-1656.85	-1666.17
70	-1585.97	-1788.28	-1794.89	-1988.15	-1757.59	-1776.77	-1836.88	-1816.35	-1784.92
90	-1585.97	-2067.13	-2070.49	-2302.6	-1962.75	-1920.96	-1996.29	-2035.63	-1927.91
110	-1585.97	-2542.65	-2544.58	-2715.96	-1960.33	-2099.19	-2199.9	-2324.82	-2109.41
130	-1585.97	-3368.78	-3367.01	-3174.32	-1884.56	-2306.72	-2442.05	-2679.79	-2322.87

Summer Solar Congested

Storage Size (MW)	No Storage	BGen3 (0 Bus)	B9 (1 Bus)	B6 (2 Bus)	B8 (2 Bus)	B7 (3 Bus)	B4 (3 Bus)	B5 (4 Bus)	Bgen2 (4 Bus)
0	241608.16	241608.16	241608.16	241608.16	241608.16	241608.16	241608.16	241608.16	241608.16
10	241608.16	241584.19	241590.19	241595.95	241594.46	241648.12	241642.68	241576.36	241646.44
20	241608.16	241583.3	241589.89	241634.82	241610.54	241685.04	241693.65	241616.16	241685.42
30	241608.16	241629.9	241637.6	241719.68	241654.41	241739.14	241759.28	241675.3	241741.4
40	241608.16	241712.84	241719.95	241834.07	241725.39	241818.1	241839.39	241775.35	241821.56

50	241608.16	241834.99	241841.54	241986.14	241823.77	241907.08	241936.82	241889.24	241912.12
60	241608.16	242012.12	242018.36	242173.57	241950.21	242012.06	242050.46	242027.57	242019.14
70	241608.16	242217.09	242223.32	242395.89	242113.61	242118.28	242193.19	242190.34	242127.82
80	241608.16	242461.04	242466.9	242659.89	242073.63	242252.94	242341.64	242376.46	242265.51
90	241608.16	242692.63	242697.8	242962.53	242053.42	242353.46	242508.04	242589.32	242367.63
100	241608.16	242795.45	242799.86	243251.73	242484.25	242464.69	242686.63	242826.95	242480.36
110	241608.16	243428.34	243429.17	243558.42	243184.49	242587.11	242882.25	243091.36	242605.64
120	241608.16	244203.24	244201.52	243945.63	244055.75	242728.12	243095.24	243372.16	242748.84
130	241608.16	244830.98	244830.67	244340.72	244680.53	242877.01	243326.4	243628.67	242900.85

Summer Solar Less Congested

Storage Size (MW)	No Storage	BGen3 (0 Bus)	B9 (1 Bus)	B6 (2 Bus)	B8 (2 Bus)	B7 (3 Bus)	B4 (3 Bus)	B5 (4 Bus)	Bgen2 (4 Bus)
0	239959.34	239959.34	239959.34	239959.34	239959.34	239959.34	239959.34	239959.34	239959.34
10	239959.34	239952.71	239955.84	239944.85	239971.27	239990.04	239987.8	239980.84	239981.28
30	239959.34	239998.85	240000.39	240023.32	240024.87	240057.17	240069.37	240055.72	240049.47
50	239959.34	240117.63	240119.01	240164.86	240129.58	240153.32	240178.45	240168.2	240145.82
70	239959.34	240315.14	240316.84	240384.18	240285.48	240283.27	240315.78	240331.98	240270.97
90	239959.34	240584.21	240585.32	240665.32	240493.04	240439.99	240483.94	240534.2	240433.16
110	239959.34	240933.84	240934.93	241014.16	240752.12	240625.95	240681.76	240779.28	240619.12
130	239959.34	241353.39	241353.61	241429.49	241068.19	240840.04	240907.79	241066.54	240834.31

Difference Between Congested and Less Congested

Size (MW)	No Storage	0 Bus	B9 (1 Bus)	B6 (2 Bus)	B8 (2 Bus)	B7 (3 Bus)	B4 (3 Bus)	B5 (4 Bus)	Bgen2 (4 Bus)
0	-1648.82	-1648.82	-1648.82	-1648.82	-1648.82	-1648.82	-1648.82	-1648.82	-1648.82
10	-1648.82	-1631.48	-1634.35	-1651.1	-1623.19	-1658.08	-1654.88	-1595.52	-1665.16
30	-1648.82	-1631.05	-1637.21	-1696.36	-1629.54	-1681.97	-1689.91	-1619.58	-1691.93
50	-1648.82	-1717.36	-1722.53	-1821.28	-1694.19	-1753.76	-1758.37	-1721.04	-1766.3
70	-1648.82	-1901.95	-1906.48	-2011.71	-1828.13	-1835.01	-1877.41	-1858.36	-1856.85
90	-1648.82	-2108.42	-2112.48	-2297.21	-1560.38	-1913.47	-2024.1	-2055.12	-1934.47
110	-1648.82	-2494.5	-2494.24	-2544.26	-2432.37	-1961.16	-2200.49	-2312.08	-1986.52
130	-1648.82	-3477.59	-3477.06	-2911.23	-3612.34	-2036.97	-2418.61	-2562.13	-2066.54

Summer Wind Congested

Storage Size (MW)	No Storage	BGen3 (0 Bus)	B9 (1 Bus)	B6 (2 Bus)	B8 (2 Bus)	B7 (3 Bus)	B4 (3 Bus)	B5 (4 Bus)	Bgen2 (4 Bus)
0	200838.22	200838.22	200838.22	200838.22	200838.22	200838.22	200838.22	200838.22	200838.22
10	200838.22	200858.64	200871.95	200831.44	200849.73	200893.2	200867.23	200799.3	200889.75
20	200838.22	200908.69	200920.81	200853.05	200886.3	200947.76	200900.07	200811.7	200945.51
30	200838.22	200986.46	200998.62	200916.44	200952.74	201008.53	200951.26	200852.44	201007.29
40	200838.22	201121.04	201133	201016.72	201040.69	201102.29	201021.44	200920.74	201102.86
50	200838.22	201285.76	201296.45	201153.21	201156.39	201202.92	201106.45	201011.19	201205.95
60	200838.22	201489.29	201502.54	201324.7	201302.28	201319.78	201207.08	201126.47	201324.96
70	200838.22	201720.72	201732.73	201535.69	201474.17	201452.4	201323.67	201265.52	201460.02
80	200838.22	202002.19	202011.2	201781.02	201676.18	201601.17	201456.6	201429.2	201611.61
90	200838.22	202325.25	202329.56	202064.51	201919.45	201768.85	201605.24	201617.04	201782.21

100	200838.22	202646.8	202653.33	202323.34	202173.04	201945.51	201770.73	201830.17	201962.39
110	200838.22	203089.25	203093.2	202619.45	202094.92	202141.85	201951.73	202068.02	202164.07
120	200838.22	203533.87	203532.2	202991.07	202303.83	202354.27	202148.25	202310.87	202382.4
130	200838.22	204029.05	204021.17	203435.52	202998.67	202582.86	202361.52	202540.32	202614.48

Summer Wind Less Congested

Storage Size (MW)	No Storage	BGen3 (0 Bus)	B9 (1 Bus)	B6 (2 Bus)	B8 (2 Bus)	B7 (3 Bus)	B4 (3 Bus)	B5 (4 Bus)	Bgen2 (4 Bus)
0	199221.34	199221.34	199221.36	199221.36	199221.36	199221.36	199221.36	199221.36	199221.36
10	199221.34	199241.29	199245.12	199203.08	199244.61	199256.83	199241.61	199231.66	199248.71
30	199221.34	199336.51	199340.58	199270.21	199322.46	199342.18	199306.24	199285.32	199334.84
50	199221.34	199506.94	199511.52	199401.54	199450.97	199451.66	199400.41	199377.54	199443.54
70	199221.34	199757.25	199753.96	199602.33	199630.33	199599.34	199523.37	199515.17	199592.68
90	199221.34	200075.49	200079.63	199870.82	199860.91	199771.5	199674.44	199695.94	199764.61
110	199221.34	200468.15	200471	200206.08	200143.54	199972.66	199855.86	199918.89	199966.2
130	199221.34	200935.08	200937.13	200609.2	200476.46	200203.64	200066.65	200184.59	200197.53

Difference Between Congested and Less Congested

Size (MW)	No Storage	0 Bus	B9 (1 Bus)	B6 (2 Bus)	B8 (2 Bus)	B7 (3 Bus)	B4 (3 Bus)	B5 (4 Bus)	Bgen2 (4 Bus)
0	-1616.88	-1616.88	-1616.86	-1616.86	-1616.86	-1616.86	-1616.86	-1616.86	-1616.86
10	-1616.88	-1617.35	-1626.83	-1628.36	-1605.12	-1636.37	-1625.62	-1567.64	-1641.04
30	-1616.88	-1649.95	-1658.04	-1646.23	-1630.28	-1666.35	-1645.02	-1567.12	-1672.45
50	-1616.88	-1778.82	-1784.93	-1751.67	-1705.42	-1751.26	-1706.04	-1633.65	-1762.41
70	-1616.88	-1963.47	-1978.77	-1933.36	-1843.84	-1853.06	-1800.3	-1750.35	-1867.34
90	-1616.88	-2249.76	-2249.93	-2193.69	-2058.54	-1997.35	-1930.8	-1921.1	-2017.6
110	-1616.88	-2621.1	-2622.2	-2413.37	-1951.38	-2169.19	-2095.87	-2149.13	-2197.87
130	-1616.88	-3093.97	-3084.04	-2826.32	-2522.21	-2379.22	-2294.87	-2355.73	-2416.95

Appendix F: 14-Bus Specifications

Original 14-bus Network Specifications in EPC format:

0,   100.00, 33, 0, 0, 60.00   / October 01, 2013 18:37:53

 08/19/93 UW ARCHIVE   100.0 1962 W IEEE 14 Bus Test Case

   1,'Bus 1   ', 138.0000,3, 1,   1, 1,1.06000, 0.0000

   2,'Bus 2   ', 138.0000,2, 1,   1, 1,1.04500, -4.9826

   3,'Bus 3   ', 138.0000,2, 1,   1, 1,1.01000, -12.7250

   4,'Bus 4   ', 138.0000,1, 1,   1, 1,1.01767, -10.3128

   5,'Bus 5   ', 138.0000,1, 1,   1, 1,1.01951, -8.7738

   6,'Bus 6   ', 138.0000,2, 1,   1, 1,1.07000, -14.2209

   7,'Bus 7   ', 138.0000,1, 1,   1, 1,1.06152, -13.3596

   8,'Bus 8   ', 138.0000,2, 1,   1, 1,1.09000, -13.3596

   9,'Bus 9   ', 138.0000,1, 1,   1, 1,1.05593, -14.9385

   10,'Bus 10   ', 138.0000,1, 1,   1, 1,1.05099, -15.0972

   11,'Bus 11   ', 138.0000,1, 1,   1, 1,1.05691, -14.7906

   12,'Bus 12   ', 138.0000,1, 1,   1, 1,1.05519, -15.0755

   13,'Bus 13   ', 138.0000,1, 1,   1, 1,1.05038, -15.1562

   14,'Bus 14   ', 138.0000,1, 1,   1, 1,1.03553, -16.0336

0 / END OF BUS DATA, BEGIN LOAD DATA

   2,'1 ',1, 1, 1,   21.700, 12.700,   0.000,   0.000,   0.000, -0.000, 1,1

   3,'1 ',1, 1, 1,   94.200, 19.000,   0.000,   0.000,   0.000, -0.000, 1,1

   4,'1 ',1, 1, 1,   47.800, -3.900,   0.000,   0.000,   0.000, -0.000, 1,1

   5,'1 ',1, 1, 1,   7.600,   1.600,   0.000,   0.000,   0.000, -0.000, 1,1

   6,'1 ',1, 1, 1,   11.200,   7.500,   0.000,   0.000,   0.000, -0.000, 1,1

   9,'1 ',1, 1, 1,   29.500, 16.600,   0.000,   0.000,   0.000, -0.000, 1,1

   10,'1 ',1, 1, 1,   9.000,   5.800,   0.000,   0.000,   0.000, -0.000, 1,1

   11,'1 ',1, 1, 1,   3.500,   1.800,   0.000,   0.000,   0.000, -0.000, 1,1

   12,'1 ',1, 1, 1,   6.100,   1.600,   0.000,   0.000,   0.000, -0.000, 1,1

   13,'1 ',1, 1, 1,   13.500,   5.800,   0.000,   0.000,   0.000, -0.000, 1,1

   14,'1 ',1, 1, 1,   14.900,   5.000,   0.000,   0.000,   0.000, -0.000, 1,1

0 / END OF LOAD DATA, BEGIN FIXED SHUNT DATA

9,' 1', 1,   0.000,   19.000

0 / END OF FIXED SHUNT DATA, BEGIN GENERATOR DATA

   1,'1 ', 232.392, -16.549,   0.000,   0.000,1.06000, 0, 615.000, 0.00000, 1.00000, 0.00000, 0.00000,1.00000,1,
100.0, 10000.000,-10000.000, 1,1.0000, 0,1.0000, 0,1.0000, 0,1.0000,0, 1.0000

   2,'1 ',   40.000,   43.556,   50.000, -40.000,1.04500, 0,   60.000, 0.00000, 1.00000, 0.00000, 0.00000,1.00000,1,
100.0, 10000.000,-10000.000, 1,1.0000, 0,1.0000, 0,1.0000, 0,1.0000,0, 1.0000

   3,'1 ',   0.000,   25.075,   40.000,   0.000,1.01000, 0,   60.000, 0.00000, 1.00000, 0.00000, 0.00000,1.00000,1,
100.0, 10000.000,-10000.000, 1,1.0000, 0,1.0000, 0,1.0000, 0,1.0000,0, 1.0000

   6,'1 ',   0.000,   12.730,   24.000,   -6.000,1.07000, 0,   25.000, 0.00000, 1.00000, 0.00000, 0.00000,1.00000,1,
100.0, 10000.000,-10000.000, 1,1.0000, 0,1.0000, 0,1.0000, 0,1.0000,0, 1.0000

   8,'1 ',   0.000,   17.623,   24.000,   -6.000,1.09000, 0,   25.000, 0.00000, 1.00000, 0.00000, 0.00000,1.00000,1,
100.0, 10000.000,-10000.000, 1,1.0000, 0,1.0000, 0,1.0000, 0,1.0000,0, 1.0000

0 / END OF GENERATOR DATA, BEGIN BRANCH DATA

   1,   2,'1 ', 0.01938, 0.05917,0.05280, 0.00, 0.00, 0.00, 0.00000, 0.00000, 0.00000, 0.00000,1,1, 0.0, 1,1.0000,
  0,1.0000, 0,1.0000, 0,1.0000

   1,   5,'1 ', 0.05403, 0.22304,0.04920, 0.00, 0.00, 0.00, 0.00000, 0.00000, 0.00000, 0.00000,1,1, 0.0, 1,1.0000,
  0,1.0000, 0,1.0000, 0,1.0000

   2,   3,'1 ', 0.04699, 0.19797,0.04380, 0.00, 0.00, 0.00, 0.00000, 0.00000, 0.00000, 0.00000,1,1, 0.0, 1,1.0000,
  0,1.0000, 0,1.0000, 0,1.0000

   2,   4,'1 ', 0.05811, 0.17632,0.03400, 0.00, 0.00, 0.00, 0.00000, 0.00000, 0.00000, 0.00000,1,1, 0.0, 1,1.0000,
  0,1.0000, 0,1.0000, 0,1.0000

   2,   5,'1 ', 0.05695, 0.17388,0.03460, 0.00, 0.00, 0.00, 0.00000, 0.00000, 0.00000, 0.00000,1,1, 0.0, 1,1.0000,
  0,1.0000, 0,1.0000, 0,1.0000

   3,   4,'1 ', 0.06701, 0.17103,0.01280, 0.00, 0.00, 0.00, 0.00000, 0.00000, 0.00000, 0.00000,1,1, 0.0, 1,1.0000,
  0,1.0000, 0,1.0000, 0,1.0000

   4,   5,'1 ', 0.01335, 0.04211,0.00000, 0.00, 0.00, 0.00, 0.00000, 0.00000, 0.00000, 0.00000,1,1, 0.0, 1,1.0000,
  0,1.0000, 0,1.0000, 0,1.0000

   6,   11,'1 ', 0.09498, 0.19890,0.00000, 0.00, 0.00, 0.00, 0.00000, 0.00000, 0.00000, 0.00000,1,1, 0.0, 1,1.0000,
  0,1.0000, 0,1.0000, 0,1.0000

   6,   12,'1 ', 0.12291, 0.25581,0.00000, 0.00, 0.00, 0.00, 0.00000, 0.00000, 0.00000, 0.00000,1,1, 0.0, 1,1.0000,
  0,1.0000, 0,1.0000, 0,1.0000

   6,   13,'1 ', 0.06615, 0.13027,0.00000, 0.00, 0.00, 0.00, 0.00000, 0.00000, 0.00000, 0.00000,1,1, 0.0, 1,1.0000,
  0,1.0000, 0,1.0000, 0,1.0000

   7,   8,'1 ', 0.00000, 0.17615,0.00000, 0.00, 0.00, 0.00, 0.00000, 0.00000, 0.00000, 0.00000,1,1, 0.0, 1,1.0000,
  0,1.0000, 0,1.0000, 0,1.0000

   7,   9,'1 ', 0.00000, 0.11001,0.00000, 0.00, 0.00, 0.00, 0.00000, 0.00000, 0.00000, 0.00000,1,1, 0.0, 1,1.0000,
  0,1.0000, 0,1.0000, 0,1.0000

   9,   10,'1 ', 0.03181, 0.08450,0.00000, 0.00, 0.00, 0.00, 0.00000, 0.00000, 0.00000, 0.00000,1,1, 0.0, 1,1.0000,
  0,1.0000, 0,1.0000, 0,1.0000

9,   14,'1 ', 0.12711, 0.27038,0.00000, 0.00, 0.00, 0.00, 0.00000, 0.00000, 0.00000, 0.00000,1,1, 0.0, 1,1.0000,
0,1.0000, 0,1.0000, 0,1.0000

   10,   11,'1 ', 0.08205, 0.19207,0.00000, 0.00, 0.00, 0.00, 0.00000, 0.00000, 0.00000, 0.00000,1,1, 0.0, 1,1.0000,
0,1.0000, 0,1.0000, 0,1.0000

   12,   13,'1 ', 0.22092, 0.19988,0.00000, 0.00, 0.00, 0.00, 0.00000, 0.00000, 0.00000, 0.00000,1,1, 0.0, 1,1.0000,
0,1.0000, 0,1.0000, 0,1.0000

   13,   14,'1 ', 0.17093, 0.34802,0.00000, 0.00, 0.00, 0.00, 0.00000, 0.00000, 0.00000, 0.00000,1,1, 0.0, 1,1.0000,
0,1.0000, 0,1.0000, 0,1.0000

0 / END OF BRANCH DATA, BEGIN TRANSFORMER DATA

   4,   7,   0,'1 ',1,1,1, 0.00000, 0.00000,2,'   ',1, 1,1.0000, 0,1.0000, 0,1.0000, 0,1.0000

 0.00000, 0.20912, 100.00

0.97800, 0.000, 0.000, 0.00, 0.00, 0.00,0,   0, 1.50000, 0.51000, 1.50000, 0.51000,159, 0, 0.00000, 0.00000

1.00000, 0.000

   4,   9,   0,'1 ',1,1,1, 0.00000, 0.00000,2,'   ',1, 1,1.0000, 0,1.0000, 0,1.0000, 0,1.0000

 0.00000, 0.55618, 100.00

0.96900, 0.000, 0.000, 0.00, 0.00, 0.00,0,   0, 1.50000, 0.51000, 1.50000, 0.51000,159, 0, 0.00000, 0.00000

1.00000, 0.000

   5,   6,   0,'1 ',1,1,1, 0.00000, 0.00000,2,'   ',1, 1,1.0000, 0,1.0000, 0,1.0000, 0,1.0000

 0.00000, 0.25202, 100.00

0.93200, 0.000, 0.000, 0.00, 0.00, 0.00,0,   0, 1.50000, 0.51000, 1.50000, 0.51000,159, 0, 0.00000, 0.00000

1.00000, 0.000

0 / END OF TRANSFORMER DATA, BEGIN AREA DATA

   1,   2,   0.000, 999.990,'IEEE14   '

0 / END OF AREA DATA, BEGIN TWO-TERMINAL DC DATA

0 / END OF TWO-TERMINAL DC DATA, BEGIN VOLTAGE SOURCE CONVERTER DATA

0 / END OF VOLTAGE SOURCE CONVERTER DATA, BEGIN IMPEDANCE CORRECTION DATA

0 / END OF IMPEDANCE CORRECTION DATA, BEGIN MULTI-TERMINAL DC DATA

0 / END OF MULTI-TERMINAL DC DATA, BEGIN MULTI-SECTION LINE DATA

0 / END OF MULTI-SECTION LINE DATA, BEGIN ZONE DATA

   1,'IEEE 14 '

0 / END OF ZONE DATA, BEGIN INTER-AREA TRANSFER DATA

0 / END OF INTER-AREA TRANSFER DATA, BEGIN OWNER DATA

   1,'1'

0 / END OF OWNER DATA, BEGIN FACTS CONTROL DEVICE DATA

0 / END OF FACTS CONTROL DEVICE DATA, BEGIN SWITCHED SHUNT DATA

0 /END OF SWITCHED SHUNT DATA, BEGIN GNE DEVICE DATA

0 /END OF GNE DEVICE DATA

Modified 13-bus Network Specifications in EPC format:

0,   100.00, 33, 0, 0, 60.00   / October 01, 2013 18:37:53

 08/19/93 UW ARCHIVE   100.0 1962 W IEEE 14 Bus Test Case

   1,'Bus 1   ', 138.0000,3, 1,   1, 1,1.06000, 0.0000

   2,'Bus 2   ', 138.0000,2, 1,   1, 1,1.04500, -4.9826

   3,'Bus 3   ', 138.0000,2, 1,   1, 1,1.01000, -12.7250

   4,'Bus 4   ', 138.0000,1, 1,   1, 1,1.01767, -10.3128

   5,'Bus 5   ', 138.0000,1, 1,   1, 1,1.01951, -8.7738

   6,'Bus 6   ', 138.0000,2, 1,   1, 1,1.07000, -14.2209

   7,'Bus 7   ', 138.0000,1, 1,   1, 1,1.06152, -13.3596

   8,'Bus 8   ', 138.0000,2, 1,   1, 1,1.09000, -13.3596

   9,'Bus 9   ', 138.0000,1, 1,   1, 1,1.05593, -14.9385

  10,'Bus 10   ', 138.0000,1, 1,   1, 1,1.05099, -15.0972

  11,'Bus 11   ', 138.0000,1, 1,   1, 1,1.05691, -14.7906

  12,'Bus 12   ', 138.0000,1, 1,   1, 1,1.05519, -15.0755

  13,'Bus 13   ', 138.0000,1, 1,   1, 1,1.05038, -15.1562

0 / END OF BUS DATA, BEGIN LOAD DATA

   2,'1 ',1, 1, 1,   21.700, 12.700,   0.000,   0.000,   0.000, -0.000, 1,1

   3,'1 ',1, 1, 1,   94.200, 19.000,   0.000,   0.000,   0.000, -0.000, 1,1

   4,'1 ',1, 1, 1,   47.800, -3.900,   0.000,   0.000,   0.000, -0.000, 1,1

   5,'1 ',1, 1, 1,   7.600,   1.600,   0.000,   0.000,   0.000, -0.000, 1,1

   6,'1 ',1, 1, 1,   11.200,   7.500,   0.000,   0.000,   0.000, -0.000, 1,1

   9,'1 ',1, 1, 1,   29.500, 16.600,   0.000,   0.000,   0.000, -0.000, 1,1

  10,'1 ',1, 1, 1,   9.000,   5.800,   0.000,   0.000,   0.000, -0.000, 1,1

  11,'1 ',1, 1, 1,   3.500,   1.800,   0.000,   0.000,   0.000, -0.000, 1,1

  12,'1 ',1, 1, 1,   6.100,   1.600,   0.000,   0.000,   0.000, -0.000, 1,1

  13,'1 ',1, 1, 1,   13.500,   5.800,   0.000,   0.000,   0.000, -0.000, 1,1

0 / END OF LOAD DATA, BEGIN FIXED SHUNT DATA

   9,' 1', 1,   0.000,   19.000

0 / END OF FIXED SHUNT DATA, BEGIN GENERATOR DATA

   1,'1 ', 232.392, -16.549,   0.000,   0.000,1.06000, 0, 615.000, 0.00000, 1.00000, 0.00000, 0.00000,1.00000,1,
100.0, 10000.000,-10000.000, 1,1.0000, 0,1.0000, 0,1.0000, 0,1.0000,0, 1.0000

   2,'1 ',   40.000,   43.556, 50.000, -40.000,1.04500, 0,   60.000, 0.00000, 1.00000, 0.00000, 0.00000,1.00000,1,
100.0, 10000.000,-10000.000, 1,1.0000, 0,1.0000, 0,1.0000, 0,1.0000,0, 1.0000

   3,'1 ',   0.000,   25.075, 40.000,   0.000,1.01000, 0,   60.000, 0.00000, 1.00000, 0.00000, 0.00000,1.00000,1,
100.0, 10000.000,-10000.000, 1,1.0000, 0,1.0000, 0,1.0000, 0,1.0000,0, 1.0000

   6,'1 ',   0.000,   12.730, 24.000,   -6.000,1.07000, 0,   25.000, 0.00000, 1.00000, 0.00000, 0.00000,1.00000,1,
100.0, 10000.000,-10000.000, 1,1.0000, 0,1.0000, 0,1.0000, 0,1.0000,0, 1.0000

   8,'1 ',   0.000,   17.623, 24.000,   -6.000,1.09000, 0,   25.000, 0.00000, 1.00000, 0.00000, 0.00000,1.00000,1,
100.0, 10000.000,-10000.000, 1,1.0000, 0,1.0000, 0,1.0000, 0,1.0000,0, 1.0000

0 / END OF GENERATOR DATA, BEGIN BRANCH DATA

   1,   2,'1 ', 0.01938, 0.05917,0.05280, 0.00, 0.00, 0.00, 0.00000, 0.00000, 0.00000, 0.00000,1,1, 0.0, 1,1.0000,
0,1.0000, 0,1.0000, 0,1.0000

   1,   5,'1 ', 0.05403, 0.22304,0.04920, 0.00, 0.00, 0.00, 0.00000, 0.00000, 0.00000, 0.00000,1,1, 0.0, 1,1.0000,
0,1.0000, 0,1.0000, 0,1.0000

   2,   3,'1 ', 0.04699, 0.19797,0.04380, 0.00, 0.00, 0.00, 0.00000, 0.00000, 0.00000, 0.00000,1,1, 0.0, 1,1.0000,
0,1.0000, 0,1.0000, 0,1.0000

   2,   4,'1 ', 0.05811, 0.17632,0.03400, 0.00, 0.00, 0.00, 0.00000, 0.00000, 0.00000, 0.00000,1,1, 0.0, 1,1.0000,
0,1.0000, 0,1.0000, 0,1.0000

   2,   5,'1 ', 0.05695, 0.17388,0.03460, 0.00, 0.00, 0.00, 0.00000, 0.00000, 0.00000, 0.00000,1,1, 0.0, 1,1.0000,
0,1.0000, 0,1.0000, 0,1.0000

   3,   4,'1 ', 0.06701, 0.17103,0.01280, 0.00, 0.00, 0.00, 0.00000, 0.00000, 0.00000, 0.00000,1,1, 0.0, 1,1.0000,
0,1.0000, 0,1.0000, 0,1.0000

   4,   5,'1 ', 0.01335, 0.04211,0.00000, 0.00, 0.00, 0.00, 0.00000, 0.00000, 0.00000, 0.00000,1,1, 0.0, 1,1.0000,
0,1.0000, 0,1.0000, 0,1.0000

   6,   11,'1 ', 0.09498, 0.19890,0.00000, 0.00, 0.00, 0.00, 0.00000, 0.00000, 0.00000, 0.00000,1,1, 0.0, 1,1.0000,
0,1.0000, 0,1.0000, 0,1.0000

   6,   12,'1 ', 0.12291, 0.25581,0.00000, 0.00, 0.00, 0.00, 0.00000, 0.00000, 0.00000, 0.00000,1,1, 0.0, 1,1.0000,
0,1.0000, 0,1.0000, 0,1.0000

   6,   13,'1 ', 0.06615, 0.13027,0.00000, 0.00, 0.00, 0.00, 0.00000, 0.00000, 0.00000, 0.00000,1,1, 0.0, 1,1.0000,
0,1.0000, 0,1.0000, 0,1.0000

   7,   8,'1 ', 0.00000, 0.17615,0.00000, 0.00, 0.00, 0.00, 0.00000, 0.00000, 0.00000, 0.00000,1,1, 0.0, 1,1.0000,
0,1.0000, 0,1.0000, 0,1.0000

   7,   9,'1 ', 0.00000, 0.11001,0.00000, 0.00, 0.00, 0.00, 0.00000, 0.00000, 0.00000, 0.00000,1,1, 0.0, 1,1.0000,
0,1.0000, 0,1.0000, 0,1.0000

   9,   10,'1 ', 0.03181, 0.08450,0.00000, 0.00, 0.00, 0.00, 0.00000, 0.00000, 0.00000, 0.00000,1,1, 0.0, 1,1.0000,
0,1.0000, 0,1.0000, 0,1.0000

10,   11,'1 ', 0.08205, 0.19207,0.00000, 0.00, 0.00, 0.00, 0.00000, 0.00000, 0.00000, 0.00000,1,1, 0.0, 1,1.0000,
0,1.0000, 0,1.0000, 0,1.0000

12,   13,'1 ', 0.22092, 0.19988,0.00000, 0.00, 0.00, 0.00, 0.00000, 0.00000, 0.00000, 0.00000,1,1, 0.0, 1,1.0000,
0,1.0000, 0,1.0000, 0,1.0000

0 / END OF BRANCH DATA, BEGIN TRANSFORMER DATA

   4,   7,   0,'1 ',1,1,1, 0.00000, 0.00000,2,'   ',1, 1,1.0000, 0,1.0000, 0,1.0000, 0,1.0000

 0.00000, 0.20912, 100.00

0.97800, 0.000, 0.000, 0.00, 0.00, 0.00,0,   0, 1.50000, 0.51000, 1.50000, 0.51000,159, 0, 0.00000, 0.00000

1.00000, 0.000

   4,   9,   0,'1 ',1,1,1, 0.00000, 0.00000,2,'   ',1, 1,1.0000, 0,1.0000, 0,1.0000, 0,1.0000

 0.00000, 0.55618, 100.00

0.96900, 0.000, 0.000, 0.00, 0.00, 0.00,0,   0, 1.50000, 0.51000, 1.50000, 0.51000,159, 0, 0.00000, 0.00000

1.00000, 0.000

   5,   6,   0,'1 ',1,1,1, 0.00000, 0.00000,2,'   ',1, 1,1.0000, 0,1.0000, 0,1.0000, 0,1.0000

 0.00000, 0.25202, 100.00

0.93200, 0.000, 0.000, 0.00, 0.00, 0.00,0,   0, 1.50000, 0.51000, 1.50000, 0.51000,159, 0, 0.00000, 0.00000

1.00000, 0.000

0 / END OF TRANSFORMER DATA, BEGIN AREA DATA

  1,   2,   0.000, 999.990,'IEEE14   '

0 / END OF AREA DATA, BEGIN TWO-TERMINAL DC DATA

0 / END OF TWO-TERMINAL DC DATA, BEGIN VOLTAGE SOURCE CONVERTER DATA

0 / END OF VOLTAGE SOURCE CONVERTER DATA, BEGIN IMPEDANCE CORRECTION DATA

0 / END OF IMPEDANCE CORRECTION DATA, BEGIN MULTI-TERMINAL DC DATA

0 / END OF MULTI-TERMINAL DC DATA, BEGIN MULTI-SECTION LINE DATA

0 / END OF MULTI-SECTION LINE DATA, BEGIN ZONE DATA

  1,'IEEE 14 '

0 / END OF ZONE DATA, BEGIN INTER-AREA TRANSFER DATA

0 / END OF INTER-AREA TRANSFER DATA, BEGIN OWNER DATA

  1,'1'

0 / END OF OWNER DATA, BEGIN FACTS CONTROL DEVICE DATA

0 / END OF FACTS CONTROL DEVICE DATA, BEGIN SWITCHED SHUNT DATA

0 /END OF SWITCHED SHUNT DATA, BEGIN GNE DEVICE DATA

0 /END OF GNE DEVICE DATA

Appendix G: 14-Bus Scaled Load Calculations

Summer Load Profile:

Hour	Actual Load [MW]	Total Scaled [MW]	Load 2 MW	Load 3 MW	Load 4 MW	Load 5 MW	Load 6 MW	Load 9 MW	Load 10 MW	Load 11 MW	Load 12 MW	Load 13-1 MW	Load 13-2 MW
0	15425	174.17	14.6	63.3	32.1	5.1	7.5	19.8	6.1	2.4	4.1	9.1	10.0
1	14366	162.21	13.6	59.0	29.9	4.8	7.0	18.5	5.6	2.2	3.8	8.5	9.3
2	13728	155.01	13.0	56.4	28.6	4.5	6.7	17.7	5.4	2.1	3.7	8.1	8.9
3	13324	150.45	12.6	54.7	27.8	4.4	6.5	17.1	5.2	2.0	3.5	7.8	8.7
4	13238	149.47	12.5	54.4	27.6	4.4	6.5	17.0	5.2	2.0	3.5	7.8	8.6
5	13546	152.95	12.8	55.6	28.2	4.5	6.6	17.4	5.3	2.1	3.6	8.0	8.8
6	14460	163.27	13.7	59.4	30.1	4.8	7.1	18.6	5.7	2.2	3.8	8.5	9.4
7	16342	184.52	15.5	67.1	34.1	5.4	8.0	21.0	6.4	2.5	4.3	9.6	10.6
8	18017	203.44	17.0	74.0	37.5	6.0	8.8	23.2	7.1	2.7	4.8	10.6	11.7
9	19400	219.05	18.4	79.7	40.4	6.4	9.5	24.9	7.6	3.0	5.2	11.4	12.6
10	20638	233.03	19.5	84.8	43.0	6.8	10.1	26.5	8.1	3.1	5.5	12.1	13.4
11	21477	242.50	20.3	88.2	44.8	7.1	10.5	27.6	8.4	3.3	5.7	12.6	14.0
12	22075	249.26	20.9	90.7	46.0	7.3	10.8	28.4	8.7	3.4	5.9	13.0	14.3
13	22594	255.12	21.4	92.8	47.1	7.5	11.0	29.1	8.9	3.4	6.0	13.3	14.7
14	22781	257.23	21.6	93.6	47.5	7.5	11.1	29.3	8.9	3.5	6.1	13.4	14.8
15	22938	259.00	21.7	94.2	47.8	7.6	11.2	29.5	9.0	3.5	6.1	13.5	14.9
16	22876	258.30	21.6	93.9	47.7	7.6	11.2	29.4	9.0	3.5	6.1	13.5	14.9
17	22916	258.75	21.7	94.1	47.8	7.6	11.2	29.5	9.0	3.5	6.1	13.5	14.9
18	22791	257.34	21.6	93.6	47.5	7.6	11.1	29.3	8.9	3.5	6.1	13.4	14.8
19	22304	251.84	21.1	91.6	46.5	7.4	10.9	28.7	8.8	3.4	5.9	13.1	14.5
20	21440	242.09	20.3	88.0	44.7	7.1	10.5	27.6	8.4	3.3	5.7	12.6	13.9
21	21051	237.69	19.9	86.5	43.9	7.0	10.3	27.1	8.3	3.2	5.6	12.4	13.7
22	19710	222.55	18.6	80.9	41.1	6.5	9.6	25.3	7.7	3.0	5.2	11.6	12.8
23	17819	201.20	16.9	73.2	37.1	5.9	8.7	22.9	7.0	2.7	4.7	10.5	11.6
24	16251	183.50	15.4	66.7	33.9	5.4	7.9	20.9	6.4	2.5	4.3	9.6	10.6
Hour	Actual Load [MW]	Total Scaled [MVar]	Load 2 Mvar	Load 3 Mvar	Load 4 Mvar	Load 5 Mvar	Load 6 Mvar	Load 9 Mvar	Load 10 Mvar	Load 11 Mvar	Load 12 Mvar	Load 13-1 Mvar	Load 13-2 Mvar
0	15425	49.43	8.5	12.8	-2.6	1.1	5.0	11.2	3.9	1.2	1.1	3.9	3.4
1	14366	46.03	8.0	11.9	-2.4	1.0	4.7	10.4	3.6	1.1	1.0	3.6	3.1
2	13728	43.99	7.6	11.4	-2.3	1.0	4.5	9.9	3.5	1.1	1.0	3.5	3.0
3	13324	42.69	7.4	11.0	-2.3	0.9	4.4	9.6	3.4	1.0	0.9	3.4	2.9
4	13238	42.42	7.3	11.0	-2.3	0.9	4.3	9.6	3.3	1.0	0.9	3.3	2.9
5	13546	43.41	7.5	11.2	-2.3	0.9	4.4	9.8	3.4	1.1	0.9	3.4	3.0

6	14460	46.33	8.0	12.0	-2.5	1.0	4.7	10.5	3.7	1.1	1.0	3.7	3.2
7	16342	52.36	9.0	13.5	-2.8	1.1	5.3	11.8	4.1	1.3	1.1	4.1	3.6
8	18017	57.73	10.0	14.9	-3.1	1.3	5.9	13.0	4.6	1.4	1.3	4.6	3.9
9	19400	62.16	10.7	16.1	-3.3	1.4	6.3	14.0	4.9	1.5	1.4	4.9	4.2
10	20638	66.13	11.4	17.1	-3.5	1.4	6.7	14.9	5.2	1.6	1.4	5.2	4.5
11	21477	68.82	11.9	17.8	-3.7	1.5	7.0	15.5	5.4	1.7	1.5	5.4	4.7
12	22075	70.73	12.2	18.3	-3.8	1.5	7.2	16.0	5.6	1.7	1.5	5.6	4.8
13	22594	72.40	12.5	18.7	-3.8	1.6	7.4	16.4	5.7	1.8	1.6	5.7	4.9
14	22781	73.00	12.6	18.9	-3.9	1.6	7.4	16.5	5.8	1.8	1.6	5.8	5.0
15	22938	73.50	12.7	19.0	-3.9	1.6	7.5	16.6	5.8	1.8	1.6	5.8	5.0
16	22876	73.30	12.7	18.9	-3.9	1.6	7.5	16.6	5.8	1.8	1.6	5.8	5.0
17	22916	73.43	12.7	19.0	-3.9	1.6	7.5	16.6	5.8	1.8	1.6	5.8	5.0
18	22791	73.03	12.6	18.9	-3.9	1.6	7.5	16.5	5.8	1.8	1.6	5.8	5.0
19	22304	71.47	12.3	18.5	-3.8	1.6	7.3	16.1	5.6	1.8	1.6	5.6	4.9
20	21440	68.70	11.9	17.8	-3.6	1.5	7.0	15.5	5.4	1.7	1.5	5.4	4.7
21	21051	67.45	11.7	17.4	-3.6	1.5	6.9	15.2	5.3	1.7	1.5	5.3	4.6
22	19710	63.16	10.9	16.3	-3.4	1.4	6.4	14.3	5.0	1.5	1.4	5.0	4.3
23	17819	57.10	9.9	14.8	-3.0	1.2	5.8	12.9	4.5	1.4	1.2	4.5	3.9
24	16251	52.07	9.0	13.5	-2.8	1.1	5.3	11.8	4.1	1.3	1.1	4.1	3.5

Fall Load Profile:

Hour	Actual Load [MW]	Total Scaled [MW]	Load 2 MW	Load 3 MW	Load 4 MW	Load 5 MW	Load 6 MW	Load 9 MW	Load 10 MW	Load 11 MW	Load 12 MW	Load 13-1 MW	Load 13-2 MW
0	10613	201.37	16.9	73.2	37.2	5.9	8.7	22.9	7.0	2.7	4.7	10.5	11.6
1	10006	189.86	15.9	69.1	35.0	5.6	8.2	21.6	6.6	2.6	4.5	9.9	10.9
2	9716	184.35	15.4	67.1	34.0	5.4	8.0	21.0	6.4	2.5	4.3	9.6	10.6
3	9556	181.32	15.2	65.9	33.5	5.3	7.8	20.7	6.3	2.5	4.3	9.5	10.4
4	9603	182.21	15.3	66.3	33.6	5.3	7.9	20.8	6.3	2.5	4.3	9.5	10.5
5	9814	186.21	15.6	67.7	34.4	5.5	8.1	21.2	6.5	2.5	4.4	9.7	10.7
6	10416	197.64	16.6	71.9	36.5	5.8	8.5	22.5	6.9	2.7	4.7	10.3	11.4
7	11260	213.65	17.9	77.7	39.4	6.3	9.2	24.3	7.4	2.9	5.0	11.1	12.3
8	12066	228.94	19.2	83.3	42.3	6.7	9.9	26.1	8.0	3.1	5.4	11.9	13.2
9	12367	234.66	19.7	85.3	43.3	6.9	10.1	26.7	8.2	3.2	5.5	12.2	13.5
10	12285	233.10	19.5	84.8	43.0	6.8	10.1	26.6	8.1	3.2	5.5	12.2	13.4
11	12082	229.25	19.2	83.4	42.3	6.7	9.9	26.1	8.0	3.1	5.4	11.9	13.2
12	11827	224.41	18.8	81.6	41.4	6.6	9.7	25.6	7.8	3.0	5.3	11.7	12.9
13	11610	220.29	18.5	80.1	40.7	6.5	9.5	25.1	7.7	3.0	5.2	11.5	12.7
14	11418	216.65	18.2	78.8	40.0	6.4	9.4	24.7	7.5	2.9	5.1	11.3	12.5
15	11499	218.19	18.3	79.4	40.3	6.4	9.4	24.9	7.6	2.9	5.1	11.4	12.6
16	11792	223.75	18.7	81.4	41.3	6.6	9.7	25.5	7.8	3.0	5.3	11.7	12.9

Hour	Actual Load [MW]	Total Scaled [MVar]	Load 2 Mvar	Load 3 Mvar	Load 4 Mvar	Load 5 Mvar	Load 6 Mvar	Load 9 Mvar	Load 10 Mvar	Load 11 Mvar	Load 12 Mvar	Load 13-1 Mvar	Load 13-2 Mvar
17	12328	233.92	19.6	85.1	43.2	6.9	10.1	26.6	8.1	3.2	5.5	12.2	13.5
18	13044	247.50	20.7	90.0	45.7	7.3	10.7	28.2	8.6	3.3	5.8	12.9	14.2
19	13650	259.00	21.7	94.2	47.8	7.6	11.2	29.5	9.0	3.5	6.1	13.5	14.9
20	13293	252.23	21.1	91.7	46.5	7.4	10.9	28.7	8.8	3.4	5.9	13.1	14.5
21	12761	242.13	20.3	88.1	44.7	7.1	10.5	27.6	8.4	3.3	5.7	12.6	13.9
22	12050	228.64	19.2	83.2	42.2	6.7	9.9	26.0	7.9	3.1	5.4	11.9	13.2
23	11118	210.96	17.7	76.7	38.9	6.2	9.1	24.0	7.3	2.9	5.0	11.0	12.1
24	10346	196.31	16.4	71.4	36.2	5.8	8.5	22.4	6.8	2.7	4.6	10.2	11.3
		5436.533333	455.493333	1977.3028573	1003.3447622	159.527619	235.0933333	619.2190476	188.9142857	73.466666 7	128.0419048	283.3714286	312.7580952

Hour	Actual Load [MW]	Total Scaled [MVar]	Load 2 Mvar	Load 3 Mvar	Load 4 Mvar	Load 5 Mvar	Load 6 Mvar	Load 9 Mvar	Load 10 Mvar	Load 11 Mvar	Load 12 Mvar	Load 13-1 Mvar	Load 13-2 Mvar
0	10613	57.15	9.9	14.8	-3.0	1.2	5.8	12.9	4.5	1.4	1.2	4.5	3.9
1	10006	53.88	9.3	13.9	-2.9	1.2	5.5	12.2	4.3	1.3	1.2	4.3	3.7
2	9716	52.32	9.0	13.5	-2.8	1.1	5.3	11.8	4.1	1.3	1.1	4.1	3.6
3	9556	51.46	8.9	13.3	-2.7	1.1	5.3	11.6	4.1	1.3	1.1	4.1	3.5
4	9603	51.71	8.9	13.4	-2.7	1.1	5.3	11.7	4.1	1.3	1.1	4.1	3.5
5	9814	52.84	9.1	13.7	-2.8	1.2	5.4	11.9	4.2	1.3	1.2	4.2	3.6
6	10416	56.09	9.7	14.5	-3.0	1.2	5.7	12.7	4.4	1.4	1.2	4.4	3.8
7	11260	60.63	10.5	15.7	-3.2	1.3	6.2	13.7	4.8	1.5	1.3	4.8	4.1
8	12066	64.97	11.2	16.8	-3.4	1.4	6.6	14.7	5.1	1.6	1.4	5.1	4.4
9	12367	66.59	11.5	17.2	-3.5	1.4	6.8	15.0	5.3	1.6	1.4	5.3	4.5
10	12285	66.15	11.4	17.1	-3.5	1.4	6.8	14.9	5.2	1.6	1.4	5.2	4.5
11	12082	65.06	11.2	16.8	-3.5	1.4	6.6	14.7	5.1	1.6	1.4	5.1	4.4
12	11827	63.68	11.0	16.5	-3.4	1.4	6.5	14.4	5.0	1.6	1.4	5.0	4.3
13	11610	62.52	10.8	16.2	-3.3	1.4	6.4	14.1	4.9	1.5	1.4	4.9	4.3
14	11418	61.48	10.6	15.9	-3.3	1.3	6.3	13.9	4.9	1.5	1.3	4.9	4.2
15	11499	61.92	10.7	16.0	-3.3	1.3	6.3	14.0	4.9	1.5	1.3	4.9	4.2
16	11792	63.50	11.0	16.4	-3.4	1.4	6.5	14.3	5.0	1.6	1.4	5.0	4.3
17	12328	66.38	11.5	17.2	-3.5	1.4	6.8	15.0	5.2	1.6	1.4	5.2	4.5
18	13044	70.24	12.1	18.2	-3.7	1.5	7.2	15.9	5.5	1.7	1.5	5.5	4.8
19	13650	73.50	12.7	19.0	-3.9	1.6	7.5	16.6	5.8	1.8	1.6	5.8	5.0
20	13293	71.58	12.4	18.5	-3.8	1.6	7.3	16.2	5.6	1.8	1.6	5.6	4.9
21	12761	68.71	11.9	17.8	-3.6	1.5	7.0	15.5	5.4	1.7	1.5	5.4	4.7
22	12050	64.88	11.2	16.8	-3.4	1.4	6.6	14.7	5.1	1.6	1.4	5.1	4.4
23	11118	59.87	10.3	15.5	-3.2	1.3	6.1	13.5	4.7	1.5	1.3	4.7	4.1
24	10346	55.71	9.6	14.4	-3.0	1.2	5.7	12.6	4.4	1.4	1.2	4.4	3.8

Appendix H: 14-Bus Generation Cost Data

Gen ID	Season	Fuel Source/ Gen Type	Gen Size (MW)	Capacity Factor (C)	Unit Fuel Cost ($/MMBTU)	Variable O&M Costs ($/MWh)	Fixed Cost Independent Value ($/hr)	Cubic Cost Model B (BTU/kWh)
1	Summer	NatGas (Conv CCGT)	332.4	8760	$2.76	$16.00	$16.67	10,783
2	Summer	NatGas (Conv CCGT)	140	8760	$2.76	$16.00	$7.02	10,783
3/6	Summer	NatGas (Conv CCGT)	100	8760	$2.76	$16.00	$5.02	10,783
8	Summer	Solar (PV)	100	8760	$0.00	$0.00	$16.99	9,516
8	Summer	Wind	100	8760	$0.00	$0.00	$10.26	9,516
1	Fall	NatGas (Conv CCGT)	332.4	8760	$3.28	$16.00	$16.67	10,783
2	Fall	NatGas (Conv CCGT)	140	8760	$3.28	$16.00	$7.02	10,783
3/6	Fall	NatGas (Conv CCGT)	100	8760	$3.28	$16.00	$5.02	10,783
8	Fall	Solar (PV)	100	8760	$0.00	$0.00	$16.99	9,516
8	Fall	Wind	100	8760	$0.00	$0.00	$10.26	9,516
4	F/S_4.1	Pumped Hydro Storage (PHS)	10	8760	$0.00	$4.30	$0.94	9,516
	F/S_4.2		20	8760	$0.00	$4.30	$1.88	9,516
	F/S_4.3		30	8760	$0.00	$4.30	$2.82	9,516
	F/S_4.4		40	8760	$0.00	$4.30	$3.76	9,516
	F/S_4.5		50	8760	$0.00	$4.30	$4.70	9,516
	F/S_4.6		60	8760	$0.00	$4.30	$5.64	9,516
	F/S_4.7		70	8760	$0.00	$4.30	$6.58	9,516
	F/S_4.8		80	8760	$0.00	$4.30	$7.53	9,516
	F/S_4.9		90	8760	$0.00	$4.30	$8.47	9,516
	F/S_4.10		100	8760	$0.00	$4.30	$9.41	9,516

Appendix I: 14-Bus Solar Generation Data

IC, Total Insolation	Scaled Energy Prod, [MW], Summer Data	IC, Total Insolation	Scaled Energy Prod, [MW], Fall Data
672.8524	0.0	-288.288454	0.0
697.4313	0.0	-284.496698	0.0
790.4614	0.0	-273.693255	0.0
1081.787	0.0	-257.840278	0.0
4063.828	0.0	-241.687682	0.0
23.95463	2.6	-241.46305	0.0
229.4364	24.5	424.7984705	0.0
345.5627	37.0	43.05778825	4.5
458.8889	49.1	348.0545668	36.0
652.0432	69.8	608.6520667	62.9
804.4004	86.1	804.1643394	83.1
901.4373	96.4	925.8820115	95.7
934.7142	100.0	967.2431699	100.0
901.4373	96.4	925.8820115	95.7
804.4004	86.1	804.1643394	83.1
652.0432	69.8	608.6520667	62.9
458.8889	49.1	348.0545668	36.0
345.5627	37.0	43.05778825	4.5
229.4364	24.5	424.7984705	0.0
23.95463	2.6	-241.46305	0.0
4063.828	0.0	-241.687682	0.0
1081.787	0.0	-257.840278	0.0
790.4614	0.0	-273.693255	0.0
697.4313	0.0	-284.496698	0.0

Appendix J: 14-Bus Results Summary

Fall Solar Congested													
Total Cost		Distance From RE											
Storage (MW)	No Storage	Bus 8 (0)	Bus 7 (1)	Bus 4 (2)	Bus 9 (2)	Bus 2 (3)	Bus 5 (3)	Bus 3 (3)	Bus 10 (3)	Bus 13 (3)	Bus 6 (4)	Bus 11 (4)	Bus 12 (4)
0	244013.6	244013.6	244013.6	244013.6	244013.6	244013.6	244013.6	244013.6	244013.6	244013.6	244013.6	244013.6	244013.6
10	244013.6	243845.9	244431.8	244465.3	244608.2	243951.8	244642.2	243924.5	244879.3	245010.7	244551.2	245007.5	245111.3
20	244013.6	243744.8	244333.5	244375.2	244512.7	243932	244596	243952.9	244879.6	245167.7	244588.5	245128.4	245515.2
30	244013.6	243726.5	244316.2	244346.5	244507.3	243956.8	244605.9	244109.2	245030	245535.2	244721.9	245454.9	246260.9
40	244013.6	243794	244363.7	244410.4	244609.4	244019.4	244670.1	244395.7	245331.7	246116.3	244952.7	245979.1	247358.8
50	244013.6	243945.6	244515.8	244566.8	244809.4	244122.2	244815	244814.8	245781.9	246909.9	245297.9	246705.1	248834.3
60	244013.6	244183.1	244755.8	244803.2	245104.1	244276.6	245042.5	245411.7	246387.5	247929.7	245744.8	247641.5	250687.4
70	244013.6	244502.9	245085.2	245111.7	245497.3	244459.8	245325	246049.8	247148.1	249166.6	246310.9	248776.9	252939.2
80	244013.6	244911.2	245516.6	245487.9	245993.2	244684.3	245713.3	246865.6	248063.4	250630.5	246978.1	250130.4	255601.7
90	244013.6	245402	246022.9	245937.9	246593	244951.5	246108.6	247814.3	249137	252322.9	247746.1	251700.7	258698.5
100	244013.6	245984.2	246618.1	246464.9	247296.4	245257.7	246572.2	248896.9	250373	254249.9	248630.8	253493.4	262266.4
Fall Wind Congested													
Total Cost		Distance From RE											
Storage (MW)	No Storage	Bus 8 (0)	Bus 7 (1)	Bus 4 (2)	Bus 9 (2)	Bus 2 (3)	Bus 5 (3)	Bus 3 (3)	Bus 10 (3)	Bus 13 (3)	Bus 6 (4)	Bus 11 (4)	Bus 12 (4)
0	187345.7	187345.7	187345.7	187345.7	187345.7	187345.7	187345.7	187345.7	187345.7	187345.7	187345.7	187345.7	187345.7
10	187345.7	187207.1	187206.6	187210.1	187213.3	187446.3	187202.2	187464	187219.1	187167.5	187195.8	187248.4	187317.9
20	187345.7	187156.9	187158.1	187156.8	187172.9	187438.4	187166.1	187484.5	187250.7	187301.4	187222	187362.6	187619.2
30	187345.7	187179.1	187181.7	187170	187218.2	187465	187190.8	187623.5	187417	187618.4	187334.4	187652.5	188233.8
40	187345.7	187279.3	187283.3	187254.2	187352.9	187529.2	187274.2	187878.4	187723.6	188130.5	187533.9	188129.2	189155.7
60	187345.7	187716.8	187711.1	187632	187882.6	187759.9	187616.7	188744.2	188748	189719.4	188194.6	189619.8	191989.4
80	187345.7	188568.4	188544.9	188358.4	188870.1	188240.5	188269.1	190184.6	190404.4	192158.5	189247.3	191912.5	196053.1
100	187345.7	190106	190027.6	189637.4	190575.8	189249.6	189399.7	192515.5	192941.8	195520.4	190789.2	195173.8	201569.6

Summer Solar Congested

Total Cost		Distance From RE											
Storage (MW)	No Storage	Bus 8 (0)	Bus 7 (1)	Bus 4 (2)	Bus 9 (2)	Bus 2 (3)	Bus 5 (3)	Bus 3 (3)	Bus 10 (3)	Bus 13 (3)	Bus 6 (4)	Bus 11 (4)	Bus 12 (4)
0	205694.3	205694.3	205694.3	205694.3	205694.3	205694.3	205694.3	205694.3	205694.3	205694.3	205694.3	205694.3	205694.3
10	205694.3	205568.4	205575.5	205586.7	205578.2	205808.9	205577.8	205856.6	205592.5	205578.9	205625.1	205647.1	205726.5
20	205694.3	205515.6	205520.7	205530.5	205538.4	205797	205543.6	205868.6	205623	205683.2	205642.1	205752	205997.2
30	205694.3	205544.7	205543.1	205545.2	205581.3	205818.4	205567.6	205985.6	205769.8	206004.9	205751.6	206011.3	206569.6
40	205694.3	205642.7	205639.5	205627.5	205708.6	205873.2	205650.3	206211.1	206042	206481.1	205944.8	206461.2	207434.5
50	205694.3	205813.1	205808.5	205777.2	205925.8	205961.3	205792.1	206548.3	206454.7	207138.5	206224.8	207066.6	208623.2
60	205694.3	206058.9	206050.6	205995.1	206205.2	206082.5	205991.6	206995.4	206992	207987.6	206592.9	207856.7	210134.4
70	205694.3	206383.2	206366.3	206282.1	206582.6	206236.9	206249	207551.1	207661.7	209041.9	207048.9	208831.5	211985.9
80	205694.3	206788.4	206757.1	206639.3	207043.8	206412.5	206571.4	208218.8	208471.7	210314.7	207609.5	209996.5	214230.2
90	205694.3	207278	207221.9	207057.3	207592	206634.1	206949.1	209000.9	209431.5	211827.8	208251.8	211354.8	217079.9
100	205694.3	207865.8	207767.8	207545.8	208227.7	206884.1	207384.9	209898	210542	213659	208993.8	212936.3	221201.6

Summer Wind Congested

Total Cost		Distance From RE											
Storage (MW)	No Storage	Bus 8 (0)	Bus 7 (1)	Bus 4 (2)	Bus 9 (2)	Bus 2 (3)	Bus 5 (3)	Bus 3 (3)	Bus 10 (3)	Bus 13 (3)	Bus 6 (4)	Bus 11 (4)	Bus 12 (4)
0	172141.8	172141.8	172141.8	172141.8	172141.8	172141.8	172141.8	172141.8	172141.8	172141.8	172141.8	172141.8	172141.8
10	172141.8	172026.9	172026.4	172029	172031.7	172260.8	172023.7	172257	172040.5	171988	172050.6	172082	172140.6
20	172141.8	171978.8	171977.3	171968.9	172002.2	172238.2	171977.1	172218.9	172064.4	172067.6	172039.7	172170	172381.9
30	172141.8	172004.3	172000.5	171972.3	172047	172247.5	171985.9	172241.4	172210.1	172322.4	172113.3	172415.1	172894.8
40	172141.8	172102.2	172094.6	172041.3	172170.4	172289.1	172052.3	172454	172477.7	172748.5	172269.2	172822.2	173685.1
60	172141.8	172511.6	172494.5	172377.2	172667.9	172467.3	172358.5	173127.1	173390.8	174134.3	172835.5	174147.4	176255.3
80	172141.8	173226.4	173180.3	172976.3	173486.2	172774.4	172892.5	174224	174826.9	176292.6	173764.9	176206.6	180108.4
100	172141.8	174332	174156	173836.8	174631.2	173211.8	173663.3	175755.4	176814.7	179346.9	175059.9	179001.5	186360.7